Climate engineering by mimicking the natural dust climate control: the Iron Salt Aerosols method

Authors:

Franz Dietrich OESTE *[1], Renaud de_RICHTER *[2], Tingzhen MING [3], Sylvain CAILLOL [2]

* corresponding author

Affiliations & Addresses:

1 gM-Ingenieurbüro, Tannenweg 2, D-35274 Kirchhain, Germany. Email: oeste@gm-ingenieurbuero.com

2 Institut Charles Gerhardt Montpellier − UMR5253 CNRS-UM2 − ENSCM-UM1 – Ecole Nationale Supérieure de Chimie de Montpellier, 8 rue de l'Ecole Normale, 34296 Montpellier Cedex 5, France. Email: renaud.derichter@gmail.com

3 School of Civil Engineering and Architecture, Wuhan University of Technology, No. 122, Luoshi Road, Hongshan District, Wuhan, 430070 China.

Abstract

Power stations, ship, and air traffic are among the most potent greenhouse gas emitters and are primarily responsible for global warming.

Iron salt aerosols (ISA), composed partly of iron and chloride, exert a cooling effect on climate in several ways. This article aims firstly to examine all direct and indirect natural climate cooling mechanisms driven by ISA tropospheric aerosol particles, showing their cooperation and interaction within the different environmental compartments. Secondly, it looks at a proposal to enhance the cooling effects by ISA in order to reach the optimistic target of the Paris climate agreement, to limit the global temperature increase between 1.5 and 2 °C.

Mineral dust played an important role during the glacial periods: by using mineral dust as a natural analogue tool and by mimicking the same method used in nature, the proposed ISA method might be able to reduce and stop climate warming. The first estimations made in this article show that by doubling the current natural iron emissions by ISA into the troposphere, i.e. by about 0.3 Tg Fe per year, artificial ISA would enable the prevention or even reversal of global warming.

The ISA method proposed integrates technical and economically feasible tools.

Keywords

Iron salt aerosols, cooling the earth, reverse global warming, methane removal, CO_2 removal phytoplankton fertilization, tropospheric ozone reduction, cloud albedo, carbon capture and storage (CCS), climate engineering

1. Introduction

The 5th assessment report of the Intergovernmental Panel on Climate Change (IPPC), released in November 2014, states that Global Warming (GW) has already begun to dramatically change continental and marine ecosystems.

A recently noticed effect is that the vertical mixing in oceans decreases and even reaches a stagnation point [1], thus weakening the net oceanic cumulative intake of atmospheric CO_2 [2, 3].

A consequence of decreasing vertical ocean mixing is a reduced or interrupted oxygen supply to the depths of the ocean. Currently, the formation of low-oxygen areas in the oceans is increasing [4, 5]. Furthermore, climate warming entails stratification of the water column and blocks vertical flows. Stratification may develop by warming the upper water layer as well as evaporation and precipitation. Generation of a fresh water layer on top of the water column by precipitation, surface water runoff and melt water inflow induce stratification [6, 7]. Even the opposite, brine generation by evaporation may induce stratification [8]. Stratification blocks the oxygen transfer through the water column and triggers the formation of oxygen-depleted zones [9] that also emit nitrous oxide (N_2O), a potent GHG and a powerful ozone depleting agent.

As iron is part of many enzymes directing the bioenergetic transformation of nitrogen in the ocean, it has an additional direct influence on the cycling of these elements through the oceanic environment [10, 11].

The severest consequence to oceanic ecosystems of such stratification is the development of anoxic milieu within stratified ocean basins. An example of the development of halocline and chemocline stratification is the Black Sea [12]. This ocean basin has a stable halocline which coincides with a chemocline, dividing an oxic salt-poor surface water layer from a saline anoxic sulfidic deep layer with a black sapropel sediment rich in organic C at the basin bottom [12].

Geological past episodes with stratified ocean basins are regularly marked by black shale or black limestone as remnants of sapropel sediments. Stratified ocean basins during the Phanerozoic epoch occurred as a consequence of elevated CO_2 levels in the atmosphere. This caused high sea surface temperatures [13] and, as a global consequence a global increase of evaporation, precipitation and production of brines of higher concentrations.

It has been pointed out that the increasing melt water run-off from past polar and subpolar ice layers may have induced the cover of denser ocean water by a melt water layer [6]. According to Praetorius et al. [14] climate warming events during the last deglacial transition induced subsurface oxygen minimum zones accompanied by sea floor anoxia in the Northern Pacific. This melt water-induced stratification had been accompanied by melt water iron-induced phytoplankton blooms. The generation of increasing precipitation and surface water run-off accompanied by increasing brine production plus elevated surface water temperatures during hot CO_2-high climate episodes had similar consequences in the past geological epochs [13].

Ocean basin stratifications may be induced by increasing precipitation with increased surface water run-off [7] or by increased brine production [8]. These ocean stratification event is characterized by regional to global ocean anoxia, black sediments with elevated organic C and hot greenhouse climate, as we learn from the whole Phanerozoic past [13] and was often accompanied by mass extinctions.

Even the largest mass extinction of ocean biota within the Phanerozoic epoch, during the Permian-Triassic transition, has been induced by high temperatures as a consequence of elevated CO_2-Levels, which induced the change of a well-mixed oxic to a stratified euxinic-anoxic ocean [15].

What we have to face now is the extraordinary process developing from the recent situation: the combination of the CO_2-dependent temperature rise-generated precipitation increase, plus melt water increase. Mankind has to find now the appropriate tool to stop this dangerous stratification process.

Warming surface waters and decreasing input of cold, oxygenated surface water, trigger a temperature rise of sediments, transforming solid methane hydrate into gaseous methane (CH_4) emissions in seawater [16]. CH_4 oxidation consumes additional oxygen, decreasing the oxygen content above those areas [17].

The same effects are expected with an anticipated increase in spring and summer coastal upwelling intensity, associated with increases in the rate of offshore advection, decreasing the nutrient supply while producing a spatial or temporal (phenological) mismatch between production and consumption in the world's most productive marine ecosystems [18].

These events have the threatening consequence of a sprawling lack of oxygen in the oceans. In such low-oxygen areas (sub-oxic to anoxic) only bacterial life is possible: higher life forms can not exist there. Accordingly, an early result of the climate warming progression could lead to a dramatic limitation of the oceanic food sources that will be needed for the projected 9-10 billion people by 2050. The same deleterious consequences on seafood supply can also result in ocean surface acidification through increased CO_2 dissolution in sea

water and decreased flow of surface water currents to ocean basin bottoms, limiting reef fish and shelled mollusk survival [19].

Any decrease of the THC has severe consequences on all kinds of ecosystems as it further triggers climate warming by different interactions. THC decrease induces a reduction or eventual disappearance of the phytoplankton fertilizers Si, P, N and Fe extracted on the ocean surface from their resources at the bottom of the ocean basins. Hydrothermal fluid cycling by mid-ocean ridges, off-axis hydrothermal fluid fluxes, subduction-dependent hydrothermal convection fluids, hydrothermal fluxes at hot spot sea mount and fluid emissions from anaerobic sediments, contain said elements as dissolved or colloidal phase [20-27]. The deeper water of all ocean basins is enriched by these fertilizers. A THC decrease within the ocean basins will result in a decrease of the assimilative transformation of CO_2 into organic carbon.

Moreover, any THC decrease would further trigger the acidification of the ocean surface by lowering or preventing the neutralization of dissolved CO_2 and HCO_3^-, due to the alkalinity decrease from hydrothermal sources [20, 28].

During the convective water flow through the huge alkaline ocean crust volume, estimated to about 20 - 540 x 10^3 km³ yr^{-1} [29], ocean water is depleted in O_2, but enriched in its reductant content such as CH_4 [20, 30]. Further elements are enriched in this convective water flow through the Earth crust, essential for the existence of life. The re-oxygenation of this huge water volume is retarded or even impossible with a minimized THC.

According to model calculations [31] the THC might have significantly changed between the last glacial and interglacial periods. During the Cenozoic epoch, ice covered pole caps limited the incorporation of carbon in the form of carbonate into the oceanic crust compared to the warm Late Mesozoic peroid [32]. The findings of Coogan & Gillis show that during ice-free periods, THCs were possible with much higher effectiveness than in modern times. Even during those warm periods with low temperature gradients between polar and equatorial oceans, an effective production of brines leading to buoyancy differences necessary for development of effective THC may have ben generated [33]. However, increased inflow rates of high density brines coming from shallow shelf regions with high evaporation rates, induced several collapses or vertical reductions of the strong Cretaceous THC. From here and for more than a million years, the lower parts of ocean basins have been filled with anoxic brines [8]. Further aspects of ocean stratification are discussed in chapter 4.1.

Remnants of these anoxic events are black shale sediments [34]. During such THC collapses, the uptake of CO_2 into the oceanic crust stayed restricted to organic carbon sediments. Additionally, the organic carbon productivity of the remaining oxic zone was decreased, as well as eolic dust input, due to phytoplankton fertilizer production being limited to continental weathering.

These examples point out the sensitivity of the THC to disturbances. Without action, the weakness of our recent THC may worsen. Any THC collapse would not only result in severe damages to ecosystems, food chains, and food resources of the oceans, but would also lead to an acceleration of the increase of atmospheric CO_2 concentration, resulting in a faster climate warming than forecasted.

The best way to prevent such disturbing situations and consequences is to stop GW.

A realistic chance of averting this development is the controlled application of a climate cooling process, used several times by nature throughout the last ice ages with high efficiency and, based on loess dust. Loess is a wind-blown dust sediment formed by progressive accumulation and composed generally of clay, sand and silt (approximately a ratio of 20:40:40 respectively), loosely cemented by calcium carbonate.

The dust concentration in the troposphere increased during every cold period in ice ages and reached a multiple of today's levels [35]. Dust deposition in the Southern Ocean during glacial periods was 3 to 10 times greater than during interglacial periods, and its major source region was probably Australia or New Zealand (Lamy et al., 2014). The windblown dust and its iron content effect on marine productivity in the Southern Ocean is thought to be a key determinant of atmospheric CO_2 concentrations [36]. During high dust level periods, the global average temperature fell down to 10°C [35, 37, 38], which is 4.5°C lower than current global average temperature. Loess sediments in the northern and southern hemisphere on continents and ocean floors originate from these cold dusty periods.

Former geoscientists had the predominant conception that the cold glacial temperatures had caused dustiness, and not the reverse [39]. Meanwhile more evidence accumulates that mineral dust was a main factor in the cause of the cold periods and that the iron (Fe) fraction of wind-blown dust aerosol fertilized the oceans' phytoplankton, activating the assimilative conversion of CO_2 into organic carbon [37-42] and carbonate which composes the main dry body substance of phytoplankton, together with silica, another component of dust [43].

Evidence about the responsibility of iron-containing dust that triggered ice ages during the late Paleozoic epoch are in discussion [44].

The biogeochemical cycles of carbon, nitrogen, oxygen, phosphorus, sulfur and water are well described in the literature, but the biogeochemical cycle of the Earth's iron is often overlooked. An overview of the progress made in the understanding of the iron cycle in the ocean is given by several authors [45, 46].

The current state of knowledge of iron in the oceans is lower than that of carbon, although numerous scientific publications deal with this topic [47-55], meanwhile the iron biogeochemical cycle in the atmosphere is described by fewer ones [56-58], on the contrary to the iron biogeochemical cycle in soil and land, as almost no recent publications details the

current knowledge of iron in soils and over the landscape [59-61], a task we attempt to do in this review.

The process of iron fertilization by injection of iron salt solution into the ocean surface had already been in discussion as an engineering scheme proposed to mitigate global warming [62]. But iron fertilization experiments with $FeSO_4$ conducted over 300 km^2 into the Sub-Antarctic Atlantic Ocean, although doubling primary productivity of Chlorophyll a, did not enhance downdraft particles' flux into the deep ocean [63]. The researchers attribute the lack of fertilization-induced export into the deep ocean to the limitation of silicon needed for diatoms. Thus, ocean fertilization using only iron can increase the uptake of CO_2 across the sea surface, but most of this uptake is transient and will probably not conduct to long-term sequestration [64]. In other experiments, the authors [65] find that iron-fertilized diatom blooms may sequester carbon for centuries in ocean bottom water, and for longer in the sediments, as up to half the diatom bloom biomass sank below 1 km depth and reached the sea floor. Meanwhile dissolution of olivine, a magnesium-iron-silicate containing silica, with a Mg:Fe ratio of nearly 9:1, resulted in 35% marine carbon uptake (with the hypothesis of 1% of the iron dissolved and biologically available), with communities of diatoms being one of the phytoplankton winners [66].

The idea of climate cooling by CO_2 carbon conversion into organic sediment carbon by addition and mixture of an iron salt solution into the ocean with the marine screw propeller has been the object of controversial debates [67-69]. The eolic iron input per square meter of ocean surface by natural ISA is in the single decadal order of mg Fe m^{-2} yr^{-1}. In comparison, the artificial Fe input by ship screws is orders of magnitude above the natural fertilizing with ISA.

The small content of water-soluble iron salts (IS) in the dust particles triggers this fertilization effect [70], and the soluble iron deposition during glaciations had been up to 10 times the modern deposition [71]. According to Spolaor et al. [72], most of the bioavailable water soluble Fe(II) has been linked, during the last 55,000 years, to the fine dust fraction, as it was demonstrated from ice cores from Antarctica. During late Paleozoic epochs, glacial stage dust fluxes of ~400 to 4,000 times those of interglacial times had been found [73], which gives an estimated carbon fixation ~2-20 times that of modern carbon fixation due to dust fertilization. Photochemistry by sunshine is the main trigger of the transformation of the primary insoluble iron fraction of dust aerosols into soluble iron salts [74], and the understanding of how the different iron content and speciation in aerosols affect the climate is growing [75]. Currently, increased sub-glacial melt water and icebergs may supply large amounts of bioavailable iron to the Southern Ocean [76]. The flux of bioavailable iron associated with glacial runoff is estimated at 0.40–2.54 Tg yr^{-1} in Greenland and 0.06–0.17 Tg yr^{-1} in Antarctica [77], which are comparable with aeolian dust fluxes to the oceans

surrounding Antarctica and Greenland, and will increase by enhanced melting in a warming climate.

However, CO_2 uptake by the oceans is not the only effect of iron dust. The full carbon cycle is well described in the literature; meanwhile we know less about the iron biogeochemical cycle. Recently the major role of soluble iron emissions from combustion sources became more evident. Today the anthropogenic combustion emissions play a significant role in the atmospheric input of soluble iron to the ocean surface [78]. Combustion processes currently contribute from 20 to 100% of the soluble iron deposition over many ocean regions [79]. Model results suggest that human activities contribute to about half of the soluble Fe supply to a significant portion of the oceans in the Northern Hemisphere [80], and that deposition of soluble iron from combustion sources contributes for more than 40% of the total soluble iron deposition over significant portions of the open ocean in the Southern Hemisphere [81]. Anthropogenic aerosol associated with coal burning are maybe the major bioavailable iron source in the surface water of the oceanic regions [82]. The higher than previously estimated Fe emission from coal combustion implies a larger atmospheric anthropogenic input of soluble Fe to the northern Atlantic and northern Pacific Oceans, which is expected to enhance the biological carbon pump in those regions [83].

The limited knowledge about dissolved or even dispersed iron distributions in the ocean confirms the work of Tagliabue et al. [55]: their calculation results about the residence time of iron in the ocean differs up to three orders of magnitude between the different published models.

The precipitation of any iron salt results from the pH and O_2 content of the ocean water milieu. But the presence of organic Fe chelators such as humic or fulvic acids [54] as well as complexing agents produced by microbes [49] and phytoplankton [84], life forms prevents iron from precipitation. In principle, this allow the transport of iron, from its sources, to any place within the ocean across huge distances with the ocean currents [25]**.** But organic material as well as humic acids have limited lifetime in oxic environments due to their depletion at last to CO_2. But within stratified anoxic ocean basins their lifetime is unlimited.

The iron inputs into the ocean regions occur by atmospheric dust, coastal and shallow sediments, sea ice, icebergs and hydrothermal fluids and deep ocean sediments [47, 49, 56, 57, 83, 85-87]**.**

Microbial life within the gradient of chemoclines dividing anoxic from oxic conditions generate organic carbon from CO_2 or HCO_3^- carbon [88-90]. The activity at these chemoclines are sources of dissolved Fe(II). Humic acid is a main product of the food chain within any life habitat. Coastal, shelf, and ocean bottom sediments, as well as hydrothermal vents and methane seeps are such habitats and known as iron sources (Boyd and Ellwood, 2010). Insoluble Fe oxides are part of the lithogenic particles suspended at the surface of the

Southern Ocean. In addition to organic phytoplankton substance, the suspended inorganics accompany the gut passage through the krill bodies. During gut passage of these animals, iron is reduced and leaves the gut in dissolved state [91]. There is no doubt that gut-microbial attack on ingested organics and inorganics produce faeces containing humic acids. This metabolic humic acid production is known from earth worm faeces [92] and human faeces [93, 94]. The effect of iron mobilization from lithogenic particles by reduction during gut passage has been found in termites too [95]. The parallel generation of Fe-chelating humic acids during gut passage guarantees, that the Fe is kept in solution after leaving the gut into the ocean. The examples demonstrate that every link of the ocean food chain may act as source of dissolved iron.

The co-generation of Fe(II) and Fe-chelating agents at any Fe sources at the bottom, surface and shelves of the oceans is the precondition to the iron transport between source and phytoplankton at the ocean surface. But the transport between sources and the phytoplankton depends on the vertical and horizontal movement activity in the ocean basins [48, 54]. Any movement between iron sources and the phytoplankton-rich surface in stratified ocean basins keeps restricted to surface near Fe input from its sources (shelf sediments, melt water, icebergs, rivers, surface water runoff and dust input).

During the glacial maxima the vertical movement activity arrived to an optimum. According to that, the Fe transport from basin bottom sources and dust sources to the phytoplankton were at their maximum and produce maximum primary productivity at the ocean surface but the carbon burial became the lowest during that time [96] although the greenhouse gases (GHGs) were at their lowest levels during the glacial maximum. Causal for this seemingly contradiction are the changing burial ratios of organic C / carbonate C at the basin bottom(s). The burial ratio is high during episodes with stratified water column and it is very low during episodes with vertical mixed water column as we demonstrate in chapter 4 in detail.

This review aims to describe the multi-stage chemistry of the iron cycle on the atmosphere, oceans, lands, sediments and ocean crust. This article is a comprehensive review of the evidence for connections between the carbon cycle and the iron cycle, and their direct and indirect planetary cooling effects. Numerous factors influence the Fe-cycle and the iron dissolution: iron speciation, photochemistry, biochemistry, red-ox chemistry, mineralogy, geology. In order to perform an accurate prediction of the impact of Fe-containing dusts, sea salt, and acidic components, the atmospheric chemistry models need to incorporate all relevant interaction compartments of the Fe-cycle with sun radiation, chlorine, sulfur, nitrogen and water. This review advocates a balanced approach to benefit from the Fe-cycle to fight global warming by enhancing natural processes of GHG depletion, albedo increase, carbon burial increase and of de-stratification of the ocean basins.

Breakdown of sections:

The next three sections describe nearly a dozen different climate cooling processes induced by iron salt aerosols (ISA) and their interaction for modeling parameter development (sections 2, 3, 4 and 5). Then estimation of the requirements in terms of ISA, to stop global warming will be given in section 6, followed by the description of a suggested ISA enhanced method to fight global warming and induce planetary cooling in section 7, and the possible risks of reducing acids and iron emissions in the future in section 8, followed by a general discussion and concluding remarks in sections 9 and 10. To our knowledge, this review completes, with atmospheric and terrestrial compartments [97], the previous ocean global iron cycle vision of Parekh [98], Archer and Johnson [50], Boyd and Ellwood [49] and of many others. It advocates a balanced approach to make use of the iron cycle to fight global warming by enhancing natural processes.

Components of the different natural cooling mechanism by ISA

The best known cooling process induced by ISA is the phytoplankton fertilizing stage described in the introduction. But this process is only part of a cascade of at least 12 climate cooling stages presented in this review. These stages are embedded within the coexisting multi-component complex networks of different reciprocal iron induced interactions across the borders of atmosphere, surface ocean, sediment and igneous bedrock as well as across the borders of chemistry, biology, and physics and across and along the borders of illuminated, dark, gaseous, liquid, solid, semi-solid, animated, unanimated, dead and different mix phase systems. Some impressions according to the complexity of iron acting in the atmospheric environment have been presented by Al-Abadleh [75].

The ISA-induced cooling effect begins in the atmosphere. Each of the negative forcing stages unfolds a climate-cooling potential for itself. Process stages 1-6 occur in the troposphere (chapter 2), stage 6 at sunlit solid surfaces, stages 7-8 in the ocean (chapter 3), and stages 9-12 in the oceanic sediment and ocean crust (chapter 4). Other possible cooling stages over terrestrial landscapes and wetlands are described in chapter 5. The more than 12 stages of this cooling process cascade operate as described below.

2. Tropospheric natural cooling effects of the iron cycle

2.1. ISA-induced cloud albedo increase

ISA consists of iron-containing particles or droplets with a chloride content. Aerosols have significant effects on the climate [99]. First, by direct scattering of radiation, and second, by inducing a cloud albedo increase. The latter effect is induced by cloud whitening and cloud life time elongation. Both effects induce a climate cooling effect by negative radiative forcing

of more than -1 W per square meter.

Aerosols have a climate impact through aerosol–cloud interactions and aerosol–radiation interactions [100]. By reflecting sunlight radiation back to space, some types of aerosols increase the local albedo (which is the fraction of solar energy that is reflected back to space), producing a cooling effect [101]. If the top of clouds reflect back a part of the incident solar radiation received, the base of clouds receive the longwave radiation emitted from the Earth surface and reemit downward a part of it. Usually, the higher a cloud is, in the atmosphere, the greater its effect on enhancing atmospheric greenhouse warming, and therefore the overall effect of high altitude clouds, such as cirrus, is a positive forcing. Meanwhile, the net effect of low altitude clouds (stratocumulus) is to cool the surface, as they are thicker and prevent more sunlight from reaching the surface. The overall effect of other types of clouds such as cumulonimbus is neutral: neither cooling nor warming.

More outgoing long-wave radiation is possible when the cirrus cover is reduced. Efficient ice nuclei (such as bismuth tri-iodide) seeding of cirrus cloud might artificially reduce their cover [102, 103].

In order to enhance the cooling effects of low altitude clouds, marine cloud brightening has been proposed [104], for instance by injecting sea salt aerosols over the oceans. The effect depends on both particle size and injection amount, but a warming effect is possible [105].

Aerosol effects on climate are complex because aerosols both reflect solar radiation to space and absorb solar radiation. In addition, atmospheric aerosols alter cloud properties and cloud cover depending on cloud type and geographical region [106]. The overall effect of aerosols on solar radiation and clouds is negative (a cooling effect), which masks some of the GHGs-induced warming. But some individual feedbacks and forcing agents (black carbon, organic carbon, and dust) have positive forcing effects (a warming effect). For instance, brown clouds are formed over large Asian urban areas [107] and have a warming effect. The forcing and feedback effects of aerosols have been clarified [101] by separating direct, indirect, semi-direct and surface albedo effects due to aerosols.

Differing to any natural dust iron-containing mineral aerosol, the ISA aerosol does not contain any residual mineral components such as Fe_2O_3 minerals known as strong radiation absorbers. Previous studies have shown that iron oxides are strong absorbers at visible wavelengths and that they can play a critical role in climate perturbation caused by dust aerosols [108, 109]. As the primary ochre colored aerosol particles emitted by the ISA (method I, see chapter 7) have small diameters of <0.05 μm and are made of pure FeOOH, they become easily and rapidly dissolved within the plume of acidic flue gas. The ISA FeOOH aerosol is emitted with the parallel generated flue gas plumes containing SO_2 and NO_x as sulfuric and nitric acid generators. ISA stays up for weeks within the troposphere before precipitating on the ocean or land surfaces. Due to their small diameter and high

surface area, the aerosol particles will immediately react with HCl, generated as reaction product between sea-salt aerosol and the flue gas borne acids. The reaction product is an orange colored $FeCl_3$ aerosol: ISA. During day time the sunlight radiation bleaches ISA into $FeCl_2$ and °Cl; at the night time the re-oxidation of ISA plus HCl absorption generates ISA again. The $FeCl_2$ aerosol particles are colorless at low humidity; pale green during high humidity episodes. The day time bleaching effect reduces the radiation absorption of ISA to much lower levels comparing to oxides such as Fe_2O_3.

Hygroscopic salt aerosols act as cloud condensation nuclei (CCN) [110, 111]. ISA particles are hygroscopic. High CCN particle concentrations have at least three different cooling effects [112, 113]. Each effect triggers the atmospheric cooling effect by a separate increase of earth reflectance (albedo) [114]:

- cloud formation (even at low super saturation);
- formation of very small cloud droplets, with an elevated number of droplets per volume, which causes elevated cloud whiteness;
- extending the lifetime of clouds, as the small cloud droplets cannot coagulate with each other to induce precipitation fall.

Figure 1 illustrates this albedo change due to ISA-CCN particles.

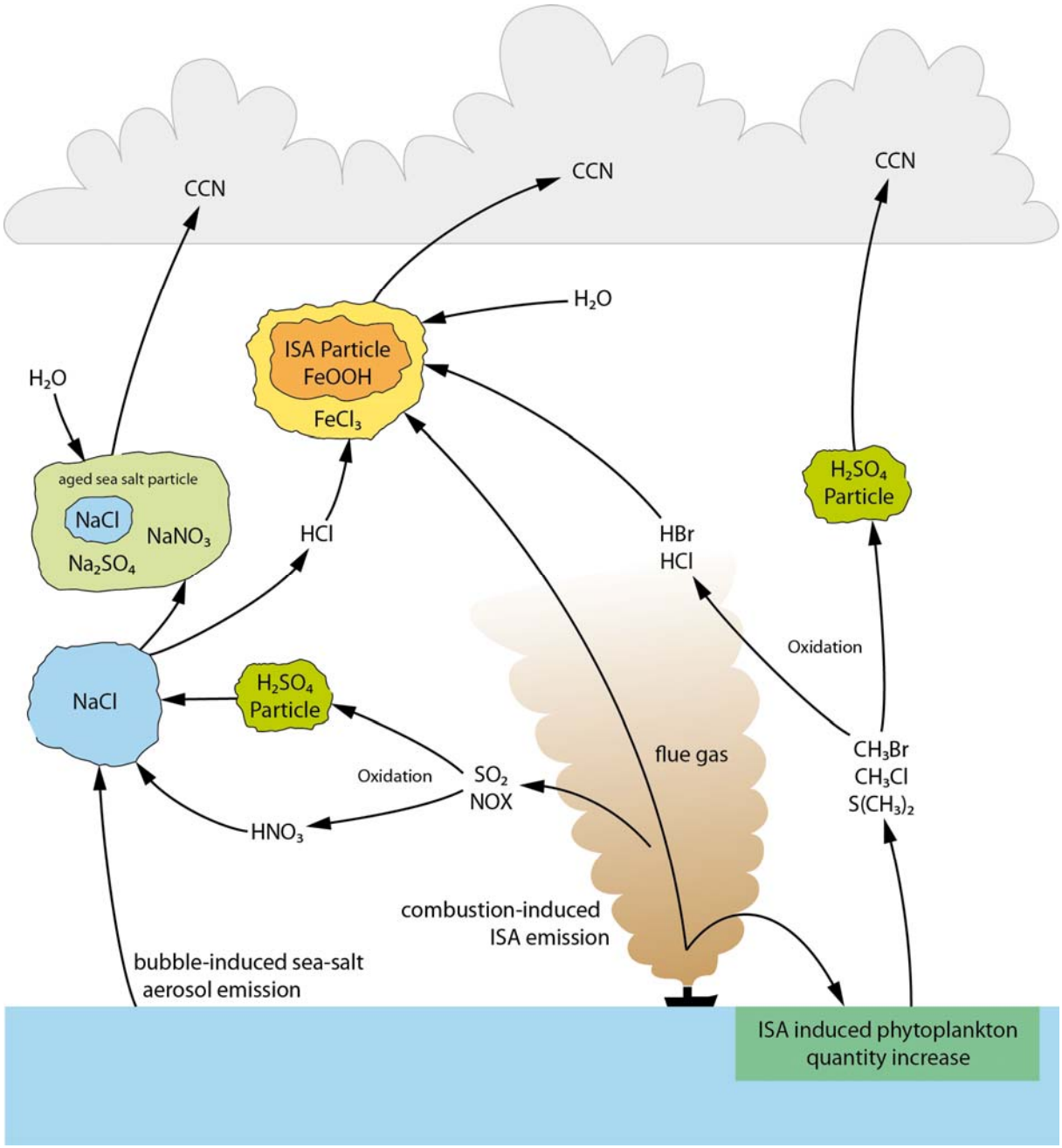

Figure 1. Process of tropospheric cooling by direct and indirect increasing of the quantity of different cloud condensation nuclei (CCN) inducing albedo increase by cloud formation at low supersaturation, cloud whitening and cloud life elongation

Additional to climate cooling effects, CCN-active aerosols might induce a weakening of tropical cyclones. The cooling potential of the ocean surface in regions of hurricane genesis and early development, by cloud whitening potential [115] shall be casual. Further effects such as delayed development, weakened intensity, early dissipation, and increased precipitation have been found [116, 117].

2.2. Oxidation of methane and further GHGs

Currently, methane (CH_4) in the troposphere is destroyed mainly by the hydroxyl radical °OH. From 3 to 4% CH_4 (25 Tg yr^{-1}) [118, 119] are oxidized by °Cl in the troposphere, and larger regional effects are predicted: up to 5.4 to 11.6% CH_4 (up to 75 Tg yr^{-1}) in the Cape Verde region [120] and ~10 to >20% of total boundary layer CH_4 oxidation in some locations [121]. According to Blasing [99, 122, 123] the increase of the GHG CH_4 since 1750 induced a radiative forcing of about +0.5 Watts per square meter. The research results of Wittmer et al. [124-127] demonstrated the possibility to reduce the CH_4 lifetime by the ISA method significantly. According to Anenberg et al. [128] the health effects of the combination of increased CH_4 and NO_x induced O_3 levels in combination with an increase of black carbon are responsible for tens of thousands deaths worldwide.

Any increase in the °Cl level will significant elevate the depletion rate of CH_4 and further volatile organic compounds (VOCs) as well as ozone (O_3) and dark carbon aerosol as described in sections 2.3 and 2.4.

Absorption of photons by semi-conductor metal oxides can provide the energy to produce an electron-hole pair able to produce either a reduced or an oxidized compound. At suitable conditions, UV and visible light can reduce a variety of metal ions in different environments [129-131]. Photo-reduced metal compounds may further act as effective chemical reductants [132, 133] and the oxidized compounds such as hydroxyl radicals or chlorine atoms, can further act as effective oxidants. Zamaraev et al. [134] proposed the decomposition of reducing atmospheric components such as CH_4 by photolytically induced oxidation power of the oxides of iron, titanium and some further metal oxide containing mineral dust components. In this sense Zamaraev designated the dust generating deserts of the globe as *"kidneys of the earth*" [135] and the atmosphere as a "*giant photocatalytic reactor*" where numerous physicochemical and photochemical processes occur [134]. Researches have proposed giant photocatalytic reactors to clean the atmosphere of several GHGs, such as N_2O [136], CFCs and HCFCs [137] and even CO_2 after direct air capture [138], as almost all GHGs can be transformed or destroyed by photocatalysis [139, 140].

Oeste suggested [141] and Wittmer et al. confirmed [124-127] the emission of CH_4 depleting chlorine atoms. This can be induced by 3 ways: sunlight photo reduction of Fe(III) to Fe(II) from $FeCl_3$ or FeOOH containing salt pans, from $FeCl_3$ or FeOOH-containing sea spray aerosols and from pure FeOOH aerosol in contact with air containing ppbv amounts of HCl. Because the H abstraction from the GHG CH_4 as the first oxidation step by °Cl is at least 16 times faster compared to the oxidation by °OH, which is the main CH_4 oxidant acting in the ISA-free atmosphere, concentration of CH_4 can be significantly reduced by ISA emission. Figure 2 illustrates by a simplified chemical reaction scheme this climate cooling mechanism by the ISA method: a direct cooling of the troposphere by CH_4 oxidation induced by ISA

particles.

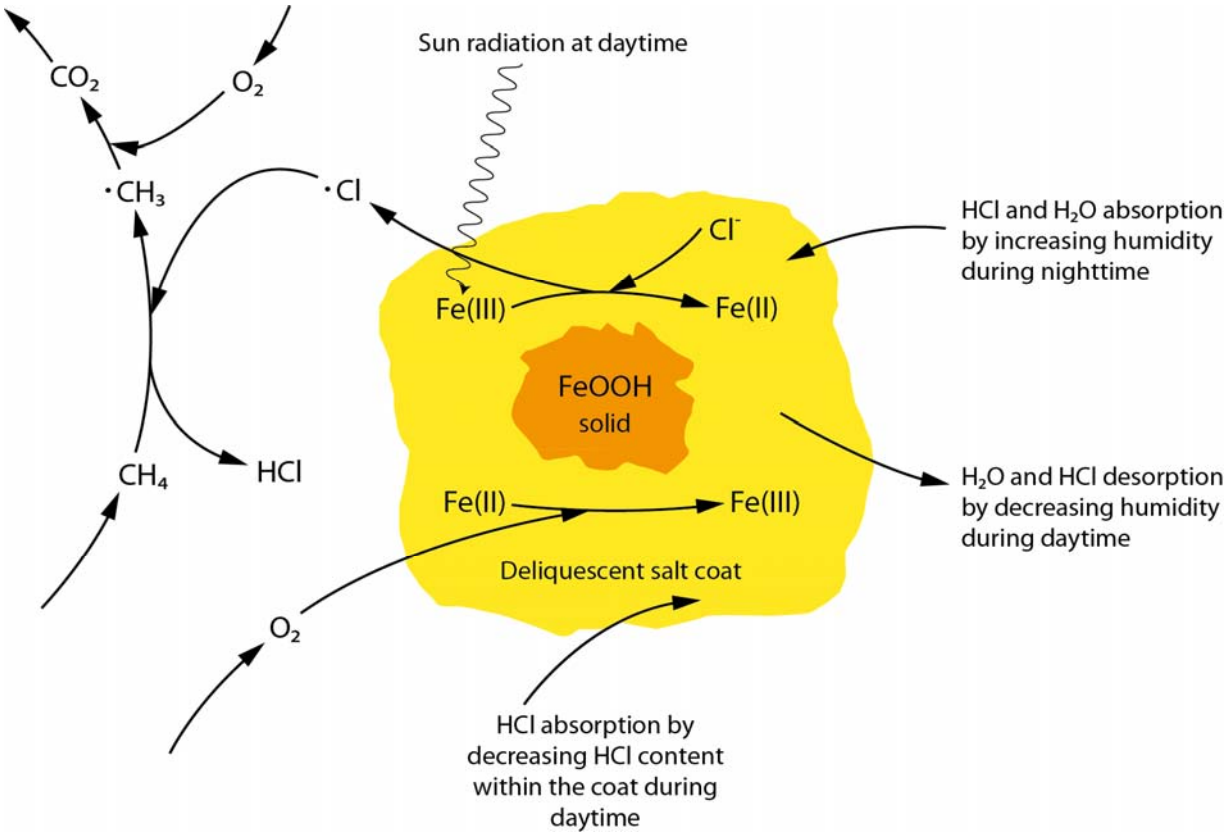

Figure 2. simplified chemical reaction scheme of the generation of chlorine radicals by iron salt aerosols under sunlight radiation and the reaction of the chlorine radicals with atmospheric methane.

At droplet or particle diameters below 1 µm, between 1 µm and 0,1 µm, contact or coagulation actions between the particles within aerosol clouds are retarded [112, 142-144]. Otherwise the aerosol lifetime would be too short to bridge any intercontinental distance or arrive in polar regions. That reduces the possible Cl^- exchange by particle contact. But absorption of gaseous HCl by reactive iron oxide aerosols resulting in Fe(III) chloride formation at the particle surfaces is possible [127]. Gaseous HCl and further gaseous chloro-compounds are available in the troposphere: HCl (300 pptv above the oceans and 100 pptv above the continents) [118], $ClNO_2$ (up to 1500 pptv near flue gas emitters) [145, 146] and CH_3Cl (550 pptv remote from urban sources) [147, 148]. By or after sorption and reactions such as photolysis, oxidation, and reduction, any kind of these chlorine species can induce chloride condensation at the ISA particle surface. Acid tropospheric aerosols and gases such as H_2SO_4, HNO_3, oxalic acid, and weaker organic acids further induce the formation of gaseous HCl from sea-salt aerosol [149-151]. Since 2004, evidence and proposals for possible catalyst-like sunshine-induced cooperative heterogeneous reaction between Fe(II),

453 Fe(III), Cl^-, °Cl, and HCl fixed on mineral dust particles and in the gaseous phase on the CH_4
454 oxidation are known [127, 141]. Further evidence of sunshine-induced catalytic cooperation
455 of Fe and Cl came from the discovery of °Cl production and CH_4 depletion in volcanic
456 eruption plumes [152, 153]. Wittmer et al. presented sunshine-induced °Cl production by iron
457 oxide aerosols in contact with gaseous HCl [127]. Further evidence comes from °Cl found in
458 tropospheric air masses above the South China Sea [154]. It is known that the troposphere
459 above the South China Sea is often in contact with Fe-containing mineral dust aerosols (~18
460 g m^{-2} a^{-1}) [155], which is further evidence that the Fe oxide-containing mineral dust aerosol
461 might be a source for the °Cl content within this area.
462 HCl, water content and pH within the surface layer of the aerosol particles depend on the
463 relative humidity. Both liquid contents, H_2O and HCl, grow with increasing humidity [156]. In
464 spite of growing HCl quantity with increasing humidity, pH increases, due to decreasing HCl
465 concentration within the surface layer. Hence, since the radiation induced °Cl production
466 decreases with decreasing pH, the °Cl emission decreases in humid conditions [127]. Under
467 dry conditions, even sulfate may be fixed as solid Na-sulfate hydrates. Solubilized sulfate
468 slightly inhibits the iron induced °Cl production [157].
469 Night or early morning humidity produces similarly the maximum chloride content on the
470 liquid aerosol particles surface. During day time, the humidity decrease induces ISA
471 photolysis and Cl^- conversion to °Cl production by decreasing water content and pH. The ISA
472 particle surface layer comes to Cl^- minima levels during after noon hours. In the continental
473 troposphere with low sea salt aerosol level, these effects enable the pure ISA iron oxide
474 aerosol particles to coat their surface with chloride solution at night and to produce chlorine
475 atom emission at daytime.
476 Freezing has different effects on the primary wet ISA particles. Changing by CCN action to
477 cloud droplets with solubilized chloride and iron content and when arriving to freezing
478 conditions, the frozen ice is covered by a mother liquor layer with elevated concentration of
479 both iron and chlorine. Some acids such as HCl do not decrease the mother liquor pH
480 proportional to concentration and the behavior of the ice surfaces, grown from low salt
481 content water, are different from high salt content water, thus the different kinds of ISA
482 behave differently [158-160]. Direct measurements of molecular chlorine levels in the Arctic
483 marine boundary layer in Barrow, Alaska, showed up to 400 pptv levels of molecular chlorine
484 [161]. The Cl concentrations fell to near-zero levels at night but peaked in the early morning
485 and late afternoon. The authors estimated that the Cl radicals oxidized on average more CH_4
486 than hydroxyl radicals, and enhanced the abundance of short-lived peroxy radicals.
487 Further investigations have to prove how the different types of ISA particles behave in clouds
488 below the freezing point or in the snow layer at different temperatures: the primary salt-poor

Fe-oxide, the poor $FeCl_3$-hydroyzed and the $FeCl_3$-NaCl mixture, because the °Cl emission depends on pH, Fe and Cl concentration.

Additional to iron photolysis, in a different and day-time independent chemical reaction, iron catalyzes the formation of °Cl or Cl_2 from chloride by tropospheric ozone [162]. Triggering the CH_4 decomposition, both kinds of iron and chlorine have a cooperative cooling effect on the troposphere: less GHG CH_4 in the atmosphere reduces the GH effect and allows more outgoing IR heat to the outer space [163].

These reactions had been active during the glacial period: Levine et al. [164] found elevated $^{13}CH_4$ / $^{12}CH_4$ isotope ratios in those Antarctic ice core segments representing the coldest glacial periods. The much greater °Cl preference for $^{12}CH_4$ oxidation than $^{13}CH_4$ oxidation than by the °OH is an explanation for this unusual isotope ratio. Additional evidence gives the decreased CH_4 concentration during elevated loess dust emission epochs [165].

As shown in more detail in the next section 2.3, ISA produces °Cl and much more hydrophilic °OH and ferryl as further possible CH_4 oxidants by the Fenton and photo-Fenton processes [75]. To gain the optimal reaction conditions within the heterogeneous gaseous / liquid / solid phase ISA system in the troposphere the CH_4 reductant and the oxidant (Fenton and photo-Fenton oxidant) have to be directed in a way, that oxidant and reductant can act within the identical medium.

As seen on table 1, according to the CH_4 Henry's law constant the preference of the 1.8 ppm tropospheric CH_4 is undoubtedly the gaseous phase. °Cl has also a preference for the gaseous phase.

Table 1: the Henry's law constants [166] and daylight stability for different gaseous or vaporous components reacting with or produced by ISA in the troposphere

Substance	Henry's law constant (mol m^{-3} Pa^{-1})	Stability against tropospheric day light (+ stable; - unstable)
CH_4	1.4×10^{-5}	+
°Cl	2.3×10^{-2}	+
Cl_2	9.2×10^{-4}	-
HCl	1.5×10^{1}	+
HOCl	6.5	-
°OH	3.8×10^{-1}	+
H_2O_2	8.3×10^{2}	-

Iron exists at least in part as Fe(III) during nighttime and at least in part as Fe(II) during daytime. The CH_4 oxidation by °Cl and °OH is restricted to the daytime as during night hours °Cl and °OH recombine fast to Cl_2, HOCl, and H_2O_2 in the dark [167]. During daylight hours, these recombination products photolyze again by regeneration of the radicals. But even

during day time these radicals and their recombination products co-exist due to the cycling between °Cl, °OH, Cl_2, HOCl, and H_2O_2. This cycling is activated by sunlight photolysis and radical recombination reactions [167, 168].

As we learn from Henry's law constants in Table 1 the oxygen species °OH and H_2O_2 have a much higher tendency to stay in the liquid phase than the chlorine species °Cl and Cl_2. Cl_2 has the tendency to react with water of neutral pH by producing HOCl. But the pH values of ISA, especially if ISA is emitted as acid flue gas plumes are lower than 3. Within this acidic region the tendency of HOCl generation from Cl_2 decreases to very low values and even at those humidity levels when the ISA particles become deliquescent the majority of the activated chlorine species will be localized in the gaseous phase containing CH_4, not in the liquid phase.

But °OH may leave the condensed phase into the gaseous phase at favorable circumstances into the gaseous phase [169] and may contribute there to the oxidation of CH_4 during clear dry conditions without liquid phase at the Fe(III) surfaces.

Comparably to the water-soluble Ammonia (5.9×10^{-1}), °OH has a similar Henry's law constant. Therefore °OH has the tendency to stay within hydrous phases during humid conditions. This tendency is 16 times lower for °Cl. This property is combined with the 16 times higher reactivity in comparison to °OH. At an equal production of °Cl and °OH, the reaction of °Cl with CH_4 has a probability of up to 250 times (16 x 16) that of the reaction of °OH with CH_4 when the ISA particles are wet and 16 times that of °OH with CH_4 when the ISA particles are dry. The probability of CH_4 oxidation by ISA derived °Cl against ISA derived °OH, may be restricted by the pH increase tendency within ISA during humid episodes (decreased °Cl generation on ISA with rising pH), to values fluctuating between the extremes 1 and 250. Independently of the kind of oxidants produced by ISA – during dry, clear sky, and sunshine episodes - the ISA deriving oxidants produce maximum oxidant concentrations within the CH_4-containing gaseous phase, producing optimum CH_4 depletion rates.

The °Cl reactivity on most VOC other than CH_4 is at least one order of magnitude higher than that of °OH [170]. Halogen organics such as dichloromethane [171] as well as the environmental persistent and bioaccumulating perfluoro organics such as perfluoro octane sulfonate may be depleted by sunlit ISA [172].

2.3. Oxidation of organic aerosol particles containing black and brown carbon

Black carbon in soot is the dominant absorber of visible solar radiation in the atmosphere [173]**.** Total global emission of black carbon is 7.5 Mt yr^{-1} [174]**.** Direct atmospheric forcing of atmospheric black carbon is +0.7 W m^{-2} [174]**.** Above its climate relevance black carbon soot induces severe health effects [128]**.**

Andreae & Gelencsér [175] defined the differences between the carbons: black carbon contains insoluble elemental carbon, brown carbon contains at least partly soluble organic carbon. Black carbon contains as well additional extractable organics of more or less volatility and/or water-solubility [175, 176]..

Black and brown carbonaceous aerosols have a positive radiative forcing (warming effect) on clouds [177] as seen in sub-section 2.1, and also after deposition on snow, glaciers, sea ice or on the polar regions, as the albedo is reduced and the surface is darkened [178]. One of the most effective methods of slowing global warming rapidly on short-term is by reducing the emissions of fossil-fuel particulate black carbon, organic matter and reducing of tropospheric ozone [179].

Both aerosol types have adverse effects to health (human, animal, livestock, vegetal) and reducing its levels will save lives and provide many benefits [180].

Thus any tropospheric lifetime reduction of both dark carbons would gain cooling effects and further positive effects.

Both carbons are characterized by aromatic functions. The black carbons contain graphene structures; the brown ones have low-molecular weight humic-like aromatic substances (HULIS). HULIS derive from tarry combustion smoke residues and/or from aged secondary organic aerosol (SOA). The source of SOA are biogenic VOCs such as terpenes [181]. HULIS contain polyphenolic red-ox mediators such as catechol and nitro-catechols [182-185].

The polyphenolic HULIS compounds are ligands with very strong binding to iron. Rainwater-dissolved HULIS prevent Fe(II) from oxidation and precipitation when mixing with seawater [186]. Wood smoke derived HULIS nano-particles penetrate into living cell walls of respiratory epithelia cells. After arrival in the cells the HULIS particles extract the cell iron from the mitochondria by formation of HULIS iron complexes [187].

Beside iron, other metals such as manganese and copper have oxygen transport properties which improve the oxidation power of H_2O_2 by Fenton reactions generating °OH [188]. H_2O_2 is a troposphere-borne oxidant [189].

Polyphenolic and carboxylate ligands of HULIS enhance the dissolution of iron oxides. These ligands bind to un-dissolved iron oxides [75].

Iron and catechols are both reversible electron shuttles:

$$Fe^{2+} \leftrightarrow Fe^{3+} + e \qquad \text{(Eq. 1);}$$

$$\text{catechol} \leftrightarrow \text{quinone} + 2e \qquad \text{(Eq. 2).}$$

The HULIS – iron connection enhances the oxidative degradation of organic compounds such as aromatic compounds [75].

Oxidant generation by reaction of oxidizable dissolved or un-dissolved metal cations such as Fe(II), Cu(I) and Mn(II) with H_2O_2 had first been discovered for instance for Fe(II) in 1894

[190]. Since then these reactions are known as Fenton reactions. Mechanisms and generated oxidants of the Fenton reactions are still under discussion.

According to the participating metal ligand oxidants such as °OH, $Fe(IV)O^{2+}$ (= Ferryl), °Cl, $°SO_4^-$, organic peroxides and quinones may appear [191].

According to Barbusinsky et al. the primary reaction intermediate from Fe^{2+} and H_2O_2 is the adduct $\{Fe(II)H_2O_2\}^{2+}$ which is transformed into the ferryl complex $\{Fe(IV)(OH)_2\}^{2+}$. The latter stabilizes as $\{Fe(IV)O\}^{2+}$ + H_2O. Reductants may also react directly with $\{Fe(IV)O\}^{2+}$ or after its decomposition to Fe^{3+} + °OH + OH- by °OH. Fe^{3+} reacts with H_2O_2 to Fe^{2+} via $°O_2H$ development; the latter decays into O_2 + H_2O.

Light enhances the Fenton reaction effectiveness. It reduces Fe^{3+} to Fe^{2+} by photolysis inducing °OH or °Cl generation, the latter in the case of available Cl^-, which reduces the H_2O_2 demand [192, 193].

This process is illustrated by figure 3.

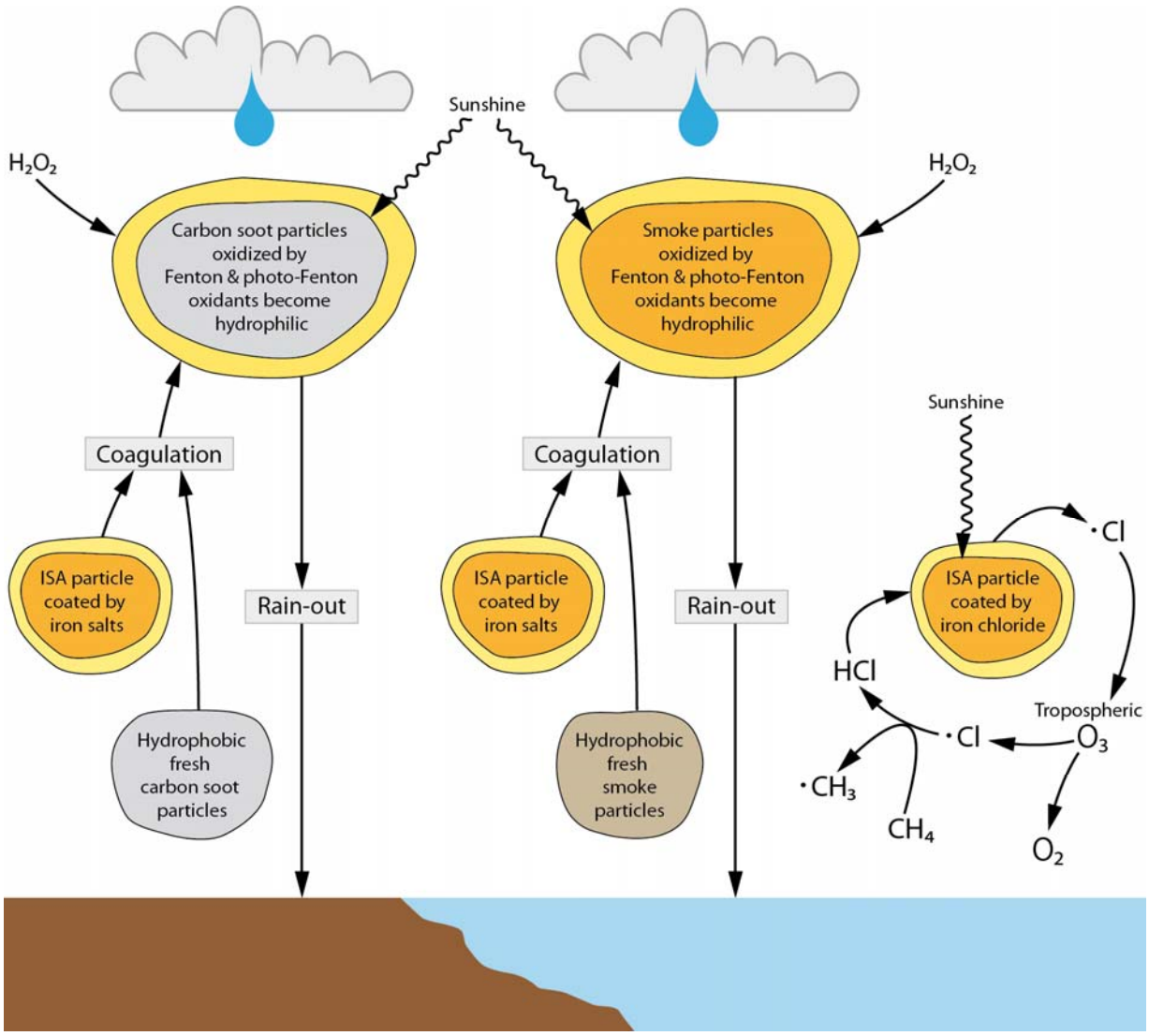

Figure 3. Schematic representation of the cooling of the troposphere, by inducing the decrease of ozone and organic aerosol particles such as soot and smoke.

The Fenton reaction mechanism is dependent on pH and on the kinds of ligands bound to the Fenton metal. The reaction mechanism with oxidants of SO_4^{2-}, NO_3^-, Cl^- and 1,2-dihydroxy benzene ligands had been studied [194].

In biological systems, 1,2-dihydroxy benzenes (catecholamines) regulate the Fenton reaction and orient it toward different reaction pathways [195].

Additionally, the fractal reaction environments like surface rich black and brown carbons and ISA are of considerable influence on the Fenton reaction. By expanding the aqueous interface, accelerations of the reaction velocity up to three orders of magnitude had been measured [196]. This may be one of the reasons why iron-containing solid surfaces made of fractal iron oxides, pyrite, activated carbon, graphite, carbon nanotubes, vermiculite, pillared clays, zeolites have been tested as efficient Fenton reagents [197-199].

Even the oxidation power of artificial Fenton and photo-Fenton systems is known to be high enough to hydroxylate aliphatic C-H bonds, inclusive CH_4 hydroxylation to methanol [200-202].

But the HULIS itself becomes depleted by the Fenton oxidation when it remains as the only reductant [195].

Like HULIS or humic substances, the different kinds of black carbons act as red-ox mediators due to their oxygen functionalities bound to the aromatic hexagon network such as hydroxyl, carbonyl, and ether [203, 204]. These functionalities act similarly as hydroquinone, quinone, aromatic ether, pyrylium and pyrone at the extended graphene planes as electron acceptor and donor moieties. Soot also possesses such red-ox mediator groups [205, 206]. Again these are ligands with well-known binding activity on iron compounds. Their difference to the HULIS ligands is that they are attached to stacks of aromatic graphene hexagon networks instead of mono- or oligo-cyclic aromatic hexagons of HULIS. As well as the HULIS red-ox mediator ligands these hydroxyl and ketone groups transfer electrons from oxidants to reductants and vice versa. Like the HULIS – iron couple, the black carbon - iron couple enhances the red-ox mediation above the levels of every individual electron shuttle [207-209]. Accordingly, any ISA doping of black carbons generates effective oxidation catalysts [210, 211].

Lit by sunlight the ISA doped soot represents an oxidation catalyst to adsorbed organics producing its own oxidants by the photo-Fenton reaction. In spite of the higher chemical stability of the graphene network of soot compared to HULIS soot, by wet oxidation further oxygen groups are fixed to the soot graphene stacks [212] increasing soot's hydrophilic property, which is necessary to arrange its rain-out. The hydroxyl radical attack resulting from the photo Fenton reaction at last breaks the graphene network into parts [213, 214]. Photo-

Fenton is much more efficient in °OH generation than Fenton, because Fe(III) reduction as regeneration step occurs by Fe(III) photo reduction, rather than consuming an organic reductant.

The oxidized hydrophilic carbon particles are more readily washed out of the atmosphere by precipitation [215]. ISA accelerates this oxidation process as the iron-induced Fenton and photo-Fenton reaction cycles produce hydroxyl and chlorine radical oxidants, speeding up the soot oxidation.

Fe(III) forms colored complexes with hydroxyl and carboxylic hydroxyl groups too, particularly if two of them are in 1,2 or 1,3 position, such as in oxalic acid. The latter belong to the group of dicarboxylic acids known to be formed as oxidation products from all kind of volatile, dissolved or particular organic carbons in the atmosphere [216]. Dicaboxylate complexes with iron are of outstanding sensitivity to destruction by photolysation [217-220]: photolysis reduces Fe(III) to Fe(II) by producing H_2O_2 and oxidation of the organic complex compounds. Then Fe(II) is re-oxidized to Fe(III) by H_2O_2 in the Fenton reaction by generation of °OH [221]. According to their elevated polarity oxidation products containing hydroxyl and carboxyl groups have increased wettability, are more water soluble and are thus rapidly washed out from the atmosphere.

Due to their elevated reactivity compared to CH_4 the gas phase, oxidation of airborne organic compounds by ISA-generated °OH or °Cl is enhanced. By eliminating black and brown carbon aerosols, ISA contributes to global warming reduction and to decreasing polar ice melting by surface albedo reduction caused by black-carbon snow contamination [173, 222].

The generation of ISA by combusting fuel oil with ferrocene or other oil soluble iron additives in ship engines or heating oil burners has additional positive effects, because soot is catalytically flame-oxidized in the presence of flame-borne ISA (detailed in chapter 6) as a combustion product of the iron additive [223, 224].

2.4. Tropospheric Ozone depletion by ISA

An additional GHG is the tropospheric ozone [179]. Carbon dioxide is the principal cause of GW and represents $^2/_3$ of the global radiative forcing, but long lived methane and short lived tropospheric ozone are both GHGs and respectively responsible of the 2nd and 3rd most important positive radiative forcing.

According to Blasing [99, 122, 123] tropospheric O_3 has an atmospheric forcing of +0.4 Watt per square meter. Any direct depleting action of tropospheric O_3 by the ISA-induced °Cl is accompanied by an indirect emission decrease of O_3 as the reduction of CH_4 and further VOC by the ISA method decreases the O_3 formation [225].

Reactive halogen species (mainly Cl, Br) cause stratospheric ozone layer destruction and thus the “ozone layer hole”. Tropospheric ozone destruction by reactive halogen species is

also a reality [226]. Since long, °Cl and °Br are known as catalysts for O_3 destruction in the Stratosphere [227]. Investigations both in laboratory and nature have shown that °Br is a much more effective catalyst of ozone depletion within the troposphere than °Cl [161, 228, 229].

As discussed at the end of chapter 2.6 clear evidence exists, that the ozone depleting "bromine explosions" known as regular phenomenons developing from cost-near snow layers at sunrise in the polar spring [230, 231] are likely to be induced by the photolysed precipitation of iron containing dust. According to Pratt, bromide enriched brines covering acidified snow particles are oxidized by photolyzation to °Br.

In coastal areas of both the northern and southern Polar Regions during springtime, inert halide salt ions (mainly Br^-) are converted by photochemistry into reactive halogen species (mainly Br atoms and BrO) that deplete ozone in the boundary layer to near zero levels [232]. During these episodes called "*tropospheric ozone depletion events"* or *"polar tropospheric ozone hole events*" O_3 is completely destroyed in the lowest kilometer of the atmosphere on areas of several million square kilometers and has a negative climate feedback or cooling effect [233].

In the tropics, halogen chemistry (mostly Br and I) is also responsible for a large fraction (~30%) of tropospheric ozone destruction [120, 234] and up to 7% of the global methane destruction is due to chlorine [121, 235]. It has been estimated that 25% of the global oxidation of CH_4 occurs in the tropical marine boundary layer [236]. A one-dimensional model has been used to simulate the chemical evolution of air masses in the tropical Atlantic Ocean [120] and to evaluate the impact of the measured halogens levels. In this model, halogens (mostly Br and I) accounted for 35−40% of total tropospheric O_3 destruction while the Cl atoms accounted for 5.4−11.6% of total CH_4 sinks. Sherwen et al. [226] estimate at -0.066 W m^{-2} the radiative forcing reduction due to O_3 pre-industrial to present-day changes.

The ISA-induced increase of °Br concentration at sea-salt containing tropospheric conditions has been confirmed [125]. This establishes ISA as part of an ozone-depleting reaction cycle and additional cooling stage. This depletion effect of the GHG tropospheric ozone is worth noting.

2.5. ISA induced phytoplankton fertilization albedo increase (by enhancing DMS-emissions) and CH_4 oxidation efficiency (by increasing MC- and DMS-emissions)

One of the largest reservoirs of gas-phase chlorine is the about 5 Tg of methyl chloride (MC) in the Earth's atmosphere [147]. Methyl-chloride is released from phytoplankton [237] and from coastal forests, terrestrial plants and fungi [238].

Dimethylsulfide (DMS) is a volatile sulfur compound that plays an important role in the global sulfur cycle. Through the emission of atmospheric aerosols, DMS may control climate by

influencing cloud albedo [239].

Currently, researchers [240] estimate that 28.1 (17.6–34.4) Tg of sulfur in the form of DMS are transferred annually from the oceans into the atmosphere.

Ocean acidification has the potential to exacerbate anthropogenic warming through reduced DMS emissions [241]. On the contrary, increased emissions of DMS and MC into the troposphere are a consequence of the ISA-induced phytoplankton growth and DMS + MC release into the troposphere. DMS is oxidized in the troposphere to sulfuric and sulfonic acid aerosols, which are highly active CCN. This process enhances the direct ISA cooling effect according to cooling section 2.1 [239].

In contact with this acidic aerosol with sea spray aerosol, sulfate and sulfonate aerosols are formed and gaseous HCl is produced. Sulfate aerosols are known to have a negative radiative forcing (a cooling effect) [242].

A further HCl source is the oxidation of MC. Both effects induce the tropospheric HCl level to rise. According to cooling stage described in section 2.2, with the increased HCl level, additional chlorine atoms are produced by reaction with ISA. This effect further accelerates the CH_4 oxidation and its removal from the atmosphere, reducing its radiative forcing.

2.6. Oxidation of CH_4 and further GHGs by sunlit solid surfaces

Mineral aerosol particles adhere strongly to sunlit, dry and solid surfaces of rocks and stones. A well-known remnant of the dust deposit in rock or stone deserts and rocky semi-arid regions is the orange, brown, red or black colored “Desert Varnish” coat covering stones and rocks. The hard desert varnish is the glued together and hardened residue of the primary dust deposit. Daily sun radiation and humidity change, as well as microbe and fungi influence grows up the varnish changing the primary aerosol deposit [243] by photolytic Fe(III) and Mn(IV) reduction during daytime and night time oxidation of Fe(II) and Mn(II). The oxidation is triggered further by Mn and Fe oxidizing microbes adapted to this habitat [244, 245]. Desert varnish preserves the Fe and Mn photo reduction ability of the aerosol: lit by light the varnish can produce chlorine from chloride containing solutions [246]. The photo, humidity, and microbial induced permanent Fe and Mn valence change between night and day [247] accompanied by adequate solubility changes seem to trigger the physico-chemical hardening of every new varnish layer.

The varnish is composed of microscopic laminations of Fe and Mn oxides. Fe plus Mn represent about $^1/_5$ of the varnish. Meanwhile $^4/_5$ of the laminations are composed of SiO_2, clay and former dust particles. Dominant mineral is SiO_2 and/or clay [248, 249]. There is little doubt that desert varnish can build up even from pure iron oxides or iron chloride aerosol deposits such as ISA. The optimum pH to photo-generate the methane oxidizing chlorine atoms from ISA is pH 2 [124]. Established by the gaseous HCl content of the troposphere

[118], a pH drop to pH 2 at the varnish surface is possible on neutral alkaline-free surfaces such as quartz, quartzite and sandstone. The humidity controlled mechanism acting between gaseous HCl and HCl dissolved in the liquid water layer absorbed on the solid iron oxide surface of ISA particles, as explained in the section 2.2, acts at the varnish surface analogue: a $FeCl_3$ stock can pile up by Fe(II) oxidation and humidity-triggered HCl absorption during night time. The $FeCl_3$ stock at the varnish surface is consumed during daytime by photolytic Fe(II) and chlorine atom generation.

ISA aerosol particles emit HCl during dry conditions. Like oxidic ISA, desert varnish absorbs H_2O and HCl from the atmosphere gathering it during night time as surface-bound H_2O, OH^-, and Cl^- coat. During sunlit day time, chloride and water desorbs from Fe(III) as °Cl, °OH and H_2O, leaving Fe(II) in the varnish surface. The surface Fe(II) (and Mn(II)) is bound by oxygen bridges to the varnish bulk of Fe(III) (and Mn(IV)); may be like the combination of Fe(II) and Fe(III) within magnetite. During night time the Fe(III) (and Mn(IV)) surface coat is regenerated by microbial and/or abiotic oxidation with O_2. It is worth mentioning, that desert varnish can exist only within dry regions.

Figure 4 illustrates the interactions of ISA at the phase borders of tropospheric aerosols, ocean surface, and dry solid surfaces.

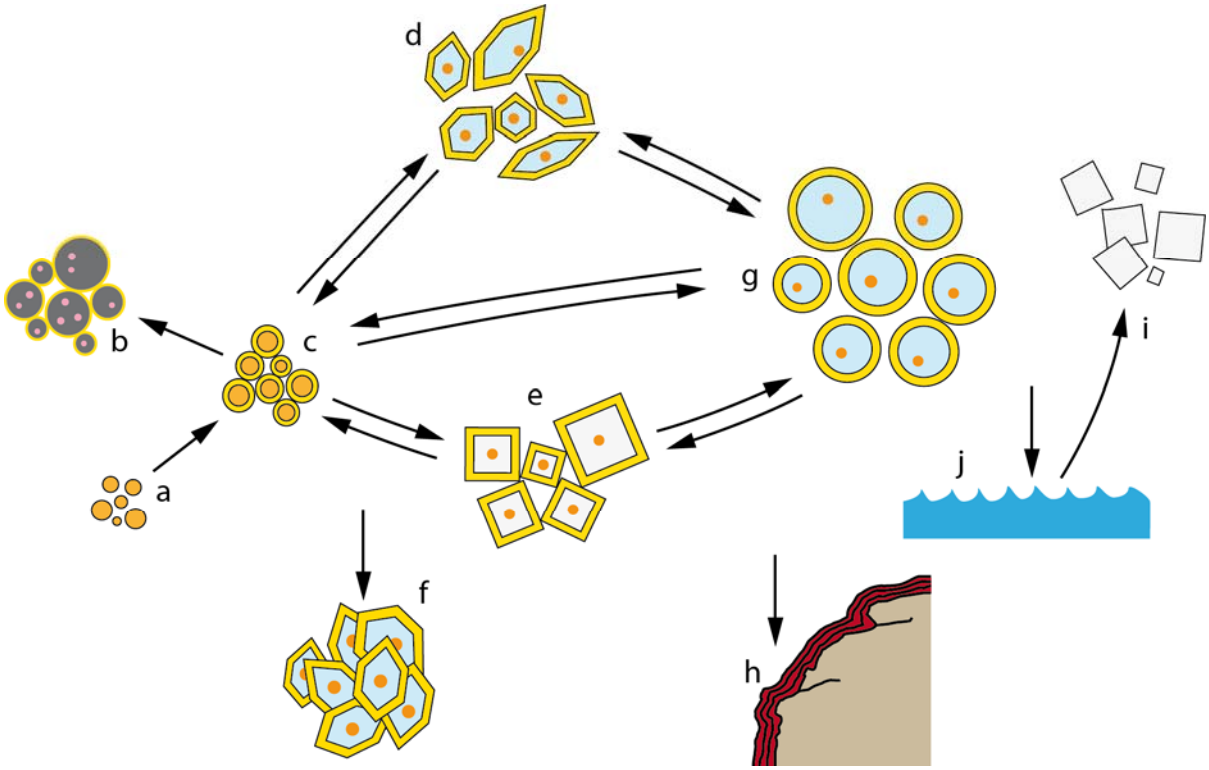

Figure 4. Schematic representation of iron salt aerosols interactions with different solid surfaces:

Primary ISA precursor FeOOH particles (a) react with gaseous HCl by generation of ISA as $FeCl_3$ coated on FeOOH particles (c).

Coagulation, condensation and chemical reaction with particles and vapors produce different kinds of liquid and/or solid ISA variants and sediments:
(b) hydrolyzed $FeCl_3$ coated on soot and/or HULIS particles
(d) hydrolyzed $FeCl_3$ coated on ice crystals
(e) hydrolyzed $FeCl_3$ coated on salt crystals
(f) hydrolyzed $FeCl_3$ coated on ice crystals of snow layers (ISA sediment)
(g) hydrolyzed $FeCl_3$ dissolved in cloud droplets
(h) $FeCl_3$ hydrolysate residue on desert varnish (ISA sediment)
(j) hydrolyzed $FeCl_3$ as dissolved residue in ocean surface water fertilizes the phytoplankton growth and at last triggers the generation of sulfuric, sulfonic and dicarboxylic acids by emission of DMS, MC and further organics. This activates the tropospheric generation of vaporous HCl by reaction of sea-salt aerosol (i) with the acids. HCl again changes the ISA precursor FeOOH aerosol (a) to ISA (c).

Similar daytime dependent microbial activated abiotic photo-reduction and photo-oxidation reaction cycles are known from aquifer environments [250]. Thus the CH_4 depletion of the former ISA deposits will persist even after change into desert varnish. As explained chapter 2.2 continental HCl (300 pptv above the oceans and 100 pptv above the continents) [118], $ClNO_2$ (up to 1500 pptv near flue gas emitters) [145, 146] and CH_3Cl (550 pptv remote from urban sources) [147, 148] and in deserts chloride salt containing dusts are direct and indirect sources of chloride which could provide desert varnishes with Cl^-.

Furthermore, analogue to ISA deposited on solid desert surfaces, ISA depositions on dry snow, snow cover and ice occurring in permanent snow-covered Mountain regions or within polar and neighboring regions preserves its CH_4 destruction activity during sunlit day, spring, and summer times [161].

The global area of the desert varnish surface does not change with changing dust precipitation rates. It only depends on the precipitation frequency. It grows through desertification and shrinks with increasing wet climate. Until now, quantitative measurements about the specific amount of CH_4 depletion per square meter of desert varnish are not known. Without this data, estimation about its influence on the CH_4 depletion and climate is impossible.

The photochemical actions inducing CH_4 depletion of the desert varnish surfaces resulting from dust precipitation are concurrent with the surfaces of deserts and semi deserts made of sand or laterite soils. Their surface is colored by ochre to red iron oxide pigments. Their iron components should act in principle by the same CH_4 depleting photochemistry such as ISA and desert varnish.

As mentioned in chapter 2.4 the Cl and Br activation by iron photolysis changes after division of the ingredients by freezing or drying of the former homogenous liquid between solid salt-poor ice and liquid brine coat or solid salt and liquid brine coat. This inhomogeneous partition phenomenon of the predominant transformation of aerosol droplets into solid, and vice versa,

applies to snow or salt layers containing a proportion of ISA.

It has been shown that cooling precipitation of the buffering influence of salts such as carbonates, sulfates and chlorides of bromide and chloride rich mother liquors on arctic snow packs or ice particles can minimize their buffering capacity against pH change [160, 231, 251]. Similar mechanisms may act when liquid aerosol particles become solid by drying.

Then, the uptake and contact over time of solid iron-bearing particles and airborne organic and inorganic acids and acid precursors on, or with, ice crystal surfaces may drop the pH of the former alkaline particle surface, into the reaction conditions of the bromide oxidation by iron(III) photo reduction.

According to Kim et al. (Kim et al., 2010) the photogeneration of Fe(III) oxides, proceeding slow at pH 3.5 in bulk solution, becomes significantly accelerated in polycrystalline arctic ice. This effect is accompanied by an acceleration of the physical dissolution of the Fe(III) oxides by freezing ice [252, 253].

The contact of arctic snow layers with iron oxides is confirmed by Kim [252]. Dorfman [254] found recent loess dust sedimentation rates in the Alaskan Arctic Burial Lake of 0.15 mm/a. According to the research results from artificial iron doped salt pans [125] iron salt doped sea-salt aerosols [124] or sea-salt doped iron oxide aerosols or pure iron oxide aerosols in contact with gaseous HCl [127] chloride and bromide in sun-lit surfaces are oxidized to °Cl and °Br by photo-reduced Fe(III) if the pH of the reaction media is 3.5 or lower.

As known from the bromine explosions, they appear on acidified first-year tundra and first-year sea ice snow lit by sunlight [230]. According to Kim et al. and Dorfman et al. the year-old snow layers contain iron(III). This confirms, that sufficient reaction conditions exist to produce bromine explosions by oxidation of iron(III) photoreduction.

Continents have considerable areas where the out flowing water is drained into “endorheic” water bodies and not into the oceans. Endorheic lakes have no outlets other than evaporation and thus dissolved salts and nutrients concentrate over time. Large surfaces of these basins are covered by salt crusts, salt marshes, salty soils, or salt lakes. Most of these areas are situated within desert or semi-desert areas [255]. These salt environments gain iron from precipitating dust or from iron containing brines they have precipitated from. As far as these environments become acidic they oxidize CH_4 by iron photolysis induced °Cl [125].

To summarize the climate-relevant action of ISA within the troposphere according to chapters 2.1-2.6: CH_4, VOC, O_3 and dark carbon aerosol plus cloud albedo, in sum, have a similar effect on the climate warming as CO_2. The ISA method will have significant reductions in CH_4, VOC, O_3 are anticipated by the test results from Wittmer et al. [124-127] and significant reductions in dark carbon aerosol and significant increase in cloud albedo are anticipated by the literature cited. We found no arguments against these statements. This allows the conclusion that only within the troposphere the ISA method should have significant climate

cooling effects.

3. Oceanic natural cooling effects of the iron cycle

3.1. Biotic CO_2 conversion into organic and carbonate carbon

Vegetation uses the oxidative power of organic metal compounds induced by photon absorption, oxidizing water to oxygen and reducing CO_2 by organic carbon generation (photosynthesis by chlorophyll, a green Mg-Porphyrin complex). This assimilation process is retarded by prevailing iron deficiency in the oceans which retards the phytoplankton growth. Meanwhile there is no doubt that ISA-containing dust precipitation fertilizes the phytoplankton which in turn affects the climate [256].

ISA triggers the phytoplankton reproduction and increases the formation of organic carbon from the GHG CO_2 [42]. The vast majority of the oxygen thus formed and only slightly water soluble (11 mg O_2 l^{-1}) escapes into the atmosphere. In contrast, the organic carbon formed remains completely in the ocean, forming the basis of the marine food and debris chain.

From the primary produced phytoplankton carbon only a small fraction arrives at the ocean bottom as organic debris and becomes part of the sediment. Cartapanis et al. [257] and Jaccard et al. [258] found direct evidence that during the glacial maxima, the accumulation rate of organic carbon was consistently higher (50 %) than during inter-glacials. This resulted from the high dust concentrations during the glacial maxima, fertilizing the phytoplankton with ISA.

The build-up of Ca-carbonate shell and frame substances by the calcification process at the ocean surface extracts additional CO_2-C from the troposphere. The bulk of calcification can be attributed to corals, foraminifera and coccolithofores; the latter are believed to contribute up to half of current oceanic $CaCO_3$ production [259].

Both carbon fixation processes increase the removal of the GHG CO_2 and thus contribute to cool the troposphere. The Fe-fertilizing process worked during the ice ages, as the evaluations of Antarctic ice cores show: the minimum CO_2 concentrations and temperatures in the troposphere are connected to the high dust phases [165].

It has been discussed that the alkalinity loss by phytoplankton calcification and $CaCO_3$ loss with phytoplankton debris from the ocean surface is said to produce calcium and alkalinity deficit at the ocean surface [260, 261], producing additional acidification at the ocean surface by CO_2 generation:

$$Ca(HCO_3)_2 \rightarrow CaCO_3 + H_2O + CO_2 \quad \text{(Eq. 3)}$$

At least in part, this acidification is compensated by assimilative generation of organic carbon by CO_2 consumption. Both organic debris and $CaCO_3$ become part of the ocean sediment. But if the organic debris is re-oxidized during its journey downwards, some acidification could

result. Acidification could result too if more CO_2 is absorbed by the ocean, then is assimilated and changed to organic debris. Sedimentation of organic debris and $CaCO_3$, increase both, according to the ISA-induced phytoplankton productivity.

The increasing amount of $CaCO_3$ sedimentation within iron fertilized ocean regions had been discussed by Salter [262]. In a sufficient mixed ocean, alkalinity loss at the surface is more than compensated by the different sources of alkali and earth alkali cations at the ocean bottom and through continental weathering: in the first place these are the mechanisms of alkalinity generated by the ocean water reactions within the ocean sediments and their bed-rock, the oceanic crust. The latter mechanisms are described in more detail in chapters 4.1 – 4.3. The convection of the primary oxic ocean bottom water through the ocean crust generates alkalinity by reduction of sulfate, nitrate and hydrogen carbonate, by dissolution of silicates by reduced humic acids and further by serpentinization of basalt and peridotite silicates [263, 264]. The alkalinity extracted from the oceanic crust keeps mainly positioned in the dark water layers of the ocean basins if the decreased THC is not able to elevate the alkaline extract into the phytoplankton layer in sufficient quantities.

The THC activation by the ISA method is described in the chapters 4.1 – 4.3.

Sudden ISA-induced phytoplankton growth generates increased calcite-shell production. This lowers the Ca-concentration at the ocean surface. Even if the vertical cycling is not fast enough to compensate the Ca-loss at once, or after a small time lag, this does no harm to the phytoplankton growth, because Ca is not essential to it. Just the opposite is true: phytoplankton uses the calcification as a detoxification measure to get rid of calcium ions from their bodies [265]. As a consequence of this effect only the relation between Ca carbonate sequestration and organic carbon sequestration will decrease during the time lag.

By additional direct alkalinity production of the phytoplankton itself, at least parts of the acidity production by the lime shell production may be compensated: ISA-controlled phytoplankton growth induces an increased synthesis of organic sulfur and of chlorine compounds [266], emitted as dimethylsulfide (DMS) and methyl chloride (MC) [267]. Synthesis of organic sulfur and halogen organics as precursors of the volatile DMS and MC emission is realized by the phytoplankton, by reduction of sulfate to organic sulfides, and oxidation of chloride to carbon chlorine compounds. This precursor synthesis excretes equivalent Na^+ and/or Ca^{2+} alkalinity, as Na_2SO_4 reduction/formation to DMS generates Na alkalinity; NaCl oxidation/formation to MC also generates Na alkalinity: cations formerly bound to SO_4^{2-} or Cl^- loose their anions, producing alkalinity. According to [268, 269] the sulfur content of phytoplankton exclusively, exceeds the Ca^{2+}, Mg^{2+}, and K^+ alkaline load of phytoplankton lost with the phytoplankton debris. Only half of the organic carbon assimilated by phytoplankton derives from dissolved CO_2. The other half derives from the ocean water $NaHCO_3$ anion content [270]. The chemical reduction (reduction of HCO_3^- to organic C + O_2

by assimilation of HCO_3^- anions) produces alkalinity as further compensation of the alkalinity loss by calcification. $NaHCO_3$ reduction/formation to organic carbon generates Na alkalinity. The cation previously bound to HCO_3^- loses its anion and produces alkalinity.

These considerations demonstrate that any of the proposed enhanced weathering measures to prevent ocean acidification by increasing the alkalinity [271] might not be necessary if the ISA method is in action and keeps the vertical ocean mixing sufficiently active.

During the down-dripping of the very fine-shaped phytoplankton debris, bacterial oxidation, fish and further food chain links minimize the organic debris up to an order of magnitude [272]. Even the dissolution of the small carbonate debris reduces the carbonate fraction until arriving at the sediment surface. In order to maximize the effect of the ISA method, within the main ISA precipitation regions, the oxidation and dissolution of the organic and carbonate phytoplankton debris during its dripping down through the ocean water column can be reduced. To reach this goal, we suggest farming fixed filter feeders such as mussels and oysters within the ISA precipitation region.

Mussels and oysters produce faeces and so called “Pseudo-faeces” in the shape of rather solid pellets. Compared to the time of sedimentation of the unconditioned phytoplankton debris, this expands the sedimentation time difference between excreted filter feeder faeces and the phytoplankton faeces pellets sedimentation on the ocean floor by an order of magnitude. Bivalve farming would significantly reduce the oxidative and solution loss of phytoplankton debris attack. Mussel and oyster farming are well-known practices which have been employed for long time as a measure to produce protein rich food. They have been proposed as an element of climate engineering [273, 274].

To further optimize the CO_2-C conversion to sediment-bound C the biomass of oysters and mussels including their shells and fixing systems might be periodically dumped into the sediment.

Additional floating supports such as coral habitats, sponges, sea lilies and sea anemones between the mussel supports might complete and again optimize the ISA precipitation areas. The oceanic water deserts can be changed into productive ecosystems and protein sources for an increasing population by these measures, among others, for an optimized CO_2 fixation induced by ISA.

A further proposal in order to maximize the CO_2 fixation induced by ISA is our suggestion to integrate a solution to the plastic waste problem on the ocean surfaces into the ISA method. About 5 to 13 million metric tons of solid plastic waste per year are entering the oceans [275]. Over the last years the plastic waste drifting on the ocean has developed into a huge problem for the oceanic ecosystems [276]. Plastic keeps sunlight away from phytoplankton, hampering it from effective growth. The plastic waste drifts with the ocean currents. It then collects within accumulation zones predicted by a global surface circulation model [277].

Most plastic-covered ocean surfaces are concentrated in central-oceanic regions with low iron content with predestination for applying the ISA method. Due to the trash, there would be a reduction in the ISA efficiency so we propose the integration of the plastic depletion problem into our ISA method: on both the side of and the outside of a container ship vessel, a specific technology can be installed: plastic trash collection, plastic trash sorting, plastic trash extrusion, plastic trash burning, ISA production and emission. The aforementioned processes are well known and need no description here. Trash or waste burning has the advantages of delivering an effective hot carrier gas with high buoyancy for uplift of ISA and for delivering HCl as co-catalyst of ISA. With the plastic extruder, most carrier parts of floating supports on the reef coral, sponge, and mussel habitats could be produced.

Beside the larger plastic fragments, the floating plastic fine debris with particle diameters in the µm range is a further problem [278]. Instead of doing the micro-trash separation by technical means, the mussel and oyster farming may clean away this ocean surface environmental problem. The floating micro-trash particles are collected by the bivalves and excreted as pseudo-faeces pellets and at last become part of the sediment layer at the ocean bottom.

Within the iron cycle, the photolytic driven oxidant production with iron participation may not be reduced to °Cl and °OH in the troposphere and O_2 by assimilation: When iron is cycled through the mantle at temperatures above 2500 K, Fe(III) is reduced to Fe(II) by release of O_2 [279]. This phenomenon may be driven by the blackbody radiation containing a great fraction of photons with wave length shorter than 2 µm at and above this temperature level.

3.2. ISA activates the O_2 input to the deep ocean

Ocean ecosystems are based on certain balances between oxidizing and reducing agents. As a result of the ISA-triggered additional input of organic carbon in the ISA emission region (i.e. the ISA precipitation region), as described in chapter 3.1, oxygen consumption by increasing organic debris precipitation could increase. The recent O_2 decline in some oceanic regions may result, at least in part, from the deposition of soluble iron deriving from flue gas pollution. Equally discussed in chapter 3.1 is the decrease of the oxidation efficiency within the water column by measures to increase the sinking velocity of the organic C containing debris. The increase of the sinking velocity of the organic C containing debris, is an effect that might completely compensate the oxygen loss by oxidation of the ISA-induced debris mass increase.

Recently, and without ISA influence, oxygen deficiency seems to develop in many parts of the ocean as described in the introduction. Oxygen deficiency is usually due to insufficient vertical water exchange owing to increased vertical density gradient rather than the result of increased phytoplankton production.

Oxygen deficiency (hypoxia) is found frequently between the oxic surface layer (the oxygenated one) and the oxic deep water layer [4, 280]. Due to the climate warming, the localities with a lack of oxygen seem to intensify and expand already today [5].

The deepest water layer of most ocean basins results from the Antarctic wintertime ocean surface ice generation by fractionating sea water into salt-poor sea ice and salt-rich dense brine. This results in the production of cold, high density oxic brines which sink to the bottom of the south ocean. The cold high density oxic brines spread as a thin oxic bottom layer up to the ocean basins north of the equator. The most recent severe climate warming, which induced disturbance of the THC, is likely to have been activated by the increasing inflow of the fresh melt water from Greenland into the North Atlantic. This inflow disturbs the down flow of the Gulf Stream water [281]. According to the increased melt of the glaciers of the Antarctic, the salt content of the ocean surface around Antarctica decreased. This effect increased the ocean surface covered by sea ice [282]. This freezing of the salt-poor melt water layer decreases the production of dense brines. This again decreases the down flow of brine, reducing again the vertical components of the ocean currents.

Through the ISA induced cooling, the oxygen and CO_2 flux into the deep ocean basins will be restored due to the input of the cold dense oxygen and CO_2 enriched polar surface water: Reduced melt water production of the Greenlandic and Antarctic ice shields by falling surface layer temperatures will restore and intensify the thermohaline circulation within the northern polar regions, by increasing the amount of Gulf Stream dumped, and by producing the circum Antarctic sea ice cover without melt water dilution, which induces the production of cold high density brines sinking to the ocean basin bottoms [283, 284]. Figure 5 illustrates the ocean basins vertical mixing circles.

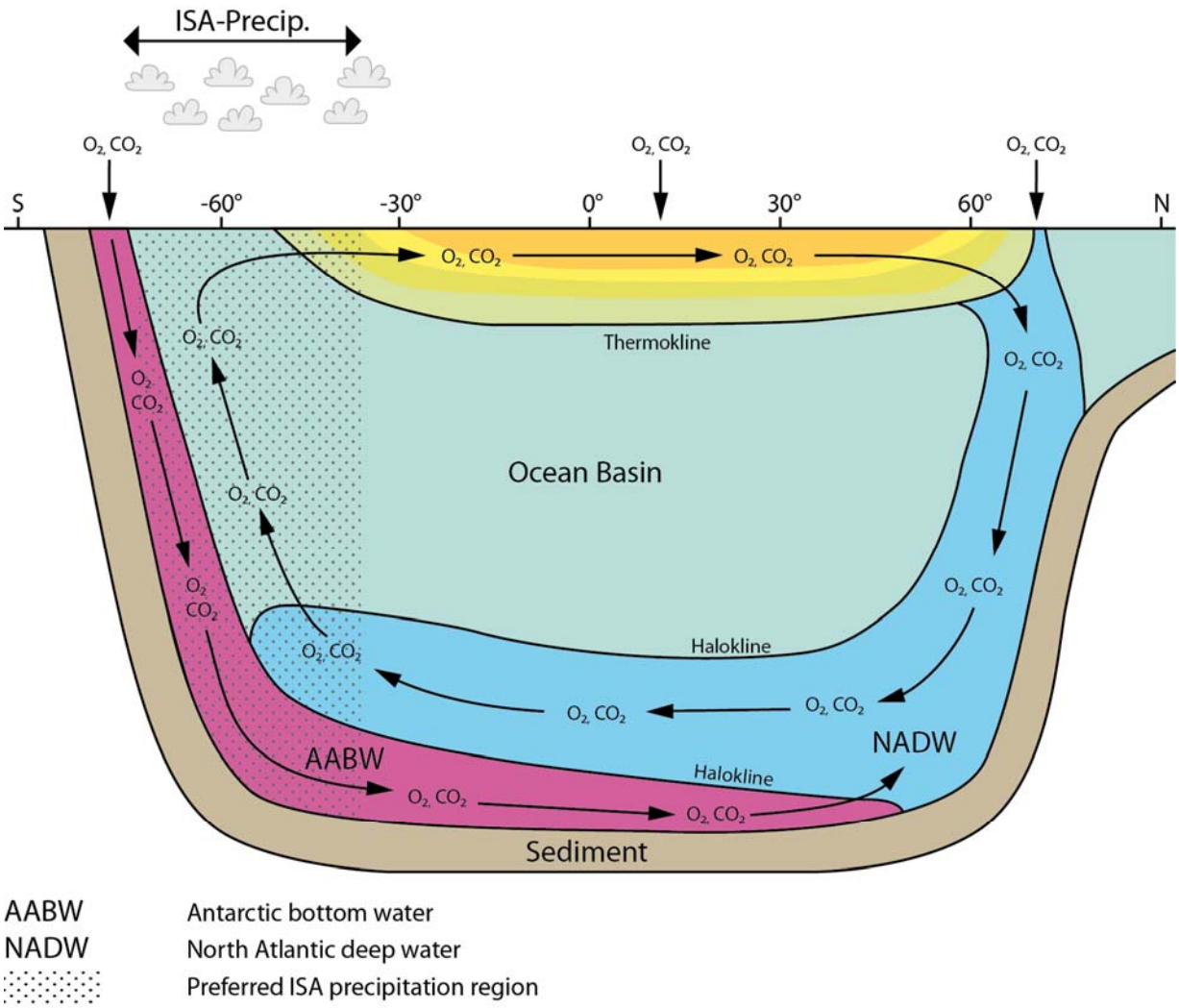

Figure 5. The motor of the Antarctic bottom water (AABW) current is the sea ice production of the Southern Ocean area bordering Antarctica. The North Atlantic Deep Water (NADW) current is driven by decreasing Gulf Stream temperature on its way north. Climate warming especially the faster temperature rise at higher latitudes shifts the region of the Gulf Stream down flow as NADW further to the north, as a result of the lowering Δt between equatorial and polar surface water. This shift sets additional Greenlandic coast regions in contact with warm Gulf Stream water and the rising air temperatures, as further component of poor increasing amounts of fresh melt water on the ocean surface. The rising melt water volume and the further north flowing Gulf Stream, increase the contact region between Gulf Stream water with fresh melt water. This produces increasing amounts of original Gulf Stream water but too low in density to sink and to become part of NADW.
Temperature rise at higher latitudes reduce the salt content of ocean surface water around Greenland and Antarctica, inducing reduced NADW and AABW volumes. According to the reduced down flow current volumes, the amounts of CO_2 and O_2 to the deep ocean basin are reduced as well as the vertical fertilizer transport from the ocean basin bottom, to the phytoplankton at the surface.

3.3. Phytoplankton fertilizer extraction from ocean sediments and underlying crust

The oceanic crust is composed of peridotites, basalts and serpentine rock and has a layer of sediment on top. Sediments and bed rock contain reductive and alkaline components extractable by sea water. The cause of the ocean water flow through the sediment layer and base rock is the temperature difference driven convection. Sediment compaction by gravity, subduction-induced compaction and subduction-induced hydroxyl mineral dehydration may be further reasons for water movement through the sediment layer at the ocean bottom.

Olivine is one of the main mineral components of oceanic crust rock layers below the sediment layer. Hauck [285] simulated the effects of the annual dissolution of 3 Gt olivine as a geoengineering climate cooling measure in the open ocean, with uniform distribution of bicarbonate, silicic acid and iron produced by the olivine dissolution. An additional aim of this work was the development of a neutralization measure against the increasing acidification of sea water. All the components of olivine: SiO_2, Fe(II) and Mg are phytoplankton fertilizers. They calculated that the iron-induced CO_2 removal saturates at on average ~1.1 PgC yr^{-1} for an iron input rate of 2.3 Tg Fe yr^{-1} (1% of the iron contained in 3 Pg olivine), while CO_2 sequestered by alkalinization is estimated to ~1.1 PgC yr^{-1} and the effect of silicic acid represents a CO_2 removal of ~0.18 PgC yr^{-1}. This data represent the enormous potential of the ocean crust rock as source of phytoplankton fertilizer.

The flow of sea water through anoxic sediments and bed rock results in the reduction of its SO_4^{2-} content, as well as extraction of the soluble fraction from the sediment such as Mn(II), Fe(II), NH_4^+ and PO_4^{3-}. The chemical and physical extraction processes are enhanced by the action of microbial attack at the border lines between oxic sea water and anoxic sediment parts within this huge aqueous system.

At suboxic conditions soluble Fe(II) and Mn(II) have optimum solubility or may be fixed as solid $Fe(II)_3(PO_4)_2$, $FeCO_3$, $MnCO_3$, FeS_2, S^0 and further Fe-S compounds [286-290].

Silicon is mobilized too, from the dissolution of silicates and SiO_2 at methanogenic conditions by complexation with reduced humic acid (HA) [286, 291]. In the reduced conditions, HA is characterized by catechol and further polyphenolic functions, which allows HA to complex with silicon [292-294] and with further metal cations.

Silicate dissolution mobilized Ca^{2+}, Mg^{2+}, Ba^{2+}, Fe^{2+}, Na^+, K^+. Fe^{2+}, Mn^{2+} and PO_4^{3-} precipitate more or less as sulfides, carbonates, within the sediment ($Fe(II)S_2$, $CaCO_3$, $MgCa(CO_3)_2$, $Fe(II)CO_3$, $Mn(II)CO_3$, $Fe(II)_3(PO_4)_2$), and within its suboxic surface ($BaSO_4$) or at its oxic surface (SiO_2, Fe(III)OOH, $Mn(IV)O_2$, clay minerals). The authigenic formed ferromanganese nodules [295] are formed by in situ microbial precipitation from sediment pore water, squeezed out to the seafloor on the sediment layer [296, 297]. Main components of the nodules are the phytoplankton fertilizer components: SiO_2, Fe- and Mn-oxides [297].

Having left the borderline between anoxic and suboxic near-surface sediment the HA catechols are changed by reversible oxidation into quinone or quinhydrone configurations by decay of the Si catechol complex. Like most of the chemical reactions within the sediment compartment, oxidation of the HA-Si complex is directed by microorganisms. The microorganisms involved use HA as external red-ox ferment [298-305]. After arrival of the pore water originating from the anoxic deeper sediment, or bed rock at the suboxic surface-near sediment layers, the oxidized HA releases $Si(OH)_4$ and, NO_3^- produced by microbial NH_4^+ nitrification [306, 307]. Depending on the $Si(OH)_4$ concentration produced, this can trigger the precipitation of layered silicates such as smectites, glauconite, and celadonite as well as silica [308-313]. Similar to HA, the clay mineral formation within the sediment, and the usage of the red-ox potential of these authigenic minerals, are, at least in part, the result of microbial action [314, 315].

According to its chelating properties, HA generate soluble to neutral Fe complexes of high stability even at oxic and weak alkaline ocean water conditions. As iron and HA have identical sources, especially chemoclines, even faeces HA can act as shuttles between Fe sources and phytoplankton [91]. But within oxic ocean milieu they become depleted, at last like every organic C substance, by oxidation.

The deep ocean currents take up the pore water percolates out of the sediment, and considerable amounts of the dissolved, colloidal or suspended sediment originating elements, are THC-conveyed to the surface [316] and activate there the phytoplankton production again. This as well, triggers the CO_2-conversion to organic C resulting in cooling the troposphere according to chapter 3.1. Repeatedly it also cools the troposphere by increasing the DMS formation according to chapters 2.5 and 3.1.

4. The main cooling effects induced by the iron cycle on the ocean crust

4.1. Carbon storage as authigenic carbonate in the ocean crust

The mechanism described in this chapter has the highest influence on the climate, due to its carbon storage capacity which is greater than that of their sediment layer. The convective water flow through the huge alkaline ocean crust volume is estimated to about 20 - 540 x 10^3 km³ yr^{-1} [29]. The oceanic crust comprises the largest aquifer system of the Earth, with an estimated rock volume of 2,3 x 10^9 km³, and a fluid volume of 2 % of the total ocean or ~10^7 km³ [20]. The system of the mid-ocean rifts (MOR) and subduction zones and the sector between these volcanic active regions are part of the Earth Mantle convection cycle, and part of said interconnected aquifer system. The bottom water of the ocean basins are in close contact to this conveyor belt-like moving rock layer of the oceanic crust. New oceanic crust is produced at the MOR: during its cooling it is pulled apart from the MOR by the moving

underlying mantel and, at last the moving mantle draws the crust down into the deeper mantle below the subduction zones. The oceanic crust has a sediment layer on top of its assemblage of multi-fractured crystalline and volcanic rocks. Both sediment and igneous bed rock interior are in an anoxic reduced and alkaline state; temperature on top of the sediment surface at the ocean bottom is round about 0 °C but temperature increases up to >1000 °C within the igneous bedrock basement. As there is no effective sealing between cold bottom water and high temperature zone, the water content of sediments and fractured basement flows through the crust in multiple thermal convection cycles positioned between cold surface and hot deep.

Alkalinity and alkalinity-inducing compounds of the ocean crust rock layers extract CO_2 and HCO_3^- from sea water by carbonate precipitation in the fissures during sea water percolation through the multi-fractured rock [317]. A carbon uptake of 22 to 29 Mt C yr^{-1} is estimated during the hydrothermal alteration of the oceanic crust [318]. This is more than the carbon uptake by the overlying sediment layer of the oceanic crust which is estimated to 13 to 23 Mt C yr^{-1} [318]. The oceanic crust is composed of peridotites, basalts and serpentine rock with a sediment layer on top. Said rock layers contain reductive and alkaline components. Sea water circling through these rock layers loses its contents of oxygen, sulfate, nitrate and even parts of hydrogen carbonate by reduction and precipitation, and becomes enriched with methane and further reductants [319-326].

Figures 6A and 6B illustrate respectively the differences between a poorly and a sufficiently mixed ocean.

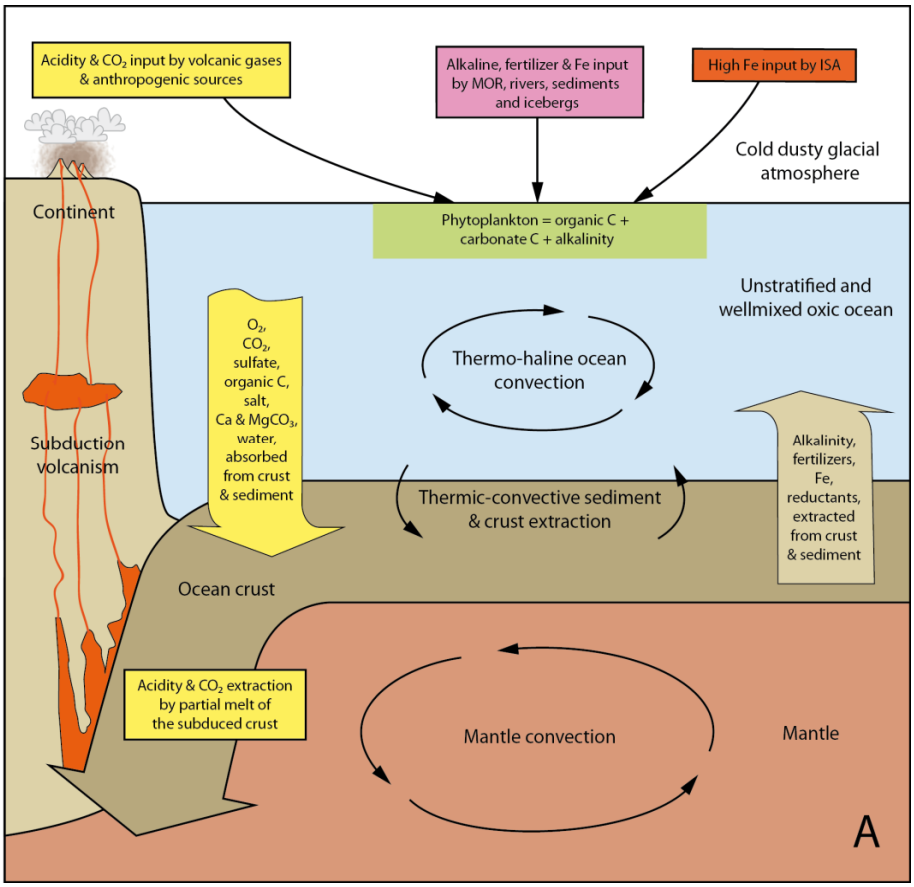

1143
1144

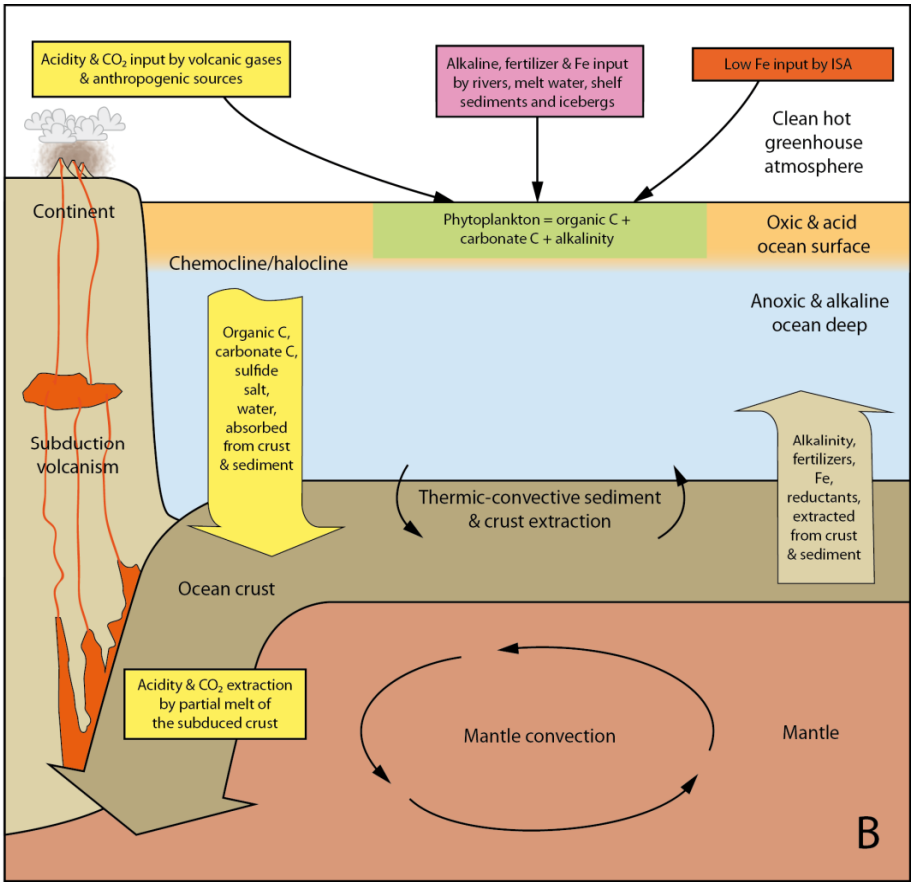

1145
1146

Figures 6A and 6B. present the essential differences between an unstratified well-mixed ocean basin under a cold and dusty atmosphere during the cold main glacial, with low atmospheric GHGs concentration (6A) and a stratified ocean basin with a melt water layer on top of a saline ocean water layer during a warm interglacial, with a hot and dust-free greenhouse atmosphere (6B).

Figure 6A: According to the unstratified well mixed water column in Basin 6A CO_2 and O_2 absorbed at the water surface are distributed within all parts of the basin. High production rates of organic carbon produced by phytoplankton in the top layer are oxidized during their way down on the sediment layer, with only minor generation of organic sediment. Carbonate carbon produced by the phytoplankton becomes dissolved to great parts within the deeper basin parts generating HCO_3^-. CO_2 and HCO_3^-. By cycling of the basin bottom water through the alkaline bottom sediment and ocean crust aquifer, CO_2 and HCO_3^- become precipitated and buried as carbonate C. The recycled bottom water becomes enriched by Fe fixed to organic chelators and is transported back to the surface. Due to the unrestricted down-flow and transfer of the CO_2 from the former surface water into sediments and into underlying base rock as carbonate carbon, the buried carbonate C exceeds the buried organic C amount.

Figure 6B: An interglacial episode with high GHGs levels accompanied by elevated surface temperatures generates increased melt water and surface water runoff. Because the saline poor water layer spreads on the saline ocean water and induces at least a regional stratification of the ocean basins water column: this stops the production of brine-induced surface water down-flow, as melt water freezing generates neither brine nor any vertical surface water movement. This stops any down transport of absorbed CO_2 and O_2 too and generates anoxic conditions within the underlying saline layer. The anoxic saline layer becomes anoxic and alkaline by sulfate and nitrate reduction. Any phytoplankton-induced organic and carbonate litter trickles down through the anoxic and alkaline layer: Ca- and $MgCO_3$ without dilution in the alkaline water and organic C without oxidation in the anoxic milieu. At the chemocline between light acidic CO_2 saturated water and the alkaline saline layer may precipitate Ca- and $MgCO_3$ in small amounts and mix with the down-falling phytoplankton-originating litter.

Due to the opposing chemical milieu differences between the oxic ocean water inflow and anoxic reduced and alkaline sediment and basement, the ocean water convection cycles through the ocean crust act as continuous chemical reaction systems and forms habitats of intensive acting microbial action [327]. The most intensive chemical reaction intensity is found at MOR, subduction zones and at volcanic sea mounts, between MOR and subduction within the abyssal plain convection cycling occurs [20]. Because the hydrogen carbonate load of the ocean water inflow comes to precipitation as carbonates of Ca, Mg, Fe, and Mn within the alkaline rock interior and by chemical reduction of sulfate, nitrate and hydrogen carbonate, the ocean basements act as huge CO_2-Carbon storages. No doubt: the ocean crust carbonate depot is the most effective carbon storage, more effective than any other organic carbon storages.

Within the huge ocean crust contact volume, sea water changes the alkaline pyroxenes and basalts into serpentine, diabase and carbonates; by producing heat, hydrogen, rock volume expansion and by permanent production of numerous fissures. The ocean water sulfates react with the silicate components to magnetite, pyrite and barite. The sea waters hydrogen carbonate load precipitates within the rock fissures as magnesite, calcite, siderite and

dolomite. By heat transfer from hot rock and chemical reaction, heat circling through the primary and new generated multiple fissures in the former mantle rock, the sea water inflow heats up, producing convective flow. At fissures where the alkalized flow of convection water containing hot CH_4 and H_2 comes out with pH 9 to 11 and, contacts the fresh sea water, carbonate precipitates and builds up skyscraper high carbonate chimneys [328].

The convective seawater flowing only through the MOR system is estimated to about 20 to 540 x 10^3 km^3 yr-1 [29]. This volume is more than the global river flow of about 50 km^3 yr-1 [329].

The weathering reaction conditions and the sea water alkalization during the intense sea water contact with the alkaline MOR rocks are much more aggressive, so respectively more effective, comparatively to reaction conditions and alkalization, during the precipitation water contact, during weathering reactions of continental rocks. This is confirmed by the alkaline pH of up to 11 of the “White Smoker” MOR outflow in spite of its haline salt buffered seawater origin [328]. Even the most alkali run-off from limestone karst spring fresh-waters or within karst cave fresh-waters does not exceed pH levels of 8.5 [330-332]. According to the enormous carbonate absorption capacity of the oceanic crust, it has been proposed to use it as a storage of CO_2 [333]. As the igneous crust rock aquifer generates H_2 during its contact with ocean water parts of the carbonate precipitation, carbonate is reduced in part to organic and / or graphitic C, depending on the reaction temperatures by botic or abiotic reduction [334-338].

There is no doubt that the efficiency of the pH dependent CO_2 absorption and carbonic acid neutralizing at the ocean surfaces and the hydrogen carbonate precipitation to carbonate processes at and within the oceanic crust, are dependent on the activity of the THC within the ocean basins. During cold climate epochs, with unstratified water column and undisturbed THC, the CO_2 conversion to ocean crust carbonate is activated, as well as the CO_2 conversion to the organic fraction of ocean sediments is activated. Just the opposite has been found to be true for the burial of organic C in ocean basin bottom sediments: according to Lopes et al. [96] the overwhelming organic debris fraction produced during main glacial episodes from the phytoplankton habitat at the surface, is oxidized and re-mineralized in the well-mixed ocean basin Lopes et al. [96]**.** As the CO_2 level in the atmosphere is at the lowest levels during the main glacials, the remaining C-sinks of the oceans seem to be of much bigger efficiency than the iron-induced production of organic C by assimilation: The most prominent C sink is the authigenic carbonate C burial in the alkaline ocean crust. There seems to be no doubt that the vertical well-mixed ocean during the main glacials works as an efficient pump, to transport dissolved CO_2 and O_2 to the ocean basin bottoms: There, O_2 act as mineralizer of organic C and CO_2-C is buried as authigenic carbonate C in the oceanic crust.

Table 2 gives an overview about some trends in C burial depending on the climate condition change between main glacial and interglacial.

Table 2: Interglacial climate episodes where hot, nearly dust-free, and had elevated levels of GHGs. The interglacials coincided with stratified water columns. The stratified ocean has a much reduced activity due to the reduced CO_2 transport to the bottom of the ocean basin. As the O_2 transport is reduced, and the lower part of the basin is anoxic, the oxidative mineralization of the organic litter fall from the phytoplankton activity at the surface is reduced and generates sediments rich in organic substances. As sulfate, nitrate and in part CO_2 within the anoxic water column are reduced to sulfide, ammonium and CH_4, the pH increases to alkaline. This can induce carbonate precipitation near the chemocline. During the glacial maxima with cold temperatures, dustiness and low greenhouse gas levels the ocean basins had well and vertical mixed water columns with highest carbonate C burial and lowest organic C burial.

Effect on		**Sediment + crust below well and vertical mixed water column**	**Sediment + crust below stratified and anoxic water column**
Mass ratio of buried sediment & crust carbon	sediment C / oceanic crust C	<<1	<1 to 1 or >1
Mass ratio of buried sediment & crust carbon	organic C / carbonate C	<<1	up to 1 or >1
Authigenic carbonate produced within the water column		No	Yes
Tropospheric parameters	Dust	High	Low
	CO_2	Low	High
	CH_4	Low	High
	Temperature	Cold	Warm

Lopes et al. [96] found just the opposite, in ocean sediment layers produced during the warm interstadial, in comparison to the cold main glacial: high burial rate of organic C in the ocean bottom sediment. But in spite of the high organic C burial rate, the interstadial CO_2 levels where kept higher than those of the main glacial. Even to this point the Lopes et al. [96] results fits well to our CO_2 sink model. During the glacials climate warming events, enormous melt water volumes were generated and induced stratification effects in ocean basins by placing a melt water blanket on the saline ocean water surface [14]. The transport of CO_2 and O_2 into the basin bottoms became interrupted. The drizzle of phytoplankton litter kept un-oxidized, and as further consequence the amount of Carbonate C burial within the ocean crust ceased.

The continuous availability of chemical activity, as chemical reaction vessel and as an alkalinity reservoir of the oceanic crust, is maintained by the continuous generation of new crustal rock material of 21 $km^3\ yr^{-1}$ [20]. This huge rock volume production capacity has enough alkalinity and fertilizer reserves to maintain the absorption, neutralization and precipitation of a multiple of the recent incoming CO_2 and HCO_3^-.

THC is the main transport medium of carbon from the atmosphere into the deep on Earth. This makes THC the most prominent climate stabilization element.

The realization of the significance of THC as stabilization element of our recent climate model induces questions about the stability of the THC. As stated in chapter 1, the main factors for destabilizing the THC seems to be stratification of the water column by the desalting of surface ocean layers by freshwater dilution from increasing ice melting [6]. The low density melt water generates a layer onto the ocean water, producing a stratified water column. The stratification hampers or prevents the transport of CO_2 and O_2-containing surface water into the deep ocean basin parts. The most severe consequence of such stratification, to oceanic ecosystems, is the development of anoxic milieu within the stratified ocean basins.

Typical marks of episodes with stratified water columns in ocean basins are the black shales and black limestones as sapropel remnants. Repeated development of stratified ocean basins during the Phanerozoic epoch occurred as a consequence of elevated CO_2 levels in the atmosphere. This caused high sea surface temperatures [13], and as a global consequence: global increase of evaporation, precipitation and as well production of brines of higher concentrations.

Hansen [6] pointed out too, that the increasing melt water run-off from polar and subpolar ice layers can induce the cover of denser ocean water by a melt water layer. But the generation of increasing precipitation and surface water run-off accompanied by increasing brine production during hot CO_2-high climate episodes has just the same consequences in the past geological epochs as we learn from Meyers [13].

Just that we now have to fear this combination, of both the CO_2-dependent temperature rise-generated precipitation increase, plus the melt water increase from glacier melt. Mankind has to find now the appropriate tool to win or to fail this challenge.

A melt increase might drive the destabilization of THC. And at first the top layers of the ocean basins will suffer from acidification and the deep layers will become alkaline and anoxic.

By starting the ISA process, the induced climate cooling will decrease the Greenland glacier melt. The minimized freshwater inflow to the North Atlantic Ocean reduces the dilution of the salty Gulf Stream and increases the down flow quantity of oxic and CO_2 containing salty surface water. In parallel, the surface increase of sea-ice produced on the South Ocean surrounding the Antarctic continent is followed by increased down-flow of oxic and CO_2

containing cold brine onto the bottoms of the oceanic basins. Both effects do increase the THC activation: the flow of alkaline, phytoplankton fertilizer enriched, and oxygen depleted deep-ocean water to the surface. This activates CO_2 absorption from the atmosphere by phytoplankton growth and by CO_2 absorption

One of the proposed alternative climate engineering measures aims to absorb atmospheric CO_2 by reducing the surface ocean acidity and by producing phytoplankton fertilizers. To transfer 1.1 x 10^9 t yr^{-1} CO_2 carbon into the ocean a crushing of 3 x 10^9 t yr^{-1} of the ocean crust and mantel rock mineral olivine to a particle diameter of 1 µm and suspend it at the ocean surface would be necessary [285, 339, 340]. These numbers seem to be two orders of magnitude too high. Keleman & Manning calculate a carbon mass subduction of about 50 x 10^6 t C yr^{-1} (C in oceanic crust, bedrock and sediment layer) [318]. Independently of which of both calculations has a mistake – technical activities to do the Hauck et al. proposal are far from any economic reality.

The proposed reaction of CO_2 with olivine is done with much better effectiveness by nature, without any costs, within the ocean crust in sufficient quantity. To minimize CO_2 emission it has been proposed to minimize power stations flue gas CO_2 by absorption by lime suspension [341]. This measure seems to be unnecessary when the ISA method comes into practice.

The fertilizing elements the phytoplankton needs, such as Si, P, and Fe, are all present in the ocean crust [342] and a property of the ocean crust water extract. Intensification of the THC would also increase the fertilizer concentration at the ocean surface in the phytoplankton layer. As demonstrated, the undisturbed THC is essential to keep the climate stabilized [32].

The ocean crust from the warm Mesocoic epoch which had no frozen polar regions contained about five times more authigenic carbonate than ocean crust younger than 60 million years [32]. Coogan interpreted this as possible consequences of higher bottom water temperature and/or different seawater composition. Insua et al. [343] found evidence, that the salinity of the ocean bottom water during the Last Glacial Maximum had been up to 4 % greater than today. It seems evident that the cause of the latter had been the higher volume of brine produced during sea-ice freezing. This fact demonstrates that disturbed or weakened THCs might be the cause of reduced carbonate C uptake of the ocean crust. The quantity of carbonate precipitation depends on the CO_2 and/or HCO_3^- input with seawater. As a consequence, the quantity of the ocean crust CO_3 uptake varies according to the activities of the THCs or stratified ocean basins: strong THCs increase the crust carbon content; weak THCs decrease it.

Independently of the cause of stratification events: by brine generation, by freezing or by evaporation, the ocean basins possess a removal mechanism which extracts salt from the brine and change the brine to sea water of normal salt concentration. This mechanism has

kept the salt concentration of sea water rather constant during the past geological epochs. This effect to achieve a constant salinity level, depletes any brine-induced stratification and restores well-mixed ocean basins again.

According to Hovland et al. [344-346] this desalination takes place by continuous salt removal from the brine or seawater within the hot ocean crust. This desalination works independently of the salt concentration of brine or seawater. The salt removal process acts within the ocean crust aquifer at near critical to super-critical seawater temperature and pressure conditions. During subduction of the salty crust rock chloride and carbonate change their cations with silicate and are dissolved as HCl and CO_2. Accompanied by H_2O, these gases are recycled to the atmosphere, mainly by subduction volcanism, but at a much smaller amount by MOR and similar alkaline volcanism.

During the time lag between the onsets of the ISA method cooling and the appearance of the alkalinity and fertilizer increase at the ocean surface, the cooling effect of ISA remains reduced. But after this time lag, the ISA method increases to optimal efficiency. Even from an economic viewpoint it seems better to compensate this by increasing the ISA emission at the beginning during the time lag, than doing the proposed suspending of olivine dust at the ocean's surface. Even lime shell wearing phytoplankton is able to accept small pH changes of CO_2 induced dependent acidification, because it uses the build-up of calcium carbonate shells as a detoxification measure to get rid of calcium ions from their bodies [265]. As a consequence of this effect, only the relation between Ca carbonate sequestration and organic carbon sequestration may decrease during the time lag.

Summing up: through the huge aquifers of the alkaline and reducing ocean crust, any transport of former surface water enriched by CO_2 or HCO_3^- induces carbonate C burial within the aquifer interior. This is the situation within well-mixed Ocean basins without stratification. Any stratification decreases carbonate burial or even stops it. Stratification changes the red-ox milieu below the stratification-induced chemocline. The MOR and sediment-induced exhalation of Fe and further metals by the black smokers into the sulfidic stratified ocean basin are prevented from contact with the planktonic surface water habitat. But surface water runoff, as well as melt water inflow and iceberg melt during warm glacial climate intervals may compensate the lack of Fe from the MOR and bottom sediment sources, as well as from the decreasing dust fall during the warm climate intervals [6, 7].

4.2. Carbon storage as organic and inorganic marine debris and as authigenic carbonate in the ocean sediment

The uptake of authigenic hydrogen carbonate from the ocean and precipitating it in the sediment, seems to play as well a major role in the carbon circle [347]. According to Kelemen [318] the carbon uptake by the sediment layer of the oceanic crust can be estimated to 13 to

23 Mt C yr^{-1}. The carbon inventory consists of life and dead organic carbon, carbonate carbon and authigenic carbonate produced by excess alkalinity deriving mainly from sulfate reduction and silicate solution by reduced humic acids. According to Sun & Turchyn the formation of calcium carbonate and its burial in marine sediments accounts for about 80 % of the total carbon removed from the Earth surface [348]. Meanwhile it seems possible to distinguish between marine formed sediment carbonate and authigenic carbonate [349].

As evidenced in chapter 4.1, stratified ocean basins can differ widely in quantity and quality of the buried C according to the prevailing climate conditions and their direct and indirect influences on ocean basin conditions. Table 2 lists some of the most prominent results.

The cooling of the Troposphere by ISA action stops melt water inflow, destructs the stratification and starts the vertical mixture. During the former stratification event, alkalized deep water layer had enormous CO_2 absorption capacity. The alkalized anoxic sediment behaves in a similar manner. This makes a much increased CO_2 absorption activity at the beginning of the movement.

Accordingly, excess alkalinity is produced by dissolution of silicates such as illite, kaolinite and feldspars, volcanic ash, pyroxene or other silicate components of ocean sediments and even opal by Si complexation with reduced HA at methanogenic conditions [286, 289, 350, 351]. Compensation by hydrogen carbonate induces authigenic precipitation of microbial dolomite [352], Ca or Fe carbonate [286, 291, 348, 350, 353, 354] and further minerals [355].

As mentioned in chapter 4.1, the biological processes of chemical sediment reduction induced by the ISA fertilization, changes NO_3^-, SO_4^{2-}, Fe(III), Mn(III/IV) and HCO_3^- to their deoxygenated and reduced species, inclusive CH_4 and NH_4^+ generation, produces a pH increase and additional alkalinity. Further pH drop is induced by H_2 evolution from FeS_2 generation from FeS and H_2S [356, 357] accompanied by CO_2 reduction to CH_4 [358] as well as N_2 reduction to NH_3 [359]. The alkalinity excess converts dissolved HCO_3^- into solid lime and dolomite [360-363]. The solid carbonates and CH_4 hydrate stabilize the sediment. Outside the polar permafrost region, methane hydrates are stable below 300 m below sea level and at ocean temperatures of nearly 0 °C [364]. The carbonate precipitation sequesters additional parts of CO_2, prevents the ocean water from acidifying and at last improves the CO_2 absorption by ocean water from the atmosphere. This again cools the troposphere.

The enhanced dissolution of silicates from the ISA induced by methanogenic sedimentation additionally compensates the enhanced alkalinity loss at the ocean surface, attributed to the calcification due to foraminifera and coccolithofores phytoplankton growth by ISA fertilization.

Summing up: within a well-mixed and unstratified ocean basin the surface layer absorb CO_2 and O_2 and become well mixed into the unstratified ocean basin by the thermo-haline basin convection. Consequences of the good mixture are nearly quantitative oxidation of the food chain debris to CO_2 produced by phytoplankton. Most C is buried as carbonate in the ocean

crust and its overlying sediment. The ratio of organic C burial to carbonate C burial is much smaller than 1. Results of Lopes et al. [96] from Northeast Pacific sediments demonstrate that, although estimated highest primary productivity during the Last Glacial Maximum, organic C burial was lowest. This coincides with our proposed optimum mixed O_2-rich milieu throughout the whole water column.

During situations with stratified water columns in the ocean basins or parts of them the THC convection is disturbed or does not exist at all. Surface water layer enriched with CO_2 and O_2 absorbed from the atmosphere cannot penetrate through the stratified water column, into the bottom of the basin. This induces sulfate reducing conditions below the surface layer. Only small parts of surface layer CO_2 are changed into carbonate C at the chemocline, with the alkaline sulfidic and anoxic parts below the chemocline. Below the chemocline, the water column is anoxic, the organic debris sediment with minor oxidation. Probably the ratio of organic C burial to carbonate C burial increases to a manifold during stratified conditions. Concerning to the huge fraction of organic C buried during the warm glacial intervals, according to the results of Lopes et al, [96] from Northeast Pacific, sediments demonstrate stratification events within their research area.

Stratification events may develop by warming the upper water layer, as well as by evaporation and precipitation [6-8].

4.3. Minimizing CH_4 emissions from sediments and igneous bedrock

The reaction product of oceanic crust minerals containing Fe(II) such as Olivine and Pyrrhotite with sea-water is hydrogen [365-367]. The hydrogen production rate at least along the MOR alone is estimated to ~10^{12} mol H_2 yr^{-1} [368]. Hydrogen is fermented by microbes with hydrogen carbonate into methane. The latter is known as constituent of the springs emitted by the ocean crust rocks (Früh-Green 2004).

Such and further CH_4 emissions, such as anoxic sediments outside the CH_4 hydrate stable pressure and temperature region, induce de-oxygenation within the overlying water layer by CH_4 emission [17, 369]. CH_4 emissions are induced for instance by hydrothermal springs [370], sediment movement [371, 372], seawater warming induced by climate change [373, 374], changing ocean circulation [375], ocean sediment subduction [376, 377]. At lower vertical sediment to ocean surface distances, the CH_4 emissions reach the troposphere. As the Arctic Ocean suffers at most from the climate change induced warming, the CH_4 release within this region rises extraordinary [16]. The most elevated Global surface-near oceanic CH_4 concentrations are located within the Arctic Ocean and the arctic troposphere [378]. This might be one of the reasons for the higher temperature rise of the Arctic region than the average surface Earth warming.

Within the sediment and within the suboxic ocean water column, CH_4 is oxidized by sulfate. Iron is an accelerator of this microbial fermentation reaction [379]. The ocean water column and the underlying sediment having had contact with ISA-originating iron are elevated in their iron content. This has different cooling effects to the troposphere: at first the elevated iron content in the uppermost suboxic sediment reduces the CH_4 content emitted by the sediment by anaerobic oxidation of methane by sulfate-reducing bacteria.

Below regions with ISA precipitation, not only the sediment, but even the whole water column of the ocean basin is enriched on iron. Any CH_4 molecule, independently of existent in the sediment, or just above in the water phase, or excreted into the water column as bubbles, is oxidized before it arrives at the water column top. By help of Fe containing enzymes the methane oxidation by sulfate is possible. This prevents the water layers above the sulfate oxidation zone from oxygen loss. Sulfate oxidizers of CH_4 are archaea and bacteria [380]. As these microbes use Fe-containing enzymes to do their anaerobic methane oxidation processes, they act better in iron-rich than in iron-poor environments [381, 382]. The iron containing debris fall of ISA-fed dead phytoplankton and phytoplankton dependent food chain links, feeds the methane depleting sulfate reducer community within or near the sediment surface.

Next, the iron content reduces the CH_4 bubble-development within the sediment layer, preventing catastrophic CH_4 eruptions by sediment destabilization, CH_4 bursts and sediment avalanches.

Third: elevated iron content prevents the ocean water column from CH_4-induced oxygen deficiency by the formation of ammonium. This oxygen deficiency prevention protects from generation of the extreme stable and very effective GHG N_2O [383].

The oxygen-dependent life will become problematic, due to its decreasing oxygen content within a decreased vertical mixed ocean basin induced by climate warming. An additional input of CH_4 would increase the oxygen deficit death zones. Any CH_4 injection into regional oxygen deficit zones, will immediately increase their volume. Climate models predict declines in oceanic dissolved oxygen with global warming. The climate warming dependent decline of the oxygen content in many ocean regions has meanwhile become manifest [384]. Braking or reversal of this trend by reducing the oxygen depleting CH_4 emissions at least should help to prevent regions within the ocean basins from methane-induced oxygen deficit.

The glacial age proved that in spite of the multiplicity of the cooling processes induced, they caused little disturbance to the ecosystems. This predestines ISA as a steering tool to prevent climate fluctuations such as the recent climate warming mankind is suffering from. The present study aims to describe in chapter 5 the technical means to realize this climate engineering project by the ISA method.

This result is contradictious to the calculations of Duprat et al. [385]. They found within the iron containing melt water trail of the giant Antarctica icebergs increased phytoplankton concentration. Duprat et al. assume that the iceberg induced carbon export increase by a factor of 5 to 10 within its influence locality and they expect an increase in carbon export by the expected increase of the iceberg production that has been predicted (for instance Joughin et al. [386]). We interpret the ongoing increase of icebergs and ice melt as a further severe warning sign that the ongoing destabilization might end soon in an insufficient mixed ocean.

The only artificially realizable restoration tool to change an insufficiently or poorly mixed ocean into a well-mixed ocean is definitely by climate cooling. The ISA method appears to be the climate cooling method by means of choice, because it accelerates the conversion of atmospheric carbons into solid and even liquid carbons with the means of nature. Comparing to the artificial aerosol systems based on TiO_2 or H_2SO_4 [387], the sea-salt aerosol has advantages, such as better controllability and economy.

5. Iron effects onshore

5.1. Importance of iron on terrestrial landscapes

As seen in previous sections, atmospheric deposition of iron together with other macronutrients and micronutrients set important controls on marine ecology and biogeochemistry: for terrestrial ecology and biogeochemistry the importance of iron is similar. Iron is one of 17 essential elements for plant growth and reproduction [388]. Iron is an essential micronutrient (or trace element) only required by plants in small amounts, for bio-functions such as production of chlorophyll and photosynthesis [389]. Iron is involved in many other important physiological processes such as nitrogen fixation and nitrate reduction and is required for certain enzyme functions [390].

Iron is the 4th most abundant element of the earth's crust (4.2%) and thus iron is seldom deficient, as despite its high abundance in soil, iron solubility is extremely low and its availability depends of the whole soil system and chemistry. Chlorosis (yellowing) is associated with iron deficiency in plants over land [59, 61], but the chemistry of iron in soils and its availability to plants [60] is out of the scope of this review, thus only a brief overview is given. However, while small amounts are necessary for growth, iron can become toxic to plants. Iron toxicity is associated with large concentrations of Fe^{2+} in the soil solution [391] and leads to oxidative stress. As a consequence, iron-uptake systems are carefully regulated to ensure that iron homeostasis is maintained. Iron availability represents a significant constraint to plant growth and plants have developed distinct strategies to ensure Fe solubilization and uptake [392]. In forests, microorganisms such as fungi and bacteria, play a role in nutrient cycling [393]. A particularly efficient iron acquisition system involves the

solubilization of iron by siderophores [394], which are biogenic chelators with high affinity and specificity for iron complexation.

Iron deficiency induced chlorosis represents the main nutritional disorder in fruit tree orchards and in crops grown on calcareous and/or alkaline soils [395] in many areas of the world. Iron deficiency is a worldwide problem has calcareous soils cover over 30% of the earth's land surface [396] specially in arid and semi-arid regions and has a large economical impact, because crop quality and yield can be severely compromised [397, 398], thus several methods of correction have been developed. Iron canopy fertilization (foliar fertilization) can be a cheaper, more environmentally-friendly alternative to soil treatments with synthetic Fe(III) chelates for the control of Fe chlorosis in fruit trees [399]. But iron chelates are expensive and have to be applied annually. Several sprays aiming to activate the Fe pools in a chlorotic leaf by foliar iron fertilization have been tested and were generally as effective as simple spay fertilization with iron sulphate (Abadía et al., 2000) and both are effective in re-greening treated leaf areas, both in peach trees and sugar beet plants [397]. Iron-deficiency chlorosis in soybean was solved by foliar sprays which significantly increased the yield of three cultivars tested and the yield responses obtained, were about 300 kg ha^{-1} [400].

Although foliar Fe fertilization seems to be potentially effective, the scientific background for this practice is still scarce and we did not found evidence that soluble iron contained in atmospheric dust aerosols has already been proved to be able to play this role.

The fertilizing role of African dust in the Amazon rainforest is well known [401] but attributed to the P input. On a basis of the 7-year average of trans-Atlantic dust transportation, Yu [402] calculated that 182 Tg yr^{-1} dust leaves the coast of North Africa (15°W), of which 43 Tg yr^{-1} reaches America (75°W). The dust reaching the Caribbean and the Amazon come mainly of the northwestern Africa (Algeria, Mali, and Mauritania) [403].

An average of dust deposition into the Amazon Basin over 7 years is estimated to be 29 kg ha^{-1} yr^{-1} [401], providing about to 23 g ha^{-1} yr^{-1} of phosphorus to fertilize the Amazon rainforest, together with Mg and Fe. Although not directly related to ISA, this dust deposition allows biomass fertilization and thus CO_2 removal from the atmosphere.

The wide spread tropical soils, mostly laterites, are deficient in phosphate and nitrogen but not in autochthon iron. The only exception to this is for all the epiphyte plants and the plants growing on the soil-free localities without any autochthon iron. These plants might gain profit from the ISA method. Such plant communities are localized for instance on top of the famous Tepuis (table mountains north of the Amazon basin near the borderlines of Brazil, Venezuela and Guyana) and on the tree branches in the rain forests without roots into the ground. From Köhler et al. [404] the epiphytes flora on the tree branches of the rain forests may contain up to 16 t ha^{-1} (Costa Rica) up to 44 t ha^{-1} (Colombia) of epiphyte plant + humus dry weight on the tree branches.

The epiphytes, but much more the Tepui plants, would gain profit from ISA and even from undissolved iron oxides, because plant roots and fungal hyphae secrete iron-solubilizing organic acids and complexants. Microbial ferments have time enough to turn all kind of undissolvable Fe into dissolvable Fe.

Is there a climate relevance to rain forest fertilizing by dust? Rizzolo et al. [405] states that the iron limited Amazon rainforest profits from the seasonal deposition of iron by Saharan dust. Especially the deposition of iron plus further nutrients on the Amazon biota is likely to increase both epiphytic growth and fungal and bacterial decomposition within the canopy [405]. The increase in iron bioavailability is also known to increase nutrient cycling within the forest.

Large fractions of the organic biomass produced by help of iron and further eolic nutrients leave the Amazon region, are transported into the South Atlantic basin and at last become part of the shelf and basin sediments. This are aquatic life plants such as Water hyazinth and Water fern, plant litter such as driftwood, leaves, and particular, colloidal, and dissolved humic and fulvic acids. According to Ertel et al. [406] the flux of dissolved organic carbon fraction at Óbidos, situated about 800 km above the Amazon mouth, is 2×10^{13} gC yr^{-1}.

Some rain forests such as the Amazonian, benefit from sporadic dust plume fertilization of Saharan origin. Others may profit from an artificial ISA precipitation resulting in a significant additional epiphyte plant growth.

5.2. Importance of iron for human food and health

All organisms on Earth ride upon a "*ferrous wheel*" made of different forms of iron that are essential for life [97]. Iron is an important micronutrient used by most organisms, including higher animals and human beings and is required for important cellular processes such as respiration, oxygen transport in the blood. Its bioavailability is of concern for all the Earth's living organisms, especially in aquatic ecosystems, including clear water and oceanic ones.

In humans, iron deficiency and anemia remain the most common nutritional disorders in the world today [407].

The World Health Organization [408] states that the lack of sufficient micro nutrients such as Fe and Zn, represents a major threat to the health and development of the world population. WHO [408] estimates that over 30 % of the world’s population are anemic and even more in developing countries (every second pregnant woman and about 40% of preschool children). Iron deficiency affects more people than any other condition, and iron deficiency exacts its heaviest overall toll in terms of ill-health, premature death and lost earnings. Iron deficiency and anemia reduce the work capacity of individuals and of entire populations, causes maternal hemorrhage, impaired physical and cognitive development, reduced school

performance and lowered productivity, bringing serious economic consequences and obstacles to national development.

Iron deficiency in humans has been associated with heart failure [409, 410]; gastric ulceration and anemia induced by Helicobacter pylori [411]; negative impacts on skeletal integrity [412], cognitive disorders [413]. Iron deficiency in infancy leads to long-term deficits in executive function and recognition memory [414]. In experiments with animals, even if the iron and the hemoglobin levels return to normal after treatment from an early induced iron deficiency, there are long-lasting cognitive, physiological and hematological effects [415]. Thus several strategies and technologies have been elaborated to manage iron deficiency in humans [416] such as food fortification (adding iron to food) [417] and biofortification (the process of enriching the nutrient content of crops, vegetables or fruit as they grow). WHO, FAO and UNICEF edit guidelines or recommendations on food fortification with micronutrients [418], for instance adding ferrous sulphate, ferrous fumarate, or iron complexes to wheat and maize flour (from 15 to 60 ppm depending on the regional average consumption ranges and on other iron food vehicles). Biofortification can be achieved by utilizing crop and soil management practices to increase micronutrient concentrations in the edible crop parts [419] and can provide a sustainable solution to malnutrition worldwide, as other methods, such as diversifying people's diets or providing dietary supplements, have proved impractical, especially in developing countries). Together with dietary modification and iron dietary supplementation, iron fortification (suitable food vehicle containing higher levels of bioavailable iron) are the main recommendations of WHO to increase iron intake, improve nutritional status and stop iron deficiency anemia. Increasing available iron levels in major staple food crops is an important strategy to reduce iron deficiency in people. WHO anticipates that benefits are substantial as timely treatment can restore personal health and raise national productivity levels by as much as 20%.

The biofortification of bioavailable iron in staple plants provides a sustainable and economical tool to use, in order to rescue iron deficiency in target populations globally [420].

In contrast with fruit trees, where foliar iron fertilization is generally used in chlorotic leaves, canopy, Fe-fertilization is increasingly being used in cereal crops to increase the Fe concentration in grains, in what is called biofortification. In these crops, which are generally treated with foliar iron sprays when there is no leaf chlorosis, applied iron has been shown to re-translocate efficiently to other plant organs, both in wheat [421] and rice [422]. Zuo and Zhang [419] have developed strategies to increase iron uptake by roots and transfer it to edible plant portions allowing absorption by humans from plant food sources.

5.3. Active inhibition of methane emissions from wetlands, lakes, and sediments

Lipson et al. [423] found that in Arctic peat ecosystem, Fe and humic reduction competes with methanogenesis as e- acceptors and inhibit some CH_4 production and that on the basis of conservative measurements of net Fe reduction rates, this process is comparable in magnitude to methanogenesis.

In wet sedge tundra landscapes Miller et al. [424] conducted experiments that showed an inverse relationship between dissolved iron and CH_4 concentrations and found that net CH_4 fluxes were significantly suppressed following the experimental addition of iron and humic acids. Iron and humic acid amendments significantly suppressed *in-situ* net methane flux.

Lipson et al. [425] conducted experiments on 2 different ecosystems: one with permafrost and naturally high levels of soil Fe and one with no permafrost and naturally low levels of soil Fe. The addition of Fe(III) and humic acids (electron acceptors) significantly reduced net CH_4 flux for at least several weeks post-treatment, without significantly altering CO_2 fluxes. There was no significant difference between the reduction of CH_4 flux caused by Fe(III) and the one caused by humic acids. The future release of GHGs from high latitude wetland ecosystems can significantly be altered by this natural and widespread phenomenon. These results also show that the suppression of CH_4 flux in this type of ecosystem can be induced by artificial addition of Fe(III), humic acids or other electron acceptors.

Zhang et al. [426, 427] found methanogenesis and sulfate reduction inhibition after ferric salt dosing to anaerobic sewer biofilms. Similar methanogenesis inhibition and even increases of rice productivity by ferric salt addition have been described by others [428-431].

Amos et al. [432] found support for the hypothesis that Fe(III) mediates CH_4 oxidation in crude contaminated aquifer.

Although some iron oxides such as magnetite and hematite have different properties and may facilitate methanogenesis by some types of micro-organisms [433] it is worth being noted that the iron solubility and bioavailability properties of the ISA are similar to the ferrihydrite which inhibits methanogenesis in the same experiments [433] and in general Fe(III)-reduction by methanogens contribute to Fe(III) inhibition of methanogenesis [434].

Experiments conducted in tropical humid tropical forest soils, which are also an important source of atmospheric CH_4 and where Fe(III)-reducing bacteria coexist with methanogens, show that upon addition of acetate, production increase of CH_4 is much greater (67 times) than that of Fe^{2+} (2 times), indicating that the two process were acetate limited and suggesting that Fe(III)-reducing bacteria were suppressing methanogenesis when acetate availability is limited [435]. For Roden and Wetzel [436] a significant suppression of CH_4 production in freshwater wetlands could be mediated by Fe(III) oxide reduction within globally extensive iron-rich tropical and subtropical soil regimes.

All these results support the hypothesis, that additional to the many photolysis dominated CH_4-depletion actions by ISA in the troposphere, even after ISA precipitation on wetlands,

marshes, lakes, rice paddies and shelf sediments it will inhibit the emission of CH_4. The degree to which Fe(III) reduction suppresses CH_4 emissions under different soil conditions should be considered by regional and global models of GHGs dynamics.

No published studies were found about the biogeochemical cycle of iron to the continents and land in specialized journals such as “Global Biogeochemical Cycles », nor in the chapter about the biogeochemical cycles of the latest IPCC report and, the recent Iron Model Intercomparison Project (FeMIP) seems concentrated in oceans interactions [55, 437].

It is now well known that in large areas of the open ocean iron is a key limiting nutrient and that in alkaline terrestrial landscapes iron deficiency induces plant chlorosis. The authors' hope is that bringing together under this review seemingly disparate lines of research from diverse disciplines, it will result a more global understanding of the global biogeochemical iron cycle, especially over terrestrial landscapes, peat-bogs, and other wetlands.

6. Estimations of the ISA demand by the ISA method

6.1. ISA can induce a significant CH_4 depletion

Wittmer [124-127] reported that the ISA method is very efficient for °Cl generation. Hence, ISA allows depletion of GHG methane by separation prior cooling effect. Therefore, ISA appears to be a very promising cooling method with technical and economic stakes. But the answer depends strongly on the volume of ISA to be produced and emitted. Indeed, ISA plume should be released high enough in the troposphere to get sufficient distribution and residence time in combination with °Cl generation quantity.

Based on results of Fe photolysis induced °Cl production, Wittmeret al. [124] estimated the feasibility of CH_4 depletion by NaCl-diluted ISA. Wittmer found a °Cl emission of 1.9 x 10^5 °Cl/cm^3 at a Cl^-/Fe(III) molar ratio of 101 within the pH range of 2.1-2.3. The same °Cl generation was found at the suboptimal pH of 3.3 – 3.5 and at a Cl^-/Fe(III) molar ratio of 51. This Cl generation is four times higher than the reference which corresponds to a significant CH_4 lifetime reduction in the troposphere [124]. A pH range of around 2 corresponds to the natural aerosol pH within the oceanic boundary layer. The optimum efficiency of °Cl production by photolysis of ISA corresponds to pH 2, whatever the source of Cl^-, NaCl or gaseous HCl and whatever if ISA is an iron(III) oxide or an iron(III) chloride aerosol [124].

According to Lim et al. [438] and to Meyer-Oeste [439] the optimum °Cl production by sunlight photolysis of $FeCl_3$ solutions or ISA, is generated in the acidic pH range. The efficient °Cl generation is necessary for an efficient CH_4 depletion by ISA. Except if made by condensation and hydrolysis of $FeCl_3$ vapor or by nebulization of pure $FeCl_3$ solution, or produced by combustion to pyrogenic FeOOH and reaction and hydrolysis with HCl and H_2O

to $FeCl_3$ solution: $FeCl_3$ has an acidic pH from the beginning because it hydrolyses according to equation 4.

$$FeCl_3 + 2H_2O \rightarrow FeCl_2OH + H_3O^+ + Cl^- \qquad \text{(Eq. 4)}$$

6.2. ISA demand calculation

Current CH_4 depletion by °Cl is estimated from 3.3% [440] to 4.3% [119]. According to the results of Wittmer [124] at a Cl^-/Fe(III) molar ratio of 101, this amount would rise fourfold: from 13 to 17%.

1. Wittmer et al. used their results obtained at a Cl^-/Fe(III) ratio of 51 at the pH of 3.3-3.5: 1.9 x 10^5 °Cl/cm^3. We consider that this pH is suboptimal. Instead it should be used the results obtained at a Cl^-/Fe(III) ratio of 101 at the pH of 2.1-2.3: 1.9 x 10^5 °Cl/cm^3.

Moreover, Wittmer et al. made two limitative estimations:

2. They only focused on the Cl delivery in the condensed state by coagulation as Cl^- transfer option between ISA particles and the Cl source sea-salt aerosol ignoring other Cl sources, Cl aggregate states, and Cl transfer mechanisms.

According to this model, the ISA particles should continuously lose in the daylight their Cl^- load by °Cl emission and as a consequence they could gain back Cl only by coagulation with sea-salt aerosol particles. As further consequences of this model the Cl^-/Fe(III) ratio of ISA particles would decrease, their diameter increase and their residence time in the troposphere would decrease.

But according to Graedel and Keene [118] and Keene et al. [441] the next prominent source of inorganic Cl in the troposphere beside sea-salt aerosol is vaporous HCl. This is the main source where the ISA particles can refill the chloride lost by photolysis. The main Cl uptake mechanism from this Cl source is the sorption from the gaseous phase.

Main HCl sources are the sea-salt reaction with acids, CH_4 and further hydrocarbon reactions with °Cl [441], flue gases of coal, biomass and garbage combustion [442], as shown in the "global reactive chlorine emissions inventory" [441], HCl from chlorocarbons being a significant part [443] in particular from CH_3Cl which is the largest, natural contributor to organic chlorine in the atmosphere [444].

3. They estimate that the global production rate of 1785 Tg yr^{-1} of sea-salt aerosol Cl^- has to be doped with iron at a Cl^-/Fe(III) molar ratio of 51 meanwhile we consider it has to be estimated at a molar ratio of 101 (according to 1.).

The calculations made with these limitative assumptions resulted in an iron demand of 56 Tg yr^{-1} Fe(III) to obtain the desired CH_4 depletion effect [124].

Whereas, with the limitative assumption that there is no further Cl^- source than sea-salt, the calculations with a Cl^-/Fe(III) ratio of 101 results in a Fe(III) demand of only 18 Tg yr^{-1}.

ISA can be produced from pyrogenic iron oxides according to method I (see chapter 7). Pyrogenic oxides have particle sizes lower than 0.1µm. Diameters of the NaCl-diluted ISA particles of the Wittmer tests [124] are round about 0.5µm. This confirms the test results of Wittmer et al. as calculation basis without any cut.

But Wittmer et al. made two other limitative assumptions:

4. ISA has the same particle size and corresponding surface range as sea-salt;
5. ISA has the same residence time as sea-salt aerosol in the troposphere."

According to their coarse aerosol particle range, the residence time of sea-salt particles in the troposphere is inferior to 1 day [445] while the artificial ISA particles with diameters lower than 0.5 µm have residence times in the troposphere of at least 10 days up to several weeks [446, 447].

Known salt aerosol generation methods by vapor condensation or nebulization [448, 449] allow not only the flame descending ISA type 1 [141], but also the condensation and nebulization descending ISA variants 2 and 3 (see chapter 7) to be produced with aerosol particle diameters between 0.1 and 0.01 µm. Diameters of salt aerosol particles according to these physical aerosol generation methods are up to, or more, than one order of magnitude smaller than of those used in the experiments by Wittmer et al. [124].

Analogue to CCN behavior in cloud processing [113] most of the small-sized ISA particles are protected by their small sizes from coagulation or coalescence with sea-salt aerosol particles. This effect prevents ISA from leaving the optimum active atomic chlorine emission conditions: low pH and low particle diameter range.

The residence time difference of more than one order of magnitude in comparison to sea-salt aerosol further reduces the Fe demand for ISA production from 18 Tg yr^{-1} to less than 1.8 Tg yr^{-1}.

6. The properties of the ISA particles produced by the most preferred ISA method variant are explained in chapter 4. Their difference to the NaCl-diluted ISA tested by Wittmer [124] are: ISA particles are made of $FeCl_3$ x nH_2O undiluted by NaCl, or FeOOH coated by $FeCl_3$ x nH_2O undiluted by NaCl [439, 450]. The Cl^-/Fe(III) molar ratios of $FeCl_3$ x nH_2O are at 3 or even lower. The Cl^-/Fe(III) molar ratio of typical ISA particles is at least 30 times smaller than the molar Cl^-/Fe(III) ratio of 101 of the tested ISA by Wittmer [124]. This reduces the Fe demand for ISA production again at least by 1 order of magnitude from <1.8 Tg yr^{-1} to about <0.2 Tg yr^{-1}.

Wittmer et al. [124] considered only sea-salt aerosol particles as transport vehicles for ISA and as only possible contact medium to gain chloride ions as °Cl source. It is well known that coal combustion is a major source of active chlorine [441-443], as well as iron [78, 79, 83, 451], thus both iron and chlorine are jointly issued by other mechanisms and sources.

As stated in our chapter 6.2 below point 5, sea salt aerosol has residence times in the troposphere lower than one day according to its coarse particle diameters without any possible bridging of intercontinental distances.

In reality the chloride transfer between sea-salt aerosol particles and ISA particles may take place without any touch or coagulation, because the troposphere is an acidic environment. Troposphere is a source of organic and inorganic acids which are in permanent contact with the sea-salt aerosol. The acid ingredients in contact with sea spray produce HCl. Further ISA is produced by combustion and is elevated by flue gas plumes: acid precursors such as SO_2 or NO_x are in higher concentrations within the flue gas plume comparing to the tropospheric environment. The acids generated by flue gas plume produce additional HCl by reaction with the sea-salt aerosol [167]. As a result, ISA and ISA precursors may absorb any chloride requirement via HCl vapor from the sea-spray source by itself [127].

Additionally to the °Cl emission increase with increasing iron concentration in the tested aerosols, the results of Wittmer verify an increase in °Cl emission with decreasing pH [124]. According to Wittmer and Meyer-Oeste [439, 450], oxidic ISA aerosol particles may be generated free from any pH-buffering alkaline components. This hampers their pH decrease by air-borne HCl to the optimum pH around pH 2. Sea-salt buffering of the absorbed HCl [452] by the alkali and earthen alkali content of sea-salt aerosol can occur only by coagulation, most probable in a minor ISA particle fraction but not in the bulk. From the beginning of its action in the troposphere, ISA keeps in the optimum °Cl emission mode: low pH, and high iron concentration levels.

Preferred ISA is produced by the ISA method variant 1 or variant 3 as described in chapter 7. Hence, ISA are composed of particles made by flame pyrolysis or iron salt vapor condensation. The mentioned ISA particles have diameters of $^{1}/_{10}$ of the particle diameters of the Wittmer tests. These ISA particles have optimum chlorine activation efficiency:

- In an appropriate chloride dotation or chloride delivering environment;
- At a pH <2;
- If they are emitted above the tropospheric boundary layer.

Then the Fe demand may fall up even shorter than the calculated 0.2 Tg Fe yr^{-1} due to their far extended surface area and far extended residence time in the atmosphere.

It has to be noted that this ISA demand calculation result refers only to the ISA cooling property according to CH_4 depletion; further cooling properties according to cloud albedo, depletion of CO_2, black and brown aerosol, ozone decrease and further causes are still kept unconsidered.

Further oxidation activity on GHGs and aerosols are induced by the °OH generation activity of ISA: volcanic eruption plumes contain high concentrations of °Cl plus °OH [152] and are characterized by decreased CH_4 concentrations [153]. Co-absorption of H_2O and HCl is the

main reason of the generation of volcanic ash particle coats containing soluble Fe salts originating from insoluble Fe oxides and Fe silicates [453, 454]. Gaseous HCl from the eruption plume entails Fe chlorides covering the surfaces of volcanic ash particles [455]. Therefore, it is reasonable that photolysis of those chlorides is the origin of both: °Cl and °OH generation in volcanic plumes.

Hydroxide radical °OH can change from the liquid aerosol phase into gaseous phase [169]. But by far, not as easy as °Cl can. Indeed, the Henry's law solubility constant of °OH is about one order of magnitude higher than that of °Cl and is in the same range than that of NH_3 [166]. But when their hygroscopic water layer shrinks in dry air or by freezing, ISA particles might act as °OH emitters. These additional °OH emissions might further increase the CH_4 oxidation potential of volcanic ash or artificial ISA and thus reduce even more the Fe demand for ISA, though this has not been tested yet, it cannot be ruled out.

In order to take care not to overstep the cooling effect too far, a reasonable goal might be to start the ISA method with a global ISA emission of 0.1 Tg Fe yr^{-1}. This quantity corresponds to the magnitude of the actual Fe input from the atmosphere into the oceans under the form of soluble salt, which is estimated to be from 0.1 up to 0.26 Tg yr^{-1} [74, 80, 456]. Doubling or even tripling of this input quantity by the ISA method is of easy technical and economic feasibility as will been seen in chapter 7.

7. The ISA method: how to increase artificial iron emissions

Preceding calculation evidenced that the ISA method has the potential to cut back the rise of CH_4 and CO_2 and, vice versa, the small decline of atmospheric oxygen content [457, 458] because it acts by a bundle of chemical and physical means. The ISA method might retard, stop or even help to restore these GHGs contents to pre-industrial levels. By the ISA method, doubling or tripling of the ISA level in the troposphere seems to be possible by feasible technical and economical means.

Since 2004 proposals have been published [141, 439, 450, 459, 460] to modify combustion processes and flue gas emissions in order to use them as ISA plume emission sources in the troposphere, by traffic and power generating combustions and their warm uplifting flue gases. Predestined for the ISA method are any hot flue gas plumes emitted by ship and air traffic, fossil and sunshine power.

At least three variants of ISA production are proposed:

- Variant 1: Emission of flame pyrolytic FeOOH aerosol with particle diameters smaller than 100 nm [461, 462] as ISA precursor by co-combustion of organic iron or carbonyl iron additives with liquid or gaseous fuels, or heating oils combusted in ship or and jet engines, or by oil or gas combustors. Co-combustion of iron compounds is a possible

measure in coal power stations and mixing the ISA precursor containing ~~oil~~ combustion flue gas to the coal combustion flue gas after the dry flue gas cleaning stage. Useful side effects of iron additives are fuel efficiency optimization and soot emission minimizing [223, 224, 463, 464]. The emitted FeOOH aerosol plumes convert immediately into the ISA plume after leaving the emission sources, due to the high reactivity of flame pyrolytic Fe oxides. The period to cover the flame pyrolytic FeOOH particle surface by HCl absorption from the gaseous phase with Fe(III) chlorides is several times shorter comparing to the generation of iron chlorides from natural iron oxide minerals in loess dust particles [452, 465].

• Variant 2: Injection of vaporous ISA precursor iron compounds such as $FeCl_3$ into a carrier gas. By contacting the carrier gas and/or the atmosphere the vaporous iron compounds condenses and/or converts by physical and/or chemical means directly into ISA. Contrary to all other ISA precursors, the sunlit $FeCl_3$ vapor is photo-reduced by concomitant generation of °Cl [466]. Thus methane depleting °Cl emission can start even before this ISA precursor has changed into hydrated $FeCl_3$.

• Variant 3: Injection of ultrasonic nebulized aqueous $FeCl_3$ solution as ISA precursor into a carrier gas. By water evaporation from the aerosol droplets ISA is generated.

The preferred heights of ISA plume generation in the troposphere are 1000 m above ground or higher altitudes in order to pass the boundary layer. There, the ISA plumes have optimum conditions to spread over sufficient life-times. The necessary buoyancy to lift up the ISA plumes can be regulated by controlling their carrier gas temperatures. Uplift towers [467], vortex generators [468] or tethered balloons [469, 470] are preferential means to direct ISA by carrier gas uplift to said heights.

The primary ochre colored FeOOH aerosol particles emitted by ISA method I have diameters of <0,05 µm. According to previous studies iron oxides are strong absorbers at visible wavelengths and might play a critical role in climate perturbation caused by dust aerosols [108, 109]. But this effect is not applicable to the ISA methods FeOOH aerosol because it is emitted by parallel generated flue gas plumes containing SO_2 and NO_x as sulfuric and nitric acid generators. Due to their small diameter dependent high surface area the aerosol particles immediately react with HCl. HCl is generated by the reaction between sea-salt aerosol and flue gas borne acids. Primary reaction product is the orange colored $FeCl_3$ aerosol: ISA. But the day time sun radiation bleaches ISA by $FeCl_2$ and °Cl generation; the night time re-oxidation of ISA plus HCl absorption regenerates $FeCl_3$ again. $FeCl_2$ is colorless at low humidity; pale green at high humidity.

Provision of the phytoplankton to optimize its growth with further nutrients such as Mn, Zn, Co, Cu, Mo, B, Si and P by the ISA method is possible by at least the variants 1-3 of the ISA method by co-combustion, co-condensation or co-nebulizing.

Global fixing regulations of GHGs emission certificate prices, values, and ISA emission certificate credit values would be simple but effective measures for the quickest world-wide implementation of the ISA flue gas conditioning method.

Anderson [471] reminded that of the 400 IPCC scenarios that keep warming below the Paris agreement target, "*344 involve the deployment of negative emissions technologies*", which he qualifies of "*speculative*" or requiring geoengineering.

A large part of the research devoted to climate engineering methods concerns SRM (sunlight reduction methods), such as mimicking the effects of large volcanic emissions by adding sulfates aerosols into the stratosphere as suggested for instance by Crutzen [242]. Numerous other types of particles have been suggested for these aerosols for instance titania by Jones [472]. But SRM only buys time and has numerous drawbacks.

On the one hand, SRM did not address the main cause of global warming (GHG emissions), nor prevents ocean acidification. On the other hand, several CDR technologies do, but their costs are much larger than SRM and the scale requested poses many technological challenges, for instance *"scaling up carbon dioxide capture and storage from megatons to gigatons*" [473].

Very few CDR methods without emission of disadvantageous pollution are known. One of those is the Terra Preta method: it is characterized by the mixing of grinded bio-char into agricultural soils. The climate relevancies of this method are sustained fixation of former CO_2 carbon, minimizing fertilizer consumption and N_2O emission reduction from the fertilized Terra Preta soils. Char has similar properties within the soil environment than humic substances, but in the environment, char is resistant against oxidation.

Comparing the Terra Preta method to other CDR methods such as fertilizing the ocean by micro nutrients, results in lower specific material expenses by CDR methods per unit of CO_2 removed from the atmosphere [474]. The ISA method we propose is a member of this CDR group, thus this result is also valid. in addition the further climate effects of the ISA method (such as depletion of CH_4, tropospheric ozone, and soot, plus cloud whitening) reduce the specific material expense level. Furthermore, the ISA method mimics a natural phenomenon (mineral iron-dust transport and deposition) and only proposes to improve the efficiency of an already existing anthropogenic pollution. Myriokefalitakis et al. [475] estimates that "*The present level of atmospheric deposition of dissolved Fe over the global ocean is calculated to be about 3 times higher than for 1850 emissions, and about a 30% decrease is projected for 2100 emissions. These changes are expected to impact most on the high-nutrient–low-chlorophyll oceanic regions.*" Their model "*results show a 5-fold decrease in Fe emissions from anthropogenic combustion sources in the year 2100 against in the present day, and about 45% reduction in mineral-Fe dissolution compared to the present day*". Meanwhile the model used by [54] predicts by 2090 an iron supply increase to HNLC surface waters

especially in the eastern equatorial Pacific attributed by the authors to changes in the meridional overturning and gyre-scale circulations that might intensify the advective supply of iron to surface waters. Furthermore, several authors [77, 87, 476-478] point out that both glacial and deep-water Fe sources may increase with continued climate warming due to Fe input from other sources, such as shelf sediments, melt water, icebergs, rivers, surface water runoff and dust input.

Recently Boyd and Bressac [67] suggested starting rapidly tests to determine efficiency and side effects of CDR ocean iron fertilizing methods, and analyzed possible geopolitical conflicts together with some other geoengineering methods [479].

Several experts, for instance Hansen et al. [6], expressed recently the urgent warning that mankind has only short time left to address and control climate warming. As a consequence mankind ought to find out as soon as possible climate controlling matter which might generate the most effective and reversible climate cooling effects within the shortest period. Lifetime of ISA emissions in the troposphere are much shorter than that of sulfates in the stratosphere. Of course, such tools and agents have to be rapidly evaluated against side-effects to ecosystems, human health, and last but not least their economic burdens.

8. Interaction of the ISA method with further measures to protect the environment

According to Wittmer & Zetzsch [127] elevated HCl content in the atmosphere triggers the methane depleting coating of oxidic ISA precursors by photolytic active Fe(III) chlorides. Any measure triggering the reduction of the HCl content of the atmosphere would impair the effectiveness of the ISA method based on this kind of method.

In this sense all kind of measures to reduce the sulfur and NO_x content of the flue gas content of gaseous, liquid or gaseous fuels belongs would decrease the effectiveness of oxidic ISA precursors, as the S and NO_x oxidation products sulfuric acid aerosol and gaseous nitric acid are the main producers of HCl by changing sea salt aerosol into sulfate and nitrate aerosol. Even the measures of reducing the energy production from fuel burning by changing to wind and photovoltaic energy would reduce this HCl source.

Sea salt aerosols produce HCl after contact with organic aerosol and organic volatile matter as the latter generates acid oxidation products from the latter such as oxalic acid [150, 480, 481]. A large fraction of organic aerosols and secondary organic aerosols originate from anthropogenic sources such as combustions. The change to wind and photovoltaic energy would reduce this HCl source.

The proposed CE measure of producing sulfuric acid aerosol within the stratosphere by inducing an albedo increase would increase the HCl content, during contact of the precipitating acid aerosol with tropospheric sea salt aerosol. Even the proposed CE measure

of increasing the sea salt aerosol content of the troposphere by artificial sea salt aerosol as cloud whitening measure could be used as ISA method trigger if flue gas is used to elevate the sea salt aerosol.

9. Discussion

In order to fight global warming, this review proposes to enhance the natural actions of Cl atoms in the troposphere, together with the synergistic action of iron in the atmosphere, ocean, oceanic sediment and land compartments, as a climate engineering method. The main results expected are a diminution of long lived well mixed atmospheric methane and carbon dioxide, but the diminution of local short lived tropospheric ozone is also possible, as well as effects on the Earth albedo, restoration of the oxygen flux into the deep ocean basins, organic carbon storage, etc.

The most important actor in the process of CO_2 C transfer from atmosphere into the Earth interior is the carbonate C precipitation in the crust rocks and sediments below the ocean. The ocean crust acts like a conveyor belt between crust evolution at MOR and its subduction zones into the mantle. Transported medium are carbonate C, small amounts of organic C, ocean salt, ocean water and sediments. This process is part of the homeostasis of the planet. Disturbances of this system part are induced by stratification processes within the ocean basins caused by density differences between different layers of the water column. Most stratification events are induced by climate warmings. Any of these homeostasis disturbances are removed by the system within geological time scales. Signs of such disturbances are more or less prominent events of extinction and of elevated organic C content in the ocean sediments. Because the recent climate warming will induce a new ocean stratification event, mankind ought to stop it. Like several interglacial stratification events in the glacial periods, the actual stratification is also induced by increasing melt water discharge. The past interruptions of the interglacial climate warmings teach us, that the interruption events were accompanied as a rule by dust events. As demonstrated, the climate cooling effects of these dust events are induced by the chemical and physical actions of ISA.

In high-nutrient, low-chlorophyll oceanic areas, where the contribution of atmospheric deposition of iron to the surface ocean could account for about 50% of C fixation, as well as in oceanic nitrogen-limited areas, where atmospheric iron relieves the iron limitation of diazotrophic organisms (thus contributing to the rate of N fixation), atmospheric deposition of iron has the potential to augment atmospherically supported rates of C fixation [482] and thus “cool the Earth” by removing CO_2 from the atmosphere.

Maybe the iron atmospheric deposition over terrestrial landscapes and wetlands has similar effects? Are there possible benefits of atmospheric deposition of soluble iron over the continents, where iron deficiency in plants occurs over 30% of them which are high pH calcareous soils that make soil Fe unavailable for plants [395]? Iron deficiency induced chlorosis in plants can be solved by addition of soluble iron complexes to the soil, or by foliar application of sprays containing mineral iron (for instance $FeSO_4$) [396] or iron chelates (Fe-EDTA among others) [399]. Iron, sulfate and several organic iron complexes such as iron-oxalate are known constituents of atmospheric dust [74], but unfortunately no published work was found about possible effects on plant chlorosis by foliar deposition of soluble iron from atmospheric dust.

We did not find studies about the impacts of atmospheric iron nutrient deposition on terrestrial ecosystems productivity. More research is needed to continue to enhance our understanding of the possible benefits of the iron cycling in freshwater and terrestrial landscape environments, as well as in atmospheric and sediment environments, in particular on its numerous potential capacities to fight global warming. The cooling effects of ISA and iron reviewed in this article already provide insight into the progress made on understanding the iron cycles from a range of perspectives.

There is abundant literature on the many geoengineering methods that have been proposed to *"cool the Earth"* [483, 484]. In particular, the injection of sulfate aerosols into the stratosphere is the most studied method, as it mimics the episodic action of natural volcanoes [163, 387]. Injected particles into the stratosphere reduce the radiative balance of Earth by scattering solar radiation back to space, so several types of particles are envisioned with a wide range of side-effects [472].

The literature also describes many options to deliver sulfates, their precursors (or other particles) to the stratosphere [469]. For instance, airplane delivery of the sulfate aerosols by the kerosene combustion process requires military jets due to commercial aircrafts limited altitude of 10 km (30,000 feet), and not the 20 km requested [469].

In the case of ISA, the altitude needed to *"cool the Earth"* is much lower: it is in the troposphere and the total quantities to deliver are 1 order of magnitude smaller. So air travel is a possible means for ISA delivery. But the global jet fuel consumption is only about 240,000 t yr^{-1}. Even by assuming the very high emission rate of 1 kg ISA precursor iron per ton of jet fuel, only 240 t yr^{-1} might be emitted. This seems far away from the order of magnitude of the target ISA emissions.

From the many other possible delivery strategies envisioned for SRM by stratospheric aerosols, many are not suited for ISA, such as artillery, missiles and rockets [469]: it will be cheaper with less pollution to use the flue gas of a reduced number of thermal power plants. That might be efficient enough to deliver the artificial iron aerosol needed over the boundary

layer, in order to the aerosols to stay several days or weeks in the troposphere and become widely distributed [485].

According to Luo [79], deposition of soluble iron from combustion already contributes from 20 to 100% of the soluble iron deposition over many ocean regions.

As an example we calculated the possible production and emission of the ISA precursor FeOOH aerosol using the flue gas of the German power station Niederaußem; with the input of 25 million t yr^{-1} of lignite (brown coal), this power station produces 3,600 MW.

According to ISA production variant 1 (chapter 6) the ISA precursor FeOOH aerosol may be produced by burning of a ferrocene ($Fe(C_5H_5)_2$) oil solution containing 1% ferrocene in a separate simple oil burner. The hot oil burner flue gas containing the ISA precursor FeOOH aerosol is injected and mixed into the cleaned power station flue gas. The power station flue gas emission rate is calculated to 9,000 m^3 flue gas per ton of lignite. As the ISA precursor containing flue gas will be elevated to heights of more than 1000 m above ground, dust levels of the ISA precursor FeOOH aerosol of 20 mg m^{-3} flue gas seem to be acceptable. This allows a quantity of 180 g of FeOOH per ton of combusted lignite (9000 m^3 t^{-1} x 0,02 g m^{-3}). At a lignite quantity of 25 million t yr^{-1}, this corresponds to 4,500 t FeOOH yr^{-1}. FeOOH has an iron content of 63%. This corresponds to a possible iron emission of 2,831 t yr^{-1} and a possible ferrocene consumption of 9,438 t yr^{-1}.

Corresponding to this calculation about 100 of such huge power stations should have the ability to produce the sufficient ISA quantity of an equivalent of 200,000 to 300,000 t Fe yr^{-1}. Further optimization of the cooling capacity of the produced ISA is possible by a co-emission of HCl, for instance by co-burning of an organic HCl precursor.

This example illustrates that ISA emission at only 100 power stations, or any similar ISA emission measures, is quite feasible compared to the alternative of CCS by CO_2 capture from the flue gas of 40 Gt yr^{-1}, compression of the CO_2 until the liquid state, followed by transportation and CO_2 storage by injection into underground rock aquifers or into old and depleted fossil fuel reservoirs.

In order to increase the effectiveness of the buoyancy capacity of the power works the usual wet cooling tower might be replaced by a dry cooling tower to mix the dry and warm air emission from the cooling tower with the hot flue gas as additional buoyancy and due point reduction mean. Further the flue gas buoyancy may increase by increasing the flue gas temperature. This or other simple techniques to realize ISA plumes may be used within the troposphere.

One alternative delivery method that seems promising and can easily be adapted to ISA method, is the use of tethered balloons [486], and will cost much less as 1 or 2 km altitude will be sufficient for ISA emissions, requiring much lower pressures in the pipes than for SO_2 delivery at 20 km for the geoengineering method. Technical and economic feasibility have

already been studied for the SPICE project [470] which was planning to release sea water spray at 1 km altitude.

Furthermore, as iron emissions only stay in the troposphere for weeks compared to SRM sulfates in the stratosphere that stay 1 or 2 years. In case any unintentional side effect or problem occurs, stopping the emissions is rapidly possible and the reversibility of its effects are much shorter than for solar radiation management by sulfates aerosols.

Other geoengineering strategies to cool the Earth, such as carbon dioxide removal by iron fertilization [64] have several pros and cons, such as localized release, less dispersion, in a form that is not readily bio-available, resulting in restricted cooling effects and high expenses.

The idea of ocean fertilization by iron to enhance the CO_2 conversion by phytoplankton assimilation came up within the last two decades. Proposed was the mixing of an iron salt solution by ships into the ocean surface. This idea was debated controversial. Example of this debate is the discussion between KS Johnson et al. and SW Chisholm et al. [68, 69]. Deeper insight into this debate is given by Boyd and Bressac [67].

The iron fertilization procedure tests done so far had been restricted to relatively small ocean regions [51, 52, 487]. These tests produced iron concentrations orders of magnitude above those produced by natural ISA processing which are in the single decadal order of milligrams of additional dissolved iron input per square meter per year. In this sense the ISA method is quite different from “iron fertilization”. As known from satellite views, phytoplankton blooms induced by natural dust emission events from the Sahara, Gobi and further dust sources, there is no doubt about the fertilizing effect of iron. Meanwhile this kind of natural iron fertilization enhancing the transfer of CO_2-Carbon into organic sediment carbon via the oceanic food chain seems to be un-contradicted and accepted [6].

The ISA method allows the use of the same atom of iron several times by catalytic and photocatalytic processes into the atmosphere, with different cooling effects (such as albedo modification and enhancement of the methane destruction) and then reaches the oceans, with further cooling effects such as the enhancement of CO_2 carbon fixation.

Harrison [488] estimates that a single ship based fertilization of the Southern Ocean will result only in a net sequestration of 0.01 t Carbon km^{-2} for 100 years at a cost of US$457 per ton of CO_2, as the economic challenge of distributing low concentrations of iron over large ocean surface areas, has been underestimated [489], as well as the numerous loss processes (i.e.: soluble iron loss and organic carbon that do not sink till the bottom of the ocean) resulting in reduced net storage of carbon per km^2 of ocean fertilized.

Figure 7 summarizes many of the cooling effects of the ISA method.

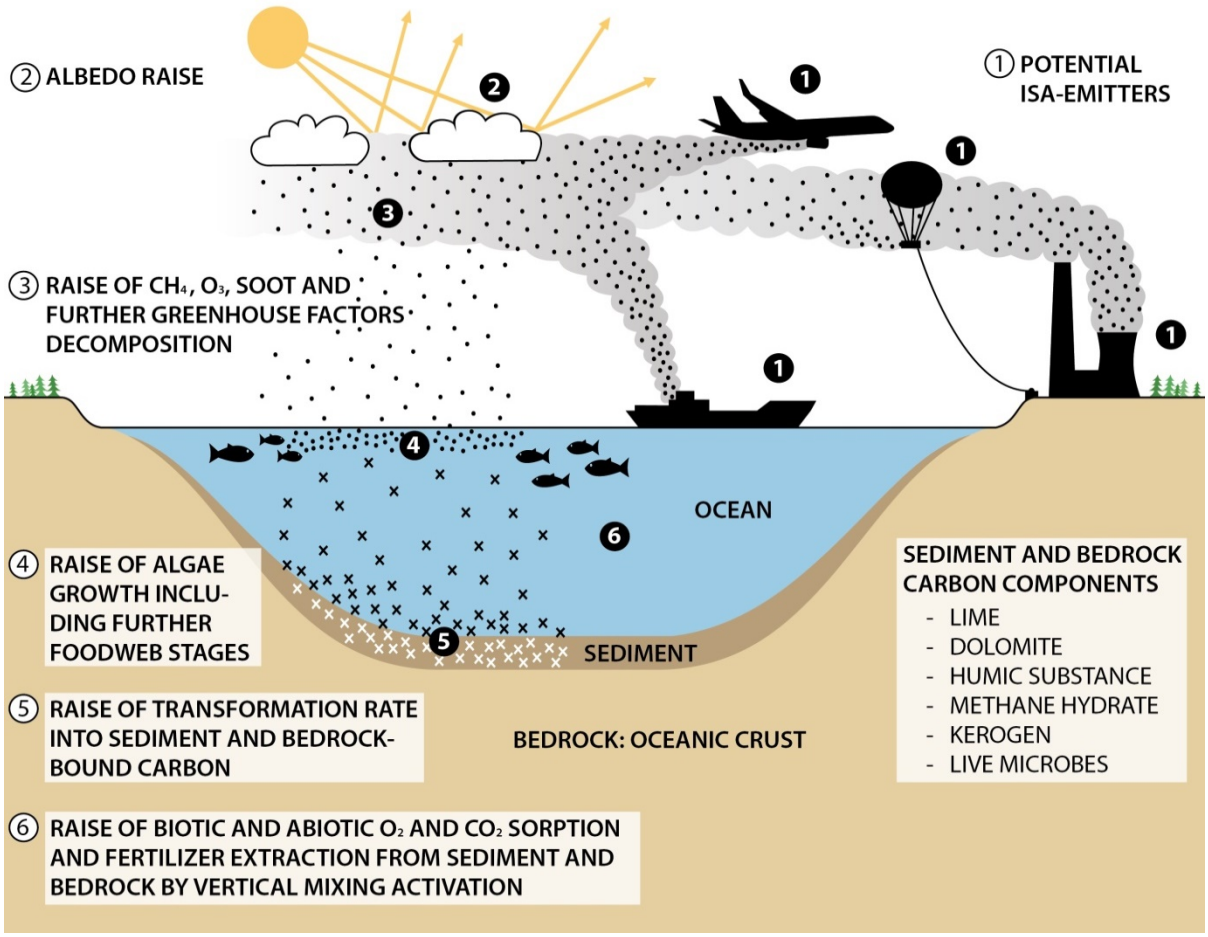

Figure 7. Summary of the principal cooling effects of the proposed iron salt aerosols method. The organic C / carbonate C burial ratio in sediments and bedrock increase after ISA method start, until a maximum. Then this ratio begins to decrease as soon as the vertical current components in the ocean basin begin to act. Then the ratio arrives to a very low permanent level, while the total of buried C arrives at a permanent maximum level when the maximum vertical mixing conditions have been obtained by the ISA method.

Why does ISA appear to be more effective than ocean iron fertilization? For ocean iron fertilization several tons of Fe(II) are dispersed in a short time (hours) over only some km^2 of ocean with several drawbacks and a massive algae bloom can change the local biotopes. Meanwhile ISA releases iron continuously, reaching the entire 510 million km^2 of Earth surface. The current iron inputs (in the form of soluble salts) into the oceans are estimated between 0.1 and 0.26 Tg yr^{-1} [74, 80, 456]. As water covers nearly 72% of Earth surface (362 million km^2), if ISA delivers 1 Tg Fe yr^{-1} evenly distributed (in addition to natural and anthropogenic current emissions), which is 4 times more than the expected needs (chapter 5.2), on average every km^2 of ocean receives 5.4 g Fe km^{-2} day^{-1} ($^1/_{510}$ t Fe km^{-2} yr^{-1}).

10 Conclusion

At ideal circumstances the ocean acts as an optimum transport medium for CO_2 carbon from the atmosphere into the ocean crust. Such circumstances are present when the vertical cycling components between ocean surface and ocean bottom are undisturbed.

Any stratification event disturbs this cycling and interrupts the CO_2 transport. Climate warming can induce stratification events by producing huge amounts of melt water. Recent research found signs of at least regional development of a beginning stratification.

The numerous climate cooling effects of natural dust show in this review, according to its soluble iron content, demonstrate that dust is of a central significance as steering element of this carbon transport from the atmosphere into the ocean crust.

This review article demonstrates the enormous effects of atmospheric iron dusts and focuses first on the tropospheric aerosol particles composed partly of iron and chloride (iron salt aerosols ISA), showing their cooperation and interactions with several components of the atmosphere for instance with CH_4, as the chlorine atom is responsible for the removal of a significant part of this GHG (3 to 4 % of CH_4) in the troposphere [118, 119]. This article summarizes a dozen of other possible direct and indirect natural climate cooling mechanisms induced by the iron biogeochemistry in all the Earth compartments: atmosphere, oceans, land (surface, soil), sediment and crust.

These dozen possible climate cooling effects due to the multi-stage chemistry of iron within the atmosphere, hydrosphere, geosphere and lithosphere are described all together for the first time and are summarized in table 3, which shows the most probable climate cooling effects of ISA. They include the ocean fertilization effect which allows enhanced algal and phytoplankton growth, which removes mineral CO_2 from the atmosphere and transforms it in organic carbon, a part of which can sink to the bottom of the oceans and be stored for long periods of time by different mechanisms that are described.

Table 3: principal effects of the ISA method proposed - or its natural equivalent - and their probable effect on the different biosphere compartments.

Compartment	Locality and/or action	Effect	Most probable cooling efficiency	Time delay between cooling on-set or off-set after ISA method start or stop
Troposphere	Boundary layer and lower	Cloud albedo increase	+++	<1 yr

	troposphere	Methane and VOC depletion	+++	<1 yr
		Black and brown carbon precipitation	++	<1 yr
		Ozone depletion	++	<1 yr
Continent	Forests and further primary producer	Organic C burial increase by assimilation increase	+	<5 yr
	Wetlands, marshes, peat bogs, lake sediments	Methane emission decrease by methanogenesis inhibition	+++	<5 yr
	Desert surfaces	Methane and VOC depletion	+ / -	<1 yr
Ocean and ocean sediment aquifer at the ocean bottom	Phytoplankton and the further food chain links	Organic and Carbonate C burial increase by assimilation increase	1) ++++	<1 yr
			2) +	<1 yr
Ocean crust aquifer	Activation of the ocean basin vertical cycling	Carbonate C burial increase in the ocean crust rock	3) +++++	>10 yr
			4) + / +++	>10 yr

1) The euxinic and alkaline bottom water of the stratified ocean have no oxidation and calcite solution capacity, thus produce a high burial rate of organic sediment C and carbonate C
2) The oxic, hydrogen carbonate and CO_2-containing bottom water of the well-mixed ocean have high oxidation capacity and high calcite dissolving capacity, thus produce a low burial rate of organic and inorganic Sediment C
3) The high inorganic C load of the oxic, hydrogen carbonate and CO_2-containing bottom water of the well-mixed ocean comes to total precipitation within the alkaline and reducing crust aquifer, thus produce a very high burial rate of inorganic C and small amounts of organic C precipitation
4) The euxinic and alkaline bottom water of the stratified ocean has low content of dissolved inorganic C and contains methane C up to saturation, thus produce low to medium C burial rate during cycling through the crust aquifer.

In order to explicitly handle the interaction of climate and biogeochemistry, the complex interactions between climate and the cycles of C, N, P, H_2O and micronutrients call for models that integrate global biogeochemical cycles of terrestrial, oceanic and atmospheric components of the biosphere.

While the iron biogeochemical cycle between the atmosphere and the ocean is considered in numerous publications, the treatment of key processes and feedbacks within the terrestrial compartment has been rather limited, and further development is urgently needed.

Mineral dust aerosols containing iron and other important nutrients or micro-nutrients are well studied components of the iron biogeochemical cycle in the atmosphere and the oceans, but the absence of recent bibliography about the full iron biogeochemical cycle over terrestrial landscapes, soils, wetlands and all clear water compartments (glaciers, ice, snow, lakes, and groundwater) points out a lack of up-to-date overview. In our opinion, the atmospheric

chemistry models need to incorporate all relevant interaction compartments of the Fe-cycle with sun radiation, chlorine, sulphur, nitrogen, oxygen, carbon and water in order to model the several planetary cooling effects of the iron cycle.

Acid rain sulphate (SO_4^{2-}) deposition on peatlands and wetlands from natural sources (volcanoes), or anthropogenic sources (fossil fuel combustion) is a known suppressant of CH_4 production [490, 491] and emissions [492-494] and may be an important process in terms of global climate. The importance of the Fe input associated with anthropogenic aerosol deposition in terrestrial biogeochemistry deserves further investigation as well as the possible impacts of a drastic diminution of anthropogenic iron and sulfates emissions from combustion processes expected by 2050 to satisfy the Paris climate agreement.

This review completes the previous global iron cycle visions [50, 52, 74, 97, 98, 495-497] and advocates a balanced approach to make profit of the iron cycle to fight global warming by enhancing natural processes.

Climate cooling by natural ISA involves the troposphere, dry solid surfaces, ocean waters, ocean sediment, ocean crust and land. Several GHG factors are controlled by ISA: CO_2, CH_4, tropospheric O_3, black carbon, dust, cloud albedo, and vertical ocean mixing.

Using mineral dust as a natural analogue tool, this article proposes to enhance the natural ISA in order to raise and heighten the cooling impacts of at least two of the dozen natural effects found: i.e. CH_4 removal by tropospheric °Cl and CO_2 removal by soluble-Fe ocean fertilization.

The ISA method proposed is feasible, probably with few to no-environmental side-effects, as it relates to chemical and/or physical combustion processes occurring currently. Actual iron production and coal combustion together with other combustions sources already release in the atmosphere a very significant part of the global bioavailable iron in the northern oceans: from 15% [80] to 80% [82, 83] depending on the iron solubility parameters taken into account.

The present level of atmospheric deposition of soluble Fe over the global ocean is evaluated to be about 3 times higher than for 1850 emissions [475], as increases in anthropogenic and biomass burning-emissions resulted in both enhanced Fe combustion emissions and a more acidic environment and thus more than double soluble Fe deposition (nearly 0.5 Tg-Fe yr^{-1} nowadays versus nearly 0.2 Tg-Fe yr^{-1} in 1850).

Inevitable reduction of aerosol emissions to improve air quality in the future might accelerate the decline of oceanic productivity per unit warming and accelerate decline in oceanic NPP [498]. Myriokefalitakis model projected results for 2100 indicate about a $^1/_4$ decrease in atmospheric deposition of soluble Fe, with a 5-fold decrease in Fe emissions from anthropogenic combustion sources (~0.070 Tg-Fe yr^{-1} nowadays against ~0.013 Tg-Fe yr^{-1} in 2100). These changes are expected to impact most on the high-nutrient–low-chlorophyll

oceanic regions. According to Myriokefalitakis [475], in view of the importance of Fe as a micronutrient for marine ecosystems, the calculated projected changes in soluble iron emissions, requires the implementation of comprehensive mineral-Fe dissolution processes as well as Fe combustion emissions in coupled climate-biogeochemistry models to account for feedbacks between climate and biogeochemical cycles. This review shows that the effects on CH_4 of ISA and of anthropogenic Fe emissions in the troposphere also deserve to be taken into account.

According to Wang et al. [83], taking into consideration the relatively high solubility of anthropogenic iron, combustion sources contribution to soluble Fe supply for northern Pacific and northern Atlantic oceanic ecosystems could be amplified by 1–2 orders of magnitude. To stop global warming, we estimated the requirements in terms of ISA by extrapolation of experiments of iron catalyzed activation by artificial sea-salt aerosols [124, 127]. Our first estimations show that by doubling the current natural Fe emissions by ISA emissions into the troposphere, i.e. by about 0.3 Tg Fe yr^{-1}, artificial ISA would enable the prevention or even the reversal of GW.

The adjustable flue gas temperatures for different types of combustions are a means to lift the ISA plumes to optimal heights within the troposphere. Thus, we believe that the ISA method proposed integrates technical and economically feasible tools that can help to stop GW.

According to our remarks in chapter 2, the reactions of ISA in the troposphere are the most prominent results for a surface temperature decrease [439]. This stops further ice melting, which activates the different vertical ocean water movements. As a result, the dissolved CO_2 is then buried as carbonate C within the ocean bottom sediments and crust.

Abbreviations:

Carbon capture and storage: CCS; Cloud condensation nuclei: CCN; Global Warming: GW; Intergovernmental Panel on Climate Change: IPPC; Iron salt: IS; Iron salt aerosols: ISA; Humic-like substances: HULIS; Hydroxyl radical: °OH; Chlorine radical: °Cl; Bromine radical: °Br; Ligand: L; Methane: CH_4; Mid-ocean rift: MOR; Secondary organic aerosol: SOA; Thermohaline circulation: THC; Volatile organic compounds: VOC.

Authors contribution:

F.D. Oeste suggested the review idea and performed initial bibliographical search completed by R. de Richter. F.D. Oeste and R. de Richter prepared the manuscript and the figures with contributions from all co-authors. T. Ming and S. Caillol also contributed to structuring the manuscript, ideas, submitting bibliography and English corrections.

Competing interests

The authors declare that they have no conflict of interest.

Acknowledgment:

This research was supported by the Scientific Research Foundation of Wuhan University of Technology (No. 40120237) and the ESI Discipline Promotion Foundation of WUT (No.35400664).

The co-authors would like to thank both reviewers S.M. Elliott and Anonymous for their constructive and thoughtful reviews which greatly improved this manuscript, in particular chapters 5, 9 and 10. We also thank Rolf Sander and Cornelius Zetzsch for their constructive comments and Louise Phillips for grammatical corrections and re-reading.

Bibliography:

[1] de Lavergne C, Palter JB, Galbraith ED, Bernardello R, Marinov I. Cessation of deep convection in the open Southern Ocean under anthropogenic climate change. Nature Climate Change. 2014;4:278-82.

[2] Bernardello R, Marinov I, Palter JB, Galbraith ED, Sarmiento JL. Impact of Weddell Sea deep convection on natural and anthropogenic carbon in a climate model. Geophysical Research Letters. 2014;41:7262-9.

[3] Bernardello R, Marinov I, Palter JB, Sarmiento JL, Galbraith ED, Slater RD. Response of the ocean natural carbon storage to projected twenty-first-century climate change. Journal of Climate. 2014;27:2033-53.

[4] Capone DG, Hutchins DA. Microbial biogeochemistry of coastal upwelling regimes in a changing ocean. Nature geoscience. 2013;6:711-7.

[5] Kalvelage T, Lavik G, Lam P, Contreras S, Arteaga L, Löscher CR, et al. Nitrogen cycling driven by organic matter export in the South Pacific oxygen minimum zone. Nature geoscience. 2013;6:228-34.

[6] Hansen J, Sato M, Hearty P, Ruedy R, Kelley M, Masson-Delmotte V, et al. Ice melt, sea level rise and superstorms: evidence from paleoclimate data, climate modeling, and modern observations that 2° C global warming is highly dangerous. Atmospheric Chemistry and Physics Discussions. 2016;15:20059-179.

[7] van Helmond NA, Sluijs A, Sinninghe Damsté JS, Reichart G-J, Voigt S, Erbacher J, et al. Freshwater discharge controlled deposition of Cenomanian–Turonian black shales on the NW European epicontinental shelf (Wunstorf, northern Germany). Climate of the Past. 2015;11:495-508.

[8] Friedrich O, Erbacher J, Moriya K, Wilson PA, Kuhnert H. Warm saline intermediate waters in the Cretaceous tropical Atlantic Ocean. Nature Geoscience. 2008;1:453-7.

[9] Voss M, Bange HW, Dippner JW, Middelburg JJ, Montoya JP, Ward B. The marine nitrogen cycle: recent discoveries, uncertainties and the potential relevance of climate change. Philosophical Transactions of the Royal Society B: Biological Sciences. 2013;368:20130121.

[10] Klotz MG, Stein LY. Nitrifier genomics and evolution of the nitrogen cycle. FEMS microbiology letters. 2008;278:146-56.

[11] Simon J, Klotz MG. Diversity and evolution of bioenergetic systems involved in microbial nitrogen compound transformations. Biochimica et Biophysica Acta (BBA)-Bioenergetics. 2013;1827:114-35.

[12] Eckert S, Brumsack H-J, Severmann S, Schnetger B, März C, Fröllje H. Establishment of euxinic conditions in the Holocene Black Sea. Geology. 2013;41:431-4.

[13] Meyers PA. Why are the δ13Corg values in Phanerozoic black shales more negative than in modern marine organic matter? Geochemistry, Geophysics, Geosystems. 2014;15:3085-106.

[14] Praetorius S, Mix A, Walczak M, Wolhowe M, Addison J, Prahl F. North Pacific deglacial hypoxic events linked to abrupt ocean warming. Nature. 2015;527:362-6.

[15] Kaiho K, Saito R, Ito K, Miyaji T, Biswas R, Tian L, et al. Effects of soil erosion and anoxic–euxinic ocean in the Permian–Triassic marine crisis. Heliyon. 2016;2:e00137.

[16] Phrampus BJ, Hornbach MJ, Ruppel CD, Hart PE. Widespread gas hydrate instability on the upper US Beaufort margin. Journal of Geophysical Research: Solid Earth. 2014;119:8594-609.

[17] Yamamoto A, Yamanaka Y, Oka A, Abe-Ouchi A. Ocean oxygen depletion due to decomposition of submarine methane hydrate. Geophysical Research Letters. 2014;41:5075-83.

[18] Bakun A, Black B, Bograd SJ, Garcia-Reyes M, Miller A, Rykaczewski R, et al. Anticipated effects of climate change on coastal upwelling ecosystems. Current Climate Change Reports. 2015;1:85-93.

[19] Branch TA, DeJoseph BM, Ray LJ, Wagner CA. Impacts of ocean acidification on marine seafood. Trends in ecology & evolution. 2013;28:178-86.

[20] Orcutt BN, Sylvan JB, Knab NJ, Edwards KJ. Microbial ecology of the dark ocean above, at, and below the seafloor. Microbiology and Molecular Biology Reviews. 2011;75:361-422.
[21] Sousa FL, Thiergart T, Landan G, Nelson-Sathi S, Pereira IA, Allen JF, et al. Early bioenergetic evolution. Philosophical Transactions of the Royal Society of London B: Biological Sciences. 2013;368:20130088.
[22] Dick GJ, Anantharaman K, Baker BJ, Li M, Reed DC, Sheik CS. The microbiology of deep-sea hydrothermal vent plumes: ecological and biogeographic linkages to seafloor and water column habitats. Hydrothermal microbial ecosystems. 2015:79.
[23] Postec A, Quéméneur M, Méline Bes NM, Benaïssa F, Payri C, Pelletier B, et al. Microbial diversity in a submarine carbonate edifice from the serpentinizing hydrothermal system of the Prony Bay (New Caledonia) over a 6-year period. Frontiers in microbiology. 2015;6.
[24] Martin W, Russell MJ. On the origin of biochemistry at an alkaline hydrothermal vent. Philosophical Transactions of the Royal Society of London B: Biological Sciences. 2007;362:1887-926.
[25] Resing JA, Sedwick PN, German CR, Jenkins WJ, Moffett JW, Sohst BM, et al. Basin-scale transport of hydrothermal dissolved metals across the South Pacific Ocean. Nature. 2015;523:200-3.
[26] Hawkes JA, Connelly D, Gledhill M, Achterberg EP. The stabilisation and transportation of dissolved iron from high temperature hydrothermal vent systems. Earth and Planetary Science Letters. 2013;375:280-90.
[27] Holm NG, Neubeck A. Reduction of nitrogen compounds in oceanic basement and its implications for HCN formation and abiotic organic synthesis. Geochem Trans. 2009;10.
[28] Monnin C, Chavagnac V, Boulart C, Ménez B, Gérard M, Gérard E, et al. Fluid chemistry of the low temperature hyperalkaline hydrothermal system of Prony Bay (New Caledonia). Biogeosciences. 2014;11:5687-706.
[29] Nielsen SG, Rehkämper M, Teagle DA, Butterfield DA, Alt JC, Halliday AN. Hydrothermal fluid fluxes calculated from the isotopic mass balance of thallium in the ocean crust. Earth and Planetary Science Letters. 2006;251:120-33.
[30] Kawagucci S, Chiba H, Ishibashi J-i, Yamanaka T, Toki T, Muramatsu Y, et al. Hydrothermal fluid geochemistry at the Iheya North field in the mid-Okinawa Trough: Implication for origin of methane in subseafloor fluid circulation systems. Geochemical Journal. 2011;45:109-24.
[31] Watson AJ, Vallis GK, Nikurashin M. Southern Ocean buoyancy forcing of ocean ventilation and glacial atmospheric CO2. Nature Geoscience. 2015.
[32] Coogan LA, Gillis KM. Evidence that low-temperature oceanic hydrothermal systems play an important role in the silicate-carbonate weathering cycle and long-term climate regulation. Geochemistry, Geophysics, Geosystems. 2013;14:1771-86.
[33] Otto-Bliesner BL, Brady EC, Shields C. Late Cretaceous ocean: coupled simulations with the national center for atmospheric research climate system model. Journal of Geophysical Research: Atmospheres. 2002;107.
[34] Takashima R, Nishi H, Huber BT, Leckie EM. Greenhouse world and the Mesozoic Ocean. The Oceanography Society. 2006;19:82-92.
[35] Martínez-Garcia A, Rosell-Melé A, Jaccard SL, Geibert W, Sigman DM, Haug GH. Southern Ocean dust-climate coupling over the past four million years. Nature. 2011;476:312-5.
[36] Maher BA, Dennis P. Evidence against dust-mediated control of glacial–interglacial changes in atmospheric CO2. Nature. 2001;411:176-80.
[37] Lamy F, Gersonde R, Winckler G, Esper O, Jaeschke A, Kuhn G, et al. Increased dust deposition in the Pacific Southern Ocean during glacial periods. Science. 2014;343:403-7.
[38] Martin JH. Glacial-interglacial CO2 change: the Iron hypothesis. Paleoceanography. 1990;5:1-13.
[39] Maher B, Prospero J, Mackie D, Gaiero D, Hesse P, Balkanski Y. Global connections between aeolian dust, climate and ocean biogeochemistry at the present day and at the last glacial maximum. Earth-Science Reviews. 2010;99:61-97.
[40] Anderson RF, Barker S, Fleisher M, Gersonde R, Goldstein SL, Kuhn G, et al. Biological response to millennial variability of dust and nutrient supply in the Subantarctic South Atlantic Ocean. Philosophical Transactions of the Royal Society of London A: Mathematical, Physical and Engineering Sciences. 2014;372:20130054.
[41] Ziegler M, Diz P, Hall IR, Zahn R. Millennial-scale changes in atmospheric CO2 levels linked to the Southern Ocean carbon isotope gradient and dust flux. Nature Geoscience. 2013;6:457-61.
[42] Martínez-García A, Sigman DM, Ren H, Anderson RF, Straub M, Hodell DA, et al. Iron fertilization of the Subantarctic Ocean during the last ice age. Science. 2014;343:1347-50.
[43] Tréguer P, Pondaven P. Global change: silica control of carbon dioxide. Nature. 2000;406:358-9.
[44] Sur S, Owens JD, Soreghan GS, Lyons TW, Raiswell R, Heavens NG, et al. Extreme eolian delivery of reactive iron to late Paleozoic icehouse seas. Geology. 2015;43:1099-102.
[45] Breitbarth E, Achterberg EP, Ardelan M, Baker AR, Bucciarelli E, Chever F, et al. Iron biogeochemistry across marine systems–progress from the past decade. Biogeosciences. 2010;7:1075-97.
[46] Raiswell R, Canfield DE. The iron biogeochemical cycle past and present. Geochemical Perspectives. 2012;1:1-2.
[47] Moore J, Braucher O. Sedimentary and mineral dust sources of dissolved iron to the world ocean. Biogeosciences. 2008;5.
[48] Moore JK, Lindsay K, Doney SC, Long MC, Misumi K. Marine ecosystem dynamics and biogeochemical cycling in the Community Earth System Model [CESM1 (BGC)]: Comparison of the 1990s with the 2090s under the RCP4. 5 and RCP8. 5 scenarios. Journal of Climate. 2013;26:9291-312.
[49] Boyd P, Ellwood M. The biogeochemical cycle of iron in the ocean. Nature Geoscience. 2010;3:675-82.
[50] Archer D, Johnson K. A model of the iron cycle in the ocean. Global Biogeochemical Cycles. 2000;14:269-79.

[51] Johnson KS, Moore JK, Smith WO. A report on the US JGOFS workshop on iron dynamics in the carbon cycle. Citeseer; 2002.
[52] Johnson KS, Moore JK, Smith WO. Workshop highlights iron dynamics in ocean carbon cycle. Eos, Transactions American Geophysical Union. 2002;83.
[53] Turner DR, Hunter KA. The biogeochemistry of iron in seawater: Wiley Chichester; 2001.
[54] Misumi K, Lindsay K, Moore JK, Doney SC, Bryan FO, Tsumune D, et al. The iron budget in ocean surface waters in the 20th and 21st centuries: projections by the Community Earth System Model version 1. Biogeosciences. 2014;11.
[55] Tagliabue A, Aumont O, DeAth R, Dunne JP, Dutkiewicz S, Galbraith E, et al. How well do global ocean biogeochemistry models simulate dissolved iron distributions? Global Biogeochemical Cycles. 2015.
[56] Mahowald NM, Baker AR, Bergametti G, Brooks N, Duce RA, Jickells TD, et al. Atmospheric global dust cycle and iron inputs to the ocean. Global biogeochemical cycles. 2005;19.
[57] Mahowald NM, Engelstaedter S, Luo C, Sealy A, Artaxo P, Benitez-Nelson C, et al. Atmospheric Iron Deposition: Global Distribution, Variability, and Human Perturbations*. Annual Review of Marine Science. 2009;1:245-78.
[58] Mahowald NM, Kloster S, Engelstaedter S, Moore JK, Mukhopadhyay S, McConnell JR, et al. Observed 20th century desert dust variability: impact on climate and biogeochemistry. Atmospheric Chemistry and Physics. 2010;10:10875-93.
[59] Anderson WB. Diagnosis and correction of iron deficiency in field crops-an overview. Journal of Plant Nutrition. 1982;5:785-95.
[60] Lindsay W, Schwab A. The chemistry of iron in soils and its availability to plants. Journal of Plant Nutrition. 1982;5:821-40.
[61] Mengel K, Geurtzen G. Iron chlorosis on calcareous soils. Alkaline nutritional condition as the cause for the chlorosis. Journal of Plant Nutrition. 1986;9:161-73.
[62] Smetacek V, Naqvi S. The next generation of iron fertilization experiments in the Southern Ocean. Philosophical Transactions of the Royal Society of London A: Mathematical, Physical and Engineering Sciences. 2008;366:3947-67.
[63] Martin P, Loeff MR, Cassar N, Vandromme P, d'Ovidio F, Stemmann L, et al. Iron fertilization enhanced net community production but not downward particle flux during the Southern Ocean iron fertilization experiment LOHAFEX. Global Biogeochemical Cycles. 2013;27:871-81.
[64] Williamson P, Wallace DW, Law CS, Boyd PW, Collos Y, Croot P, et al. Ocean fertilization for geoengineering: a review of effectiveness, environmental impacts and emerging governance. Process Safety and Environmental Protection. 2012;90:475-88.
[65] Smetacek V, Klaas C, Strass VH, Assmy P, Montresor M, Cisewski B, et al. Deep carbon export from a Southern Ocean iron-fertilized diatom bloom. Nature. 2012;487:313-9.
[66] Köhler P, Hauck J, Völker C, Wolf-Gladrow D. The role of iron during the open ocean dissolution of olivine in a simulated CO2 removal experiment—enhanced weathering, ocean alkalinization, ocean fertilization. 2015.
[67] Boyd PW, Bressac M. Developing a test-bed for robust research governance of geoengineering: the contribution of ocean iron biogeochemistry. Phil Trans R Soc A. 2016;374:20150299.
[68] Johnson KS, Karl DM. Is ocean fertilization credible and creditable? Science. 2002;296:467-8.
[69] Chisholm SW, Falkowski PG, Cullen JJ. Response to the letter of Johnson, K.S. and Karl, D.M. Science. 2002;296:467-8.
[70] Duggen S, Croot P, Schacht U, Hoffmann L. Subduction zone volcanic ash can fertilize the surface ocean and stimulate phytoplankton growth: Evidence from biogeochemical experiments and satellite data. Geophysical Research Letters. 2007;34.
[71] Conway T, Wolff E, Röthlisberger R, Mulvaney R, Elderfield H. Constraints on soluble aerosol iron flux to the Southern Ocean at the Last Glacial Maximum. Nature communications. 2015;6.
[72] Spolaor A, Vallelonga P, Cozzi G, Gabrieli J, Varin C, Kehrwald N, et al. Iron speciation in aerosol dust influences iron bioavailability over glacial-interglacial timescales. Geophysical Research Letters. 2013;40:1618-23.
[73] Soreghan GS, Sur S, Owens JD, Raiswell R, Heavens NG, Natalie M, et al. The potential biological impact of eolian delivery of reactive iron to late Paleozoic icehouse seas. 2014 GSA Annual Meeting in Vancouver, British Columbia2014.
[74] Johnson M, Meskhidze N. Atmospheric dissolved iron deposition to the global oceans: effects of oxalate-promoted Fe dissolution, photochemical redox cycling, and dust mineralogy. Geoscientific Model Development Discussions. 2013;6:1901-47.
[75] Al-Abadleh HA. Review of the bulk and surface chemistry of iron in atmospherically relevant systems containing humic-like substances. RSC Advances. 2015;5:45785-811.
[76] Death R, Wadham J, Monteiro F, Le Brocq A, Tranter M, Ridgwell A, et al. Antarctic ice sheet fertilises the Southern Ocean. Biogeosciences. 2014;11:2635-43.
[77] Hawkings JR, Wadham JL, Tranter M, Raiswell R, Benning LG, Statham PJ, et al. Ice sheets as a significant source of highly reactive nanoparticulate iron to the oceans. Nature communications. 2014;5.
[78] Sedwick PN, Sholkovitz ER, Church TM. Impact of anthropogenic combustion emissions on the fractional solubility of aerosol iron: Evidence from the Sargasso Sea. Geochemistry, Geophysics, Geosystems. 2007;8.
[79] Luo C, Mahowald N, Bond T, Chuang P, Artaxo P, Siefert R, et al. Combustion iron distribution and deposition. Global Biogeochemical Cycles. 2008;22.
[80] Ito A, Shi Z. Delivery of anthropogenic bioavailable iron from mineral dust and combustion aerosols to the ocean. Atmospheric Chemistry and Physics Discussions. 2015;15:23051-88.

[81] Ito A. Atmospheric processing of combustion aerosols as a source of bioavailable iron. Environmental Science & Technology Letters. 2015;2:70-5.
[82] Lin YC, Chen JP, Ho TY, Tsai I. Atmospheric iron deposition in the northwestern Pacific Ocean and its adjacent marginal seas: the importance of coal burning. Global Biogeochemical Cycles. 2015;29:138-59.
[83] Wang R, Balkanski Y, Boucher O, Bopp L, Chappell A, Ciais P, et al. Sources, transport and deposition of iron in the global atmosphere. Atmospheric Chemistry and Physics. 2015;15:6247-70.
[84] Shaked Y, Lis H. Disassembling iron availability to phytoplankton. Environmental Bioinorganic Chemistry of Aquatic Microbial Organisms. 2012:28.
[85] Johnson KS, Chavez FP, Friederich GE. Continental-shelf sediment as a primary source of iron for coastal phytoplankton. Nature. 1999;398:697-700.
[86] Elrod VA, Berelson WM, Coale KH, Johnson KS. The flux of iron from continental shelf sediments: A missing source for global budgets. Geophysical Research Letters. 2004;31.
[87] Raiswell R, Hawkings JR, Benning LG, Baker AR, Death R, Albani S, et al. Potentially bioavailable iron delivery by iceberg-hosted sediments and atmospheric dust to the polar oceans. Biogeosciences. 2016;13:3887.
[88] Schmidt C, Vuillemin R, Le Gall C, Gaill F, Le Bris N. Geochemical energy sources for microbial primary production in the environment of hydrothermal vent shrimps. Marine Chemistry. 2008;108:18-31.
[89] Sylvan JB, Toner BM, Edwards KJ. Life and death of deep-sea vents: bacterial diversity and ecosystem succession on inactive hydrothermal sulfides. MBio. 2012;3:e00279-11.
[90] Borch T, Kretzschmar R, Kappler A, Cappellen PV, Ginder-Vogel M, Voegelin A, et al. Biogeochemical redox processes and their impact on contaminant dynamics. Environmental Science & Technology. 2009;44:15-23.
[91] Schmidt K, Schlosser C, Atkinson A, Fielding S, Venables HJ, Waluda CM, et al. Zooplankton gut passage mobilizes lithogenic iron for ocean productivity. Current Biology. 2016;26:2667-73.
[92] Muscolo A, Sidari M, Pizzeghello D, Nardi S. Effects of humic substances isolated from earthworm faeces. Dynamic Soil, Dynamic Plant. 2009;2:45-52.
[93] Reck M, Tomasch J, Deng Z, Jarek M, Husemann P, Wagner-Döbler I. Stool metatranscriptomics: A technical guideline for mRNA stabilisation and isolation. BMC genomics. 2015;16:494.
[94] Wagner Mackenzie B, Waite DW, Taylor MW. Evaluating variation in human gut microbiota profiles due to DNA extraction method and inter-subject differences. Frontiers in microbiology. 2015;6:130.
[95] Vu AT, Nguyen NC, Leadbetter JR. Iron reduction in the metal-rich guts of wood-feeding termites. Geobiology. 2004;2:239-47.
[96] Lopes C, Kucera M, Mix AC. Climate change decouples oceanic primary and export productivity and organic carbon burial. Proceedings of the National Academy of Sciences. 2015;112:332-5.
[97] Pérez-Guzmán L, Bogner K, Lower B. Earth's Ferrous Wheel. Nature Education Knowledge. 2010;1:8.
[98] Parekh P, Follows MJ, Boyle E. Modeling the global ocean iron cycle. Global biogeochemical cycles. 2004;18.
[99] Forster P, Ramaswamy V, Artaxo P, Berntsen T, Betts R, Fahey DW, et al. Changes in atmospheric constituents and in radiative forcing. Chapter 2. . Climate Change 2007 The Physical Science Basis wwwipcch/pdf/assessment-report/ar4/wg1/ar4-wg1-chapter2pdf2007.
[100] Boucher O. Biogeochemical Effects and Climate Feedbacks of Aerosols. Atmospheric Aerosols: Springer; 2015. p. 247-69.
[101] Bauer SE, Menon S. Aerosol direct, indirect, semidirect, and surface albedo effects from sector contributions based on the IPCC AR5 emissions for preindustrial and present-day conditions. Journal of Geophysical Research: Atmospheres (1984–2012). 2012;117.
[102] Mitchell DL, Finnegan W. Modification of cirrus clouds to reduce global warming. Environmental Research Letters. 2009;4:045102.
[103] Storelvmo T, Kristjansson J, Muri H, Pfeffer M, Barahona D, Nenes A. Cirrus cloud seeding has potential to cool climate. Geophysical Research Letters. 2013;40:178-82.
[104] Latham J, Bower K, Choularton T, Coe H, Connolly P, Cooper G, et al. Marine cloud brightening. Philosophical Transactions of the Royal Society of London A: Mathematical, Physical and Engineering Sciences. 2012;370:4217-62.
[105] Alterskjær K, Kristjánsson J. The sign of the radiative forcing from marine cloud brightening depends on both particle size and injection amount. Geophysical Research Letters. 2013;40:210-5.
[106] Koch D, Del Genio A. Black carbon absorption effects on cloud cover, review and synthesis. Atmospheric Chemistry & Physics Discussions. 2010;10:7323-46.
[107] Ramanathan V, Li F, Ramana M, Praveen P, Kim D. Atmospheric brown clouds: hemispherical and regional variations in long-range transport, absorption, and radiative forcing. J Geophys Res. 2007;112:D22S1.
[108] Zhang X, Wu G, Zhang C, Xu T, Zhou Q. What is the real role of iron oxides in the optical properties of dust aerosols? Atmospheric Chemistry and Physics. 2015;15:12159-77.
[109] Sokolik IN, Toon OB. Incorporation of mineralogical composition into models of the radiative properties of mineral aerosol from UV to IR wavelengths. Journal of Geophysical Research. 1999;104:9423-44.
[110] Karydis V, Kumar P, Barahona D, Sokolik I, Nenes A. Assessing the Impact of Mineral Dust and Adsorption Activation on Cloud Droplet Formation. Advances in Meteorology, Climatology and Atmospheric Physics: Springer; 2013. p. 515-20.
[111] Levin Z, Teller A, Ganor E, Yin Y. On the interactions of mineral dust, sea-salt particles, and clouds: A measurement and modeling study from the Mediterranean Israeli Dust Experiment campaign. Journal of Geophysical Research: Atmospheres (1984–2012). 2005;110.
[112] Rosenfeld D, Freud E. Number of activated CCN as a key property in cloud aerosol interactions or, more on simplicity in complex systems. WCRP First Open Science Conference. Denver, USA2011.

[113] Rosenfeld D, Lohmann U, Raga GB, O'Dowd CD, Kulmala M, Fuzzi S, et al. Flood or drought: how do aerosols affect precipitation? science. 2008;321:1309-13.
[114] Rosenfeld D, Andreae MO, Asmi A, Chin M, Leeuw G, Donovan DP, et al. Global observations of aerosol-cloud-precipitation-climate interactions. Reviews of Geophysics. 2014;52:750-808.
[115] Latham J, Parkes B, Gadian A, Salter S. Weakening of hurricanes via marine cloud brightening (MCB). Atmospheric Science Letters. 2012;13:231-7.
[116] Wang Y, Lee K-H, Lin Y, Levy M, Zhang R. Distinct effects of anthropogenic aerosols on tropical cyclones. Nature Climate Change. 2014;4:368-73.
[117] Zhang H, McFarquhar GM, Cotton WR, Deng Y. Direct and indirect impacts of Saharan dust acting as cloud condensation nuclei on tropical cyclone eyewall development. Geophysical Research Letters. 2009;36.
[118] Graedel TE, Keene W. The budget and cycle of Earth's natural chlorine. Pure and applied chemistry. 1996;68:1689-97.
[119] Allan W, Struthers H, Lowe D. Methane carbon isotope effects caused by atomic chlorine in the marine boundary layer: Global model results compared with Southern Hemisphere measurements. Journal of Geophysical Research: Atmospheres (1984–2012). 2007;112.
[120] Sommariva R, von Glasow R. Multiphase halogen chemistry in the tropical Atlantic Ocean. Environmental science & technology. 2012;46:10429-37.
[121] Hossaini R, Chipperfield MP, Saiz-Lopez A, Fernandez R, Monks S, Brauer P, et al. A global model of tropospheric chlorine chemistry: organic versus inorganic sources and impact on methane oxidation. Journal of Geophysical Research: Atmospheres. 2016.
[122] Blasing T. Recent greenhouse gas concentrations, Carbon Dioxide Information Analysis Center, Oak Ridge National Laboratory, US Department of Energy [Online], 2009. Doi: 10.3334/CDIAC/atg.032. 2010.
[123] Blasing T. Recent Greenhouse Gas Concentrations. Carbon Dioxide Information Analysis Center CDIAC. DOI: 10.3334/CDIAC/atg.032 http://cdiac.ornl.gov/pns/current_ghg.html. DOE - Oak Ridge2016.
[124] Wittmer J, Bleicher S, Ofner J, Zetzsch C. Iron (III)-induced activation of chloride from artificial sea-salt aerosol. Environmental Chemistry. 2015;12:461-75.
[125] Wittmer J, Bleicher S, Zetzsch C. Iron (III)-Induced Activation of Chloride and Bromide from Modeled Salt Pans. The Journal of Physical Chemistry A. 2015;119:4373–85.
[126] Wittmer J, Bleicher S, Zetzsch C. Report on the Photochemical Induced Halogen Activation of Fe-containing Aerosols. J Climatol Weather Forecasting. 2016;4:2.
[127] Wittmer J, Zetzsch C. Photochemical activation of chlorine by iron-oxide aerosol. Journal of Atmospheric Chemistry Doi:101007/s10874-016-9336-6. 2016:1-18.
[128] Anenberg SC, Schwartz J, Shindell DT, Amann M, Faluvegi GS, Klimont Z, et al. Global air quality and health co-benefits of mitigating near-term climate change through methane and black carbon emission controls. 2012.
[129] Oster GK, Oster G. Photoreduction of Metal Ions by Visible Light1. Journal of the American Chemical Society. 1959;81:5543-5.
[130] Monico L, Janssens K, Hendriks E, Vanmeert F, Van der Snickt G, Cotte M, et al. Evidence for Degradation of the Chrome Yellows in Van Gogh's Sunflowers: A Study Using Noninvasive In Situ Methods and Synchrotron-Radiation-Based X-ray Techniques. Angewandte Chemie. 2015;127:14129-33.
[131] Thakur RS, Chaudhary R, Singh C. Influence of pH on photocatalytic reduction, adsorption, and deposition of metal ions: speciation modeling. Desalination and Water Treatment. 2015;56:1335-63.
[132] Ola O, Maroto-Valer MM. Transition metal oxide based TiO2 nanoparticles for visible light induced CO2 photoreduction. Applied Catalysis A: General. 2015;502:114-21.
[133] Xu H-Q, Hu J, Wang D, Li Z, Zhang Q, Luo Y, et al. Visible-Light Photoreduction of CO2 in a Metal–Organic Framework: Boosting Electron–Hole Separation via Electron Trap States. Journal of the American Chemical Society. 2015;137:13440-3.
[134] Zamaraev KI, Khramov MI, Parmon VN. Possible impact of heterogeneous photocatalysis on the global chemistry of the Earth's atmosphere. Catalysis Reviews—Science and Engineering. 1994;36:617-44.
[135] Zamaraev K. Catalytic science and technology for environmental issues. Catalysis today. 1997;35:3-13.
[136] de Richter R, Ming T, Shen S, Caillol S. Fighting global warming by greenhouse gas removal: destroying atmospheric nitrous oxide thanks to synergies between two breakthrough technologies. Environmental Science and Pollution Research. 2016;23:6119-38.
[137] de Richter R, Ming T, Caillol S, Liu W. Fighting global warming by GHG removal: Destroying CFCs and HCFCs in solar-wind power plant hybrids producing renewable energy with no-intermittency. International Journal of Greenhouse Gas Control. 2016;49:449-72.
[138] Kiesgen de_Richter R, Ming T, Caillol S. Fighting global warming by photocatalytic reduction of CO2 using giant photocatalytic reactors. Renewable and Sustainable Energy Reviews. 2013;19:82-106.
[139] de Richter R, Caillol S. Fighting global warming: the potential of photocatalysis against CO2, CH4, N2O, CFCs, tropospheric O3, BC and other major contributors to climate change. Journal of Photochemistry and Photobiology C: Photochemistry Reviews. 2011;12:1-19.
[140] de Richter R, Ming T, Davies P, Liu W, Caillol S. Removal of non-CO2 greenhouse gases by large-scale atmospheric solar photocatalysis. Progress in Energy and Combustion Science Submitted. 2017.
[141] Oeste FD. Climate cooling by interaction of artificial loess haze with seasalt haze induced by iron- or titanium-doped ship- and aircraft-fuel. Geo Leipzig 2004, Gemeinschaftstagung DGG und GGW. Schriftenreihe der Deutschen Geologischen Gesellschaft, 34, p. 344, ISBN 3-932537-06-8.2004. p. 344.
[142] Santachiara G, Prodi F, Belosi F. A review of thermo-and diffusio-phoresis in the atmospheric aerosol scavenging process. Part 1: Drop Scavenging. Atmospheric and Climate Sciences. 2012;2:148-58.

[143] Ardon-Dryer K, Huang Y-W, Cziczo D. Laboratory studies of collection efficiency of sub-micrometer aerosol particles by cloud droplets on a single droplet basis. Atmospheric Chemistry and Physics Discussions. 2015;15:6207-36.
[144] Wang P, Grover S, Pruppacher H. On the effect of electric charges on the scavenging of aerosol particles by clouds and small raindrops. Journal of the Atmospheric Sciences. 1978;35:1735-43.
[145] Osthoff HD, Roberts JM, Ravishankara A, Williams EJ, Lerner BM, Sommariva R, et al. High levels of nitryl chloride in the polluted subtropical marine boundary layer. Nature Geoscience. 2008;1:324-8.
[146] Riedel T, Wolfe G, Danas K, Gilman J, Kuster W, Bon D, et al. An MCM modeling study of nitryl chloride (ClNO 2) impacts on oxidation, ozone production and nitrogen oxide partitioning in polluted continental outflow. Atmospheric Chemistry and Physics. 2014;14:3789-800.
[147] Khalil M, Rasmussen R. Atmospheric methyl chloride. Atmospheric Environment. 1999;33:1305-21.
[148] Yokouchi Y, Noijiri Y, Barrie L, Toom-Sauntry D, Machida T, Inuzuka Y, et al. A strong source of methyl chloride to the atmosphere from tropical coastal land. Nature. 2000;403:295-8.
[149] Kim J-S, Park K. Atmospheric aging of Asian dust particles during long range transport. Aerosol Science and Technology. 2012;46:913-24.
[150] Drozd G, Woo J, Häkkinen S, Nenes A, McNeill VF. Inorganic salts interact with oxalic acid in submicron particles to form material with low hygroscopicity and volatility. Atmospheric Chemistry and Physics. 2014;14:5205-15.
[151] Pechtl S, von Glasow R. Reactive chlorine in the marine boundary layer in the outflow of polluted continental air: A model study. Geophysical research letters. 2007;34.
[152] Baker AK, Rauthe-Schöch A, Schuck TJ, Brenninkmeijer CA, van Velthoven PF, Wisher A, et al. Investigation of chlorine radical chemistry in the Eyjafjallajökull volcanic plume using observed depletions in non-methane hydrocarbons. Geophysical Research Letters. 2011;38.
[153] Rose WI, Millard GA, Mather TA, Hunton DE, Anderson B, Oppenheimer C, et al. Atmospheric chemistry of a 33–34 hour old volcanic cloud from Hekla Volcano (Iceland): Insights from direct sampling and the application of chemical box modeling. Journal of Geophysical Research: Atmospheres (1984–2012). 2006;111.
[154] Baker AK, Sauvage C, Thorenz UR, Brenninkmeijer CA, Oram DE, van Velthoven P, et al. Evidence for widespread tropospheric Cl chemistry in free tropospheric air masses from the South China Sea. EGU General Assembly Conference Abstracts2015. p. 10370.
[155] Wang SH, Hsu NC, Tsay SC, Lin NH, Sayer AM, Huang SJ, et al. Can Asian dust trigger phytoplankton blooms in the oligotrophic northern South China Sea? Geophysical Research Letters. 2012;39.
[156] von Glasow R, Sander R. Variation of sea salt aerosol pH with relative humidity. Geophysical research letters. 2001;28:247-50.
[157] Bleicher S, Buxmann J, Sander R, Riedel T, Thornton J, Platt U, et al. The influence of nitrogen oxides on the activation of bromide and chloride in salt aerosol. Atmospheric Chemistry and Physics Discussions. 2014;14:10135-66.
[158] Wren S, Donaldson D. How does deposition of gas phase species affect pH at frozen salty interfaces? Atmospheric Chemistry and Physics. 2012;12:10065-73.
[159] Kahan TF, Wren SN, Donaldson DJ. A Pinch of Salt Is All It Takes: Chemistry at the Frozen Water Surface. Accounts of chemical research. 2014;47:1587-94.
[160] Bartels-Rausch T, Jacobi H-W, Kahan TF, Thomas JL, Thomson ES, Abbatt JP, et al. A review of air–ice chemical and physical interactions (AICI): liquids, quasi-liquids, and solids in snow. Atmospheric Chemistry and Physics. 2014;14:1587-633.
[161] Liao J, Huey LG, Liu Z, Tanner DJ, Cantrell CA, Orlando JJ, et al. High levels of molecular chlorine in the Arctic atmosphere. Nature Geoscience. 2014;7:91-4.
[162] Sadanaga Y, Hirokawa J, Akimoto H. Formation of molecular chlorine in dark condition: Heterogeneous reaction of ozone with sea salt in the presence of ferric ion. Geophysical research letters. 2001;28:4433-6.
[163] Ming T, de_Richter R, Liu W, Caillol S. Fighting global warming by climate engineering: Is the Earth radiation management and the solar radiation management any option for fighting climate change? Renewable and Sustainable Energy Reviews. 2014;31:792-834.
[164] Levine JG, Wolff EW, Jones AE, Sime LC. The role of atomic chlorine in glacial-interglacial changes in the carbon-13 content of atmospheric methane. Geophysical Research Letters. 2011;38.
[165] Skinner L. Facing future climate change: is the past relevant? Philosophical Transactions of the Royal Society of London A: Mathematical, Physical and Engineering Sciences. 2008;366:4627-45.
[166] Sander R. Compilation of Henry's law constants (version 4.0) for water as solvent. Atmospheric Chemistry and Physics. 2015;15:4399-981.
[167] von Glasow R. Modeling the gas and aqueous phase chemistry of the marine boundary layer. Available at www.rolandvonglasow.de: Universität Mainz, Germany,; 2000.
[168] Luna A, Nascimento C, Chiavone-Filho O. Photodecomposition of hydrogen peroxide in highly saline aqueous medium. Brazilian Journal of Chemical Engineering. 2006;23:341-9.
[169] Nie W, Ding A, Wang T, Kerminen V-M, George C, Xue L, et al. Polluted dust promotes new particle formation and growth. Scientific reports. 2014;4.
[170] Young C, Washenfelder R, Edwards P, Parrish D, Gilman J, Kuster W, et al. Chlorine as a primary radical: evaluation of methods to understand its role in initiation of oxidative cycles. Atmospheric Chemistry and Physics. 2014;14:3427-40.
[171] Pena AL, Segura E R, Chan M A, Hoggard E P. Photodegradation of dichloromethane catalyzed by iron (III) chloride on silica gel. Current Catalysis. 2014;3:35-8.

[172] Jin L, Zhang P, Shao T, Zhao S. Ferric ion mediated photodecomposition of aqueous perfluorooctane sulfonate (PFOS) under UV irradiation and its mechanism. Journal of hazardous materials. 2014;271:9-15.
[173] Ramanathan V, Carmichael G. Global and regional climate changes due to black carbon. Nature geoscience. 2008;1:221-7.
[174] Bond TC, Doherty SJ, Fahey D, Forster P, Berntsen T, DeAngelo B, et al. Bounding the role of black carbon in the climate system: A scientific assessment. Journal of Geophysical Research: Atmospheres. 2013;118:5380-552.
[175] Andreae M, Gelencsér A. Black carbon or brown carbon? The nature of light-absorbing carbonaceous aerosols. Atmospheric Chemistry and Physics. 2006;6:3131-48.
[176] Nguyen TH, Ball WP. Absorption and adsorption of hydrophobic organic contaminants to diesel and hexane soot. Environmental science & technology. 2006;40:2958-64.
[177] Ramana M, Ramanathan V, Feng Y, Yoon S, Kim S, Carmichael G, et al. Warming influenced by the ratio of black carbon to sulphate and the black-carbon source. Nature Geoscience. 2010;3:542-5.
[178] Hadley OL, Kirchstetter TW. Black-carbon reduction of snow albedo. Nature Climate Change. 2012;2:437-40.
[179] Jacobson MZ. Control of fossil-fuel particulate black carbon and organic matter, possibly the most effective method of slowing global warming. Journal of Geophysical Research: Atmospheres (1984–2012). 2002;107:ACH 16-1-ACH -22.
[180] Shindell D, Kuylenstierna JC, Vignati E, van Dingenen R, Amann M, Klimont Z, et al. Simultaneously mitigating near-term climate change and improving human health and food security. Science. 2012;335:183-9.
[181] Fry JL, Draper DC, Barsanti KC, Smith JN, Ortega J, Winkler PM, et al. Secondary organic aerosol formation and organic nitrate yield from NO3 oxidation of biogenic hydrocarbons. Environmental science & technology. 2014;48:11944-53.
[182] Pillar EA, Camm RC, Guzman MI. Catechol oxidation by ozone and hydroxyl radicals at the air–water interface. Environmental science & technology. 2014;48:14352-60.
[183] Ofner J, Krüger H-U, Grothe H, Schmitt-Kopplin P, Whitmore K, Zetzsch C. Physico-chemical characterization of SOA derived from catechol and guaiacol–a model substance for the aromatic fraction of atmospheric HULIS. Atmospheric Chemistry and Physics. 2011;11:1-15.
[184] Hoffer A, Kiss G, Blazso M, Gelencsér A. Chemical characterization of humic-like substances (HULIS) formed from a lignin-type precursor in model cloud water. Geophysical research letters. 2004;31:L06115.
[185] Claeys M, Vermeylen R, Yasmeen F, Gómez-González Y, Chi X, Maenhaut W, et al. Chemical characterisation of humic-like substances from urban, rural and tropical biomass burning environments using liquid chromatography with UV/vis photodiode array detection and electrospray ionisation mass spectrometry. Environmental Chemistry. 2012;9:273-84.
[186] Willey JD, Kieber RJ, Seaton PJ, Miller C. Rainwater as a source of Fe (II)-stabilizing ligands to seawater. Limnology and Oceanography. 2008;53:1678.
[187] Ghio AJ, Soukup JM, Dailey LA, Tong H, Kesic MJ, Budinger GS, et al. Wood smoke particle sequesters cell iron to impact a biological effect. Chemical research in toxicology. 2015;28:2104-11.
[188] Chemizmu K, Fentona R. Fenton reaction-controversy concerning the chemistry. Ecological chemistry and engineering. 2009;16:347-58.
[189] Vione D, Maurino V, Minero C, Pelizzetti E. The atmospheric chemistry of hydrogen peroxide: A review. ANNALI DI CHIMICA-ROMA-. 2003;93:477-86.
[190] Fenton H. LXXIII.—Oxidation of tartaric acid in presence of iron. Journal of the Chemical Society, Transactions. 1894;65:899-910.
[191] Barbusiński K. Fenton reaction-controversy concerning the chemistry. Ecological chemistry and engineering. 2009;16:347-58.
[192] Southworth BA, Voelker BM. Hydroxyl radical production via the photo-Fenton reaction in the presence of fulvic acid. Environmental science & technology. 2003;37:1130-6.
[193] Machulek Jr A, Moraes JEF, Okano LT, Silvério CA, Quina FH. Photolysis of ferric ions in the presence of sulfate or chloride ions: implications for the photo-Fenton process. Photochemical & Photobiological Sciences. 2009;8:985-91.
[194] De Laat J, Le GT, Legube B. A comparative study of the effects of chloride, sulfate and nitrate ions on the rates of decomposition of H2O2 and organic compounds by Fe (II)/H2O2 and Fe (III)/H2O2. Chemosphere. 2004;55:715-23.
[195] Salgado P, Melin V, Contreras D, Moreno Y, Mansilla HD. Fenton reaction driven by iron ligands. Journal of the Chilean Chemical Society. 2013;58:2096-101.
[196] Enami S, Sakamoto Y, Colussi AJ. Fenton chemistry at aqueous interfaces. Proceedings of the National Academy of Sciences. 2014;111:623-8.
[197] Teixeira APC, Tristão JC, Araujo MH, Oliveira LC, Moura FC, Ardisson JD, et al. Iron: a versatile element to produce materials for environmental applications. Journal of the Brazilian Chemical Society. 2012;23:1579-93.
[198] Pignatello JJ, Oliveros E, MacKay A. Advanced oxidation processes for organic contaminant destruction based on the Fenton reaction and related chemistry. Critical reviews in environmental science and technology. 2006;36:1-84.
[199] Pinto IS, Pacheco PH, Coelho JV, Lorençon E, Ardisson JD, Fabris JD, et al. Nanostructured δ-FeOOH: an efficient Fenton-like catalyst for the oxidation of organics in water. Applied Catalysis B: Environmental. 2012;119:175-82.

[200] Gopakumar G, Belanzoni P, Baerends EJ. Hydroxylation catalysis by mononuclear and dinuclear iron oxo catalysts: a methane monooxygenase model system versus the Fenton reagent FeIVO (H2O) 52+. Inorganic chemistry. 2011;51:63-75.
[201] Hammond C, Forde MM, Rahim A, Hasbi M, Thetford A, He Q, et al. Direct Catalytic Conversion of Methane to Methanol in an Aqueous Medium by using Copper-Promoted Fe-ZSM-5. Angewandte Chemie International Edition. 2012;51:5129-33.
[202] Yoshizawa K, Shiota Y, Yumura T, Yamabe T. Direct methane-methanol and benzene-phenol conversions on Fe-ZSM-5 zeolite: Theoretical predictions on the reaction pathways and energetics. The Journal of Physical Chemistry B. 2000;104:734-40.
[203] Klüpfel L, Keiluweit M, Kleber M, Sander M. Redox properties of plant biomass-derived black carbon (biochar). Environmental science & technology. 2014;48:5601-11.
[204] Oh S-Y, Chiu PC. Graphite-and soot-mediated reduction of 2, 4-dinitrotoluene and hexahydro-1, 3, 5-trinitro-1, 3, 5-triazine. Environmental science & technology. 2009;43:6983-8.
[205] Studebaker ML, Huffman E, Wolfe A, Nabors L. Oxygen-containing groups on the surface of carbon black. Industrial & Engineering Chemistry. 1956;48:162-6.
[206] Drushel HV, Hallum JV. The Organic Nature of Carbon Black Surfaces. II. Quinones and Hydroquinones by Coulometry at Controlled Potential. The Journal of Physical Chemistry. 1958;62:1502-5.
[207] Lima SB, Borges SMS, Rangel MdC, Marchetti SG. Effect of iron content on the catalytic properties of activated carbon-supported magnetite derived from biomass. Journal of the Brazilian Chemical Society. 2013;24:344-54.
[208] Wang L, Yao Y, Zhang Z, Sun L, Lu W, Chen W, et al. Activated carbon fibers as an excellent partner of Fenton catalyst for dyes decolorization by combination of adsorption and oxidation. Chemical Engineering Journal. 2014;251:348-54.
[209] Kim JR, Santiano B, Kim H, Kan E. Heterogeneous oxidation of methylene blue with surface-modified iron-amended activated carbon. 2013.
[210] Oeste FD. Die H2S-Oxidation an aktiver Kohle-ein elektrochemischer Prozess? Carbon. 1977;15:225-8.
[211] Song P, Wang Y, Pan J, Xu W, Zhuang L. Structure-activity relationship in high-performance iron-based electrocatalysts for oxygen reduction reaction. Journal of Power Sources. 2015;300:279-84.
[212] Moreno-Castilla C, Lopez-Ramon M, Carrasco-Marın F. Changes in surface chemistry of activated carbons by wet oxidation. Carbon. 2000;38:1995-2001.
[213] Bai H, Jiang W, Kotchey GP, Saidi WA, Bythell BJ, Jarvis JM, et al. Insight into the mechanism of graphene oxide degradation via the photo-Fenton reaction. The Journal of Physical Chemistry C. 2014;118:10519-29.
[214] Zhou X, Zhang Y, Wang C, Wu X, Yang Y, Zheng B, et al. Photo-Fenton reaction of graphene oxide: a new strategy to prepare graphene quantum dots for DNA cleavage. Acs Nano. 2012;6:6592-9.
[215] Zuberi B, Johnson KS, Aleks GK, Molina LT, Molina MJ, Laskin A. Hydrophilic properties of aged soot. Geophysical research letters. 2005;32.
[216] Kawamura K, Umemoto N, Mochida M, Bertram T, Howell S, Huebert B. Water-soluble dicarboxylic acids in the tropospheric aerosols collected over east Asia and western North Pacific by ACE-Asia C-130 aircraft. Journal of Geophysical Research: Atmospheres (1984–2012). 2003;108.
[217] Eder JM. Über die Zersetzung des Eisenchlorides und einiger organischer Ferridsalze im Lichte. Monatshefte für Chemie/Chemical Monthly. 1880;1:755-62.
[218] Eder JM. Ausführliches Handbuch der Photographie, Erster Band, 2. Teil: Photochemie (die chemischen Wirkungen des Lichtes): Wilhelm Knapp; 1906.
[219] Zhu X, Prospero JM, Savoie DL, Millero FJ, Zika RG, Saltzman ES. Photoreduction of iron (III) in marine mineral aerosol solutions. Journal of Geophysical Research: Atmospheres (1984–2012). 1993;98:9039-46.
[220] Weller C, Tilgner A, Bräuer P, Herrmann H. Modeling the Impact of Iron–Carboxylate Photochemistry on Radical Budget and Carboxylate Degradation in Cloud Droplets and Particles. Environmental science & technology. 2014;48:5652-9.
[221] Cunningham KM, Goldberg MC, Weiner ER. Mechanisms for aqueous photolysis of adsorbed benzoate, oxalate, and succinate on iron oxyhydroxide (goethite) surfaces. Environmental science & technology. 1988;22:1090-7.
[222] Flanner MG, Zender CS, Randerson JT, Rasch PJ. Present-day climate forcing and response from black carbon in snow. Journal of Geophysical Research: Atmospheres. 2007;112.
[223] Kasper M, Sattler K, Siegmann K, Matter U. The effect of ferrocene addition on particle formation and burnout in combustion processes. Journal of Aerosol Science. 1998;29:S617-S8.
[224] Weiser V, Eisenreich N, Roth E, Pfeil A. Mechanisms of Soot Reduction in Diesel Pool Fire by Ferrocene.
[225] Cooper OR, Parrish D, Ziemke J, Balashov N, Cupeiro M, Galbally I, et al. Global distribution and trends of tropospheric ozone: An observation-based review. Elementa: Science of the Anthropocene. 2014;2:000029.
[226] Sherwen T, Evans MJ, Carpenter LJ, Schmidt JA, Mickely L. Halogen chemistry reduces tropospheric O3 radiative forcing. Atmos Chem Phys Discuss, doi. 2016;10.
[227] Crutzen PJ, Oppenheimer M. Learning about ozone depletion. Climatic Change. 2008;89:143-54.
[228] Wayne RP, Poulet G, Biggs P, Burrows J, Cox R, Crutzen P, et al. Halogen oxides: Radicals, sources and reservoirs in the laboratory and in the atmosphere. Atmospheric Environment. 1995;29:2677-881.
[229] Le Bras G, Platt U. A possible mechanism for combined chlorine and bromine catalyzed destruction of tropospheric ozone in the Arctic. Geophysical research letters. 1995;22:599-602.
[230] Pratt KA, Custard KD, Shepson PB, Douglas TA, Pöhler D, General S, et al. Photochemical production of molecular bromine in Arctic surface snowpacks. Nature Geoscience. 2013;6:351-6.

[231] Blechschmidt A-M, Richter A, Burrows J, Kaleschke L, Strong K, Theys N, et al. An exemplary case of a bromine explosion event linked to cyclone development in the Arctic. Atmospheric Chemistry and Physics. 2016;16:1773-88.
[232] Simpson W, Glasow Rv, Riedel K, Anderson P, Ariya P, Bottenheim J, et al. Halogens and their role in polar boundary-layer ozone depletion. Atmospheric Chemistry and Physics. 2007;7:4375-418.
[233] Roscoe H, Kreher K, Friess U. Ozone loss episodes in the free Antarctic troposphere, suggesting a possible climate feedback. Geophysical research letters. 2001;28:2911-4.
[234] Read KA, Mahajan AS, Carpenter LJ, Evans MJ, Faria BV, Heard DE, et al. Extensive halogen-mediated ozone destruction over the tropical Atlantic Ocean. Nature. 2008;453:1232-5.
[235] Lawler M, Finley B, Keene W, Pszenny A, Read K, Von Glasow R, et al. Pollution-enhanced reactive chlorine chemistry in the eastern tropical Atlantic boundary layer. Geophysical Research Letters. 2009;36.
[236] Bloss WJ, Evans MJ, Lee JD, Sommariva R, Heard DE, Pilling MJ. The oxidative capacity of the troposphere: Coupling of field measurements of OH and a global chemistry transport model. Faraday discussions. 2005;130:425-36.
[237] Hu L, Yvon-Lewis SA, Butler JH, Lobert JM, King DB. An improved oceanic budget for methyl chloride. Journal of Geophysical Research: Oceans. 2013;118:715-25.
[238] Khalil M, Moore R, Harper D, Lobert J, Erickson VK, Keene W. Natural emissions of chlorine-containing gases: Reactive Chlorine Emissions Inventory. 1999.
[239] Charlson RJ, Lovelock JE, Andreae MO, Warren SG. Oceanic phytoplankton, atmospheric sulphur, cloud albedo and climate. Nature. 1987;326:655-61.
[240] Lana A, Bell T, Simó R, Vallina SM, Ballabrera-Poy J, Kettle A, et al. An updated climatology of surface dimethlysulfide concentrations and emission fluxes in the global ocean. Global Biogeochemical Cycles. 2011;25.
[241] Six KD, Kloster S, Ilyina T, Archer SD, Zhang K, Maier-Reimer E. Global warming amplified by reduced sulphur fluxes as a result of ocean acidification. Nature Climate Change. 2013;3:975-8.
[242] Crutzen PJ. Albedo enhancement by stratospheric sulfur injections: a contribution to resolve a policy dilemma? Climatic change. 2006;77:211-20.
[243] Perry RS, Kolb VM, Lynne BY, Sephton MA, Mcloughlin N, Engel MH, et al. How desert varnish forms? Optics & Photonics 2005: International Society for Optics and Photonics; 2005. p. 59060V-V-12.
[244] Hungate B, Danin A, Pellerin N, Stemmler J, Kjellander P, Adams J, et al. Characterization of manganese-oxidizing (MnII→ MnIV) bacteria from Negev Desert rock varnish: implications in desert varnish formation. Canadian Journal of Microbiology. 1987;33:939-43.
[245] Allen CC, Westall F, Schelble RT. Importance of a martian hematite site for astrobiology. Astrobiology. 2001;1:111-23.
[246] Johnson L, Eggleston C. The photocatalytic actions of desert varnish. : University of Wyoming; 2013.
[247] Matsunaga K, Ohyama T, Kuma K, Kudo I, Suzuki Y. Photoreduction of manganese dioxide in seawater by organic substances under ultraviolet or sunlight. Water Research. 1995;29:757-9.
[248] Liu T, Dorn RI. Understanding the spatial variability of environmental change in drylands with rock varnish microlaminations. Annals of the Association of American Geographers. 1996;86:187-212.
[249] Dorn RI. The Rock Varnish Revolution: New Insights from Microlaminations and the Contributions of Tanzhuo Liu. Geography Compass. 2009;3:1804-23.
[250] Gammons C, Parker S, Nimick D. Diel iron cycling in acidic rivers of southwestern Spain. Goechimica et Cosmochimica Acta: Pergamon - Elsevier Science Ltd, Oxford, England; 2007. p. A305-A.
[251] Sander R, Burrows J, Kaleschke L. Carbonate precipitation in brine - a potential trigger for tropospheric ozone depletion events. Atmospheric Chemistry and Physics. 2006;6:4653-8.
[252] Kim K, Choi W, Hoffmann MR, Yoon H-I, Park B-K. Photoreductive dissolution of iron oxides trapped in ice and its environmental implications. Environmental science & technology. 2010;44:4142-8.
[253] Jeong D, Kim K, Choi W. Accelerated dissolution of iron oxides in ice. Atmospheric Chemistry and Physics. 2012;12:11125-33.
[254] Dorfman J, Stoner J, Finkenbinder M, Abbott M, Xuan C, St-Onge G. A 37,000-year environmental magnetic record of aeolian dust deposition from Burial Lake, Arctic Alaska. Quaternary Science Reviews. 2015;128:81-97.
[255] Hammer UT. Saline lake ecosystems of the world: Springer Science & Business Media; 1986.
[256] Albani S, Mahowald N, Murphy L, Raiswell R, Moore J, Anderson R, et al. Paleodust variability since the Last Glacial Maximum and implications for iron inputs to the ocean. Geophysical Research Letters. 2016;43:3944-54.
[257] Cartapanis O, Bianchi D, Jaccard SL, Galbraith ED. Global pulses of organic carbon burial in deep-sea sediments during glacial maxima. Nature communications. 2016;7.
[258] Jaccard SL, Galbraith ED, Martínez-García A, Anderson RF. Covariation of deep Southern Ocean oxygenation and atmospheric CO2 through the last ice age. Nature. 2016;530:207-10.
[259] Mackinder L, Wheeler G, Schroeder D, Riebesell U, Brownlee C. Molecular mechanisms underlying calcification in coccolithophores. Geomicrobiology Journal. 2010;27:585-95.
[260] Rost B, Riebesell U. Coccolithophores and the biological pump: responses to environmental changes. Coccolithophores: Springer; 2004. p. 99-125.
[261] Meyer J, Riebesell U. Reviews and Syntheses: Responses of coccolithophores to ocean acidification: a meta-analysis. Biogeosciences (BG). 2015;12:1671-82.
[262] Salter I, Schiebel R, Ziveri P, Movellan A, Lampitt R, Wolff GA. Carbonate counter pump stimulated by natural iron fertilization in the Polar Frontal Zone. Nature Geoscience. 2014.
[263] Alt JC, Shanks WC. Serpentinization of abyssal peridotites from the MARK area, Mid-Atlantic Ridge: sulfur geochemistry and reaction modeling. Geochimica et Cosmochimica Acta. 2003;67:641-53.

[264] Früh-Green GL, Connolly JA, Plas A, Kelley DS, Grobéty B. Serpentinization of oceanic peridotites: implications for geochemical cycles and biological activity. The subseafloor biosphere at mid-ocean ridges. 2004:119-36.
[265] Müller M, Barcelos e Ramos J, Schulz KG, Riebesell U, Kazmierczak J, Gallo F, et al. Phytoplankton calcification as an effective mechanism to prevent cellular calcium poisoning. Biogeosciences Discussions. 2015;12:12691-712.
[266] Matrai P, Keller M. Total organic sulfur and dimethylsulfoniopropionate in marine phytoplankton: intracellular variations. Marine Biology. 1994;119:61-8.
[267] Carpenter LJ, Archer SD, Beale R. Ocean-atmosphere trace gas exchange. Chemical Society Reviews. 2012;41:6473-506.
[268] Chen C-TA, Lin C-M, Huang B-T, Chang L-F. Stoichiometry of carbon, hydrogen, nitrogen, sulfur and oxygen in the particulate matter of the western North Pacific marginal seas. Marine Chemistry. 1996;54:179-90.
[269] Fujita T. Concentration of major chemical elements in marine plankton. Geochemical Journal. 1971;4:143-56.
[270] Cassar N, Laws EA, Bidigare RR, Popp BN. Bicarbonate uptake by Southern Ocean phytoplankton. Global Biogeochemical Cycles. 2004;18.
[271] Taylor LL, Quirk J, Thorley RM, Kharecha PA, Hansen J, Ridgwell A, et al. Enhanced weathering strategies for stabilizing climate and averting ocean acidification. Nature Climate Change. 2015.
[272] Weber T, Cram JA, Leung SW, DeVries T, Deutsch C. Deep ocean nutrients imply large latitudinal variation in particle transfer efficiency. Proceedings of the National Academy of Sciences. 2016:201604414.
[273] Dimitrova K, Sarkisyan A, Koleva V. Vertical mussel reef farming: Exploring climate change solutions with economic and ecologic significance. Climate Engineering Research Symposium. Berlin2015.
[274] Lenton A, Sen Gupta A. Carbon credits for oyster farming: fact or fiction? Fish2010. p. 30.
[275] Jambeck JR, Geyer R, Wilcox C, Siegler TR, Perryman M, Andrady A, et al. Plastic waste inputs from land into the ocean. Science. 2015;347:768-71.
[276] Law KL, Morét-Ferguson SE, Goodwin DS, Zettler ER, DeForce E, Kukulka T, et al. Distribution of surface plastic debris in the eastern Pacific Ocean from an 11-year data set. Environmental science & technology. 2014;48:4732-8.
[277] Cózar A, Echevarría F, González-Gordillo JI, Irigoien X, Úbeda B, Hernández-León S, et al. Plastic debris in the open ocean. Proceedings of the National Academy of Sciences. 2014;111:10239-44.
[278] van Sebille E, Wilcox C, Lebreton L, Maximenko N, Hardesty BD, van Franeker JA, et al. A global inventory of small floating plastic debris. Environmental Research Letters. 2015;10:124006.
[279] Bykova E, Dubrovinsky L, Dubrovinskaia N, Bykov M, McCammon C, Ovsyannikov S, et al. Structural complexity of simple Fe2O3 at high pressures and temperatures. Nature communications. 2016;7.
[280] Bruland K. A review of the chemistries of redox sensitive elements within suboxic zones of oxygen minimum regions. Gayana (Concepc). 2006;70:6-13.
[281] Rahmstorf S, Feulner G, Mann ME, Robinson A, Rutherford S, Schaffernicht EJ. Exceptional twentieth-century slowdown in Atlantic Ocean overturning circulation. Nature climate change. 2015;5:475-80.
[282] Bintanja R, Van Oldenborgh G, Drijfhout S, Wouters B, Katsman C. Important role for ocean warming and increased ice-shelf melt in Antarctic sea-ice expansion. Nature Geoscience. 2013;6:376-9.
[283] Rahmstorf S. Thermohaline Ocean Circulation. Encyclopedia of Quaternary Sciences. Postdam Institute for Climate Impact Research. 2006;5.
[284] Ohshima KI, Fukamachi Y, Williams GD, Nihashi S, Roquet F, Kitade Y, et al. Antarctic Bottom Water production by intense sea-ice formation in the Cape Darnley polynya. Nature Geoscience. 2013;6:235-40.
[285] Hauck J, Köhler P, Wolf-Gladrow D, Völker C. Iron fertilisation and century-scale effects of open ocean dissolution of olivine in a simulated CO2 removal experiment. Environmental Research Letters. 2016;11:024007.
[286] Wallmann K, Aloisi G, Haeckel M, Tishchenko P, Pavlova G, Greinert J, et al. Silicate weathering in anoxic marine sediments. Geochimica et Cosmochimica Acta. 2008;72:2895-918.
[287] Ohman L-O, Nordin A, Sedeh IF, Sjoberg S. Equilibrium and Structural Studies of Silicon (IV) and Aluminium (III) in Aqueous Solution. 28. Formation of Soluble Silicic Acid-Ligand Complexes as Studied by Potentiometrie and Solubility Measurements. Acta chemica scandinavica. 1991;45:335-41.
[288] Swanson KA. The effect of dissolved catechol on the dissolution of amorphous silica in seawater: Pennsylvania State University.; 1988.
[289] Roden E, Edmonds J. Phosphate mobilization in iron-rich anaerobic sediments: microbial Fe (III) oxide reduction versus iron-sulfide formation. Archiv für Hydrobiologie. 1997;139:347-78.
[290] Slomp CP, Mort HP, Jilbert T, Reed DC, Gustafsson BG, Wolthers M. Coupled dynamics of iron and phosphorus in sediments of an oligotrophic coastal basin and the impact of anaerobic oxidation of methane. 2013.
[291] Vorhies JS, Gaines RR. Microbial dissolution of clay minerals as a source of iron and silica in marine sediments. Nature Geoscience. 2009;2.
[292] Demadis KD, Mavredaki E, Somara M. Additive-Driven Dissolution Enhancement of Colloidal Silica. 2. Environmentally Friendly Additives and Natural Products. Industrial & Engineering Chemistry Research. 2011;50:13866-76.
[293] Jorgensen SS. Dissolution kinetics of silicate minerals in aqueous catechol solutions. Journal of Soil Science. 1976;27:183-95.
[294] Belton DJ, Deschaume O, Patwardhan SV, Perry CC. A solution study of silica condensation and speciation with relevance to in vitro investigations of biosilicification. The Journal of Physical Chemistry B. 2010;114:9947-55.

[295] Kastner M. Oceanic minerals: Their origin, nature of their environment, and significance. Proceedings of the National Academy of Sciences. 1999;96:3380-7.
[296] Wu Y-H, Liao L, Wang C-S, Ma W-L, Meng F-X, Wu M, et al. A comparison of microbial communities in deep-sea polymetallic nodules and the surrounding sediments in the Pacific Ocean. Deep Sea Research Part I: Oceanographic Research Papers. 2013;79:40-9.
[297] Nayak B, Das SK, Bhattacharyya KK. Detrital and authigenic (?) baddeleyite (ZrO2) in ferromanganese nodules of Central Indian Ocean Basin. Geoscience Frontiers. 2011;2:571-6.
[298] Straub KL, Kappler A, Schink B. Enrichment and isolation of ferric-iron-and humic-acid-reducing bacteria. Methods in enzymology. 2005;397:58-77.
[299] Kappler A, Benz M, Schink B, Brune A. Electron shuttling via humic acids in microbial iron (III) reduction in a freshwater sediment. FEMS Microbiology Ecology. 2004;47:85-92.
[300] Piepenbrock A, Behrens S, Kappler A. Comparison of humic substance-and Fe (III)-reducing microbial communities in anoxic aquifers. Geomicrobiology Journal. 2014;31:917-28.
[301] Bond DR, Lovley DR. Reduction of Fe (III) oxide by methanogens in the presence and absence of extracellular quinones. Environmental Microbiology. 2002;4:115-24.
[302] Coates JD, Ellis DJ, Blunt-Harris EL, Gaw CV, Roden EE, Lovley DR. Recovery of humic-reducing bacteria from a diversity of environments. Applied and Environmental Microbiology. 1998;64:1504-9.
[303] Lovley DR, Fraga JL, Coates JD, Blunt-Harris EL. Humics as an electron donor for anaerobic respiration. Environmental Microbiology. 1999;1:89-98.
[304] Lovley DR, Blunt-Harris EL. Role of humic-bound iron as an electron transfer agent in dissimilatory Fe (III) reduction. Applied and environmental microbiology. 1999;65:4252-4.
[305] Benz M, Schink B, Brune A. Humic acid reduction by Propionibacterium freudenreichii and other fermenting bacteria. Applied and environmental microbiology. 1998;64:4507-12.
[306] van Kessel MA, Speth DR, Albertsen M, Nielsen PH, den Camp HJO, Kartal B, et al. Complete nitrification by a single microorganism. Nature. 2015.
[307] Daims H, Lebedeva EV, Pjevac P, Han P, Herbold C, Albertsen M, et al. Complete nitrification by Nitrospira bacteria. Nature. 2015;528:504-9.
[308] Charpentier D, Buatier M, Jacquot E, Gaudin A, Wheat C. Conditions and mechanism for the formation of iron-rich Montmorillonite in deep sea sediments (Costa Rica margin): Coupling high resolution mineralogical characterization and geochemical modeling. Geochimica et Cosmochimica Acta. 2011;75:1397-410.
[309] Gaudin A, Buatier M, Beaufort D, Petit S, Grauby O, Decarreau A. Characterization and origin of Fe3+-montmorillonite in deep-water calcareous sediments (Pacific Ocean, Costa Rica margin). Clays and Clay Minerals. 2005;53:452-65.
[310] Pufahl P, Hiatt E. Oxygenation of the Earth's atmosphere–ocean system: a review of physical and chemical sedimentologic responses. Marine and Petroleum Geology. 2012;32:1-20.
[311] Zijlstra H. 3. Early diagenesis of chalk, in: The sedimentology of chalk. Springer; 1995.
[312] Polgári M, Hein J, Németh T, Pál-Molnár E, Vigh T. Celadonite and smectite formation in the Úrkút Mn-carbonate ore deposit (Hungary). Sedimentary Geology. 2013;294:157-63.
[313] Bjorlykke K. Petroleum geoscience: From sedimentary environments to rock physics: Springer Science & Business Media; 2010.
[314] Konhauser KO, Urrutia MM. Bacterial clay authigenesis: a common biogeochemical process. Chemical Geology. 1999;161:399-413.
[315] Kostka JE, Stucki LJW, Nealson KH, Wu J. Reduction of structural Fe (III) in smectite by a pure culture of the Fe-reducing bacterium Shewanella putrifaciens strain MR-1. Clays and Clay Minerals: Citeseer; 1996.
[316] Lam PJ, Bishop JK. The continental margin is a key source of iron to the HNLC North Pacific Ocean. Geophysical Research Letters. 2008;35.
[317] Coggon RM, Teagle D, Harris M, John C, Smith-Duque C, Alt J. Why Does Calcium Carbonate Precipitate in the Ocean Crust? AGU Fall Meeting Abstracts2012. p. 0545.
[318] Kelemen PB, Manning CE. Reevaluating carbon fluxes in subduction zones, what goes down, mostly comes up. Proceedings of the National Academy of Sciences. 2015;112:E3997-E4006.
[319] Schrenk MO, Brazelton WJ, Lang SQ. Serpentinization, carbon, and deep life. Rev Mineral Geochem. 2013;75:575-606.
[320] Janecky D, Seyfried W. Hydrothermal serpentinization of peridotite within the oceanic crust: experimental investigations of mineralogy and major element chemistry. Geochimica et Cosmochimica Acta. 1986;50:1357-78.
[321] Müntener O. Serpentine and serpentinization: A link between planet formation and life. Geology. 2010;38:959-60.
[322] Evans BW. Control of the products of serpentinization by the Fe2+ Mg− 1 exchange potential of olivine and orthopyroxene. Journal of Petrology. 2008;49:1873-87.
[323] Sanna A, Uibu M, Caramanna G, Kuusik R, Maroto-Valer M. A review of mineral carbonation technologies to sequester CO 2. Chemical Society Reviews. 2014;43:8049-80.
[324] Oelkers EH, Gislason SR, Matter J. Mineral carbonation of CO2. Elements. 2008;4:333-7.
[325] Sissmann O, Brunet F, Martinez I, Guyot Fo, Verlaguet A, Pinquier Y, et al. Enhanced olivine carbonation within a basalt as compared to single-phase experiments: reevaluating the potential of CO2 mineral sequestration. Environmental science & technology. 2014;48:5512-9.
[326] Kelemen PB, Matter J, Streit EE, Rudge JF, Curry WB, Blusztajn J. Rates and mechanisms of mineral carbonation in peridotite: natural processes and recipes for enhanced, in situ CO2 capture and storage. Annual Review of Earth and Planetary Sciences. 2011;39:545-76.

[327] Ivarsson M, Bengtson S, Neubeck A. The igneous oceanic crust–Earth's largest fungal habitat? Fungal Ecology. 2016;20:249-55.
[328] Kelley DS, Karson JA, Früh-Green GL, Yoerger DR, Shank TM, Butterfield DA, et al. A serpentinite-hosted ecosystem: the Lost City hydrothermal field. Science. 2005;307:1428-34.
[329] Rast W, Calcagno A, Williams WD. The Watershed: Water from the Mountains into the Sea. Streams And Rivers: Water Flowing Over the Land Surface. In: Programme UUNe, editor. Lakes and Reservoirs vol 22001. p. 36.
[330] Righi-Cavallaro KO, Roche KF, Froehlich O, Cavallaro MR. Structure of macroinvertebrate communities in riffles of a Neotropical karst stream in the wet and dry seasons. Acta Limnologica Brasiliensia. 2010;22:306-16.
[331] Li Q, Sun H, Wang J. Hydrochemical response of Epikarst Spring to rainfall: implications of nutrition element loss and groundwater pollution. Polish Journal of Environmental Studies. 2010;19:441-8.
[332] Raeisi E, Karami G. Hydrochemographs of Berghan karst spring as indicators of aquifer characteristics. Journal of Cave and Karst Studies. 1997;59:112-8.
[333] Kelemen PB, Matter J. In situ carbonation of peridotite for CO2 storage. Proceedings of the National Academy of Sciences. 2008;105:17295-300.
[334] Wang X, Ouyang Z, Zhuo S, Zhang M, Zheng G, Wang Y. Serpentinization, abiogenic organic compounds, and deep life. Science China Earth Sciences. 2014;57:878-87.
[335] Malvoisin B, Chopin C, Brunet F, Galvez ME. Low-temperature wollastonite formed by carbonate reduction: a marker of serpentinite redox conditions. Journal of Petrology. 2012;53:159-76.
[336] Holm NG, Oze C, Mousis O, Waite J, Guilbert-Lepoutre A. Serpentinization and the formation of H2 and CH4 on celestial bodies (planets, moons, comets). Astrobiology. 2015;15:587-600.
[337] Galvez ME, Beyssac O, Martinez I, Benzerara K, Chaduteau C, Malvoisin B, et al. Graphite formation by carbonate reduction during subduction. Nature Geoscience. 2013;6:473-7.
[338] Rumble D. Hydrothermal graphitic carbon. Elements. 2014;10:427-33.
[339] Köhler P, Hartmann J, Wolf-Gladrow DA. Geoengineering potential of artificially enhanced silicate weathering of olivine. Proceedings of the National Academy of Sciences. 2010;107:20228-33.
[340] Köhler P, Abrams JF, Völker C, Hauck J, Wolf-Gladrow DA. Geoengineering impact of open ocean dissolution of olivine on atmospheric CO2, surface ocean pH and marine biology. Environmental Research Letters. 2013;8:014009.
[341] Haas S, Weber N, Berry A, Erich E. Limestone powder carbon dioxide scrubber as the technology for Carbon Capture and Usage. Cement International. 2014;3:34-45.
[342] Lyubetskaya T, Korenaga J. Chemical composition of Earth's primitive mantle and its variance: 1. Method and results. Journal of Geophysical Research: Solid Earth. 2007;112.
[343] Insua TL, Spivack AJ, Graham D, D'Hondt S, Moran K. Reconstruction of Pacific Ocean bottom water salinity during the Last Glacial Maximum. Geophysical Research Letters. 2014;41:2914-20.
[344] Hovland M, Rueslåtten H, Johnsen HK. Buried Hydrothermal Systems: The Potential Role of Supercritical Water," ScriW", in Various Geological Processes and Occurrences in the Sub-Surface. American Journal of Analytical Chemistry. 2014;5:128.
[345] Hovland M, Rueslåtten H, Johnsen H, Kvamme B, Kuznetsova T. Salt formation associated with sub-surface boiling and supercritical water. Marine and Petroleum Geology. 2006;23:855-69.
[346] Hovland M, Kuznetsova T, Rueslåtten H, Kvamme B, Johnsen HK, Fladmark GE, et al. Sub-surface precipitation of salts in supercritical seawater. Basin Research. 2006;18:221-30.
[347] Schrag DP, Higgins JA, Macdonald FA, Johnston DT. Authigenic carbonate and the history of the global carbon cycle. Science. 2013;339:540-3.
[348] Sun X, Turchyn AV. Significant contribution of authigenic carbonate to marine carbon burial. Nature Geoscience. 2014;7:201-4.
[349] Zhao M-Y, Zheng Y-F, Zhao Y-Y. Seeking a geochemical identifier for authigenic carbonate. Nature communications. 2016;7.
[350] Solomon EA, Spivack AJ, Kastner M, Torres ME, Robertson G. Gas hydrate distribution and carbon sequestration through coupled microbial methanogenesis and silicate weathering in the Krishna–Godavari basin, offshore India. Marine and Petroleum Geology. 2014;58:233-53.
[351] Meister P, Gutjahr M, Frank M, Bernasconi SM, Vasconcelos C, McKenzie JA. Dolomite formation within the methanogenic zone induced by tectonically driven fluids in the Peru accretionary prism. Geology. 2011;39:563-6.
[352] Roberts JA, Bennett PC, González LA, Macpherson G, Milliken KL. Microbial precipitation of dolomite in methanogenic groundwater. Geology. 2004;32:277-80.
[353] Merinero R, Lunar R, Martínez-Frías J, Somoza L, Díaz-del-Río V. Iron oxyhydroxide and sulphide mineralization in hydrocarbon seep-related carbonate submarine chimneys, Gulf of Cadiz (SW Iberian Peninsula). Marine and Petroleum Geology. 2008;25:706-13.
[354] Dewangan P, Basavaiah N, Badesab F, Usapkar A, Mazumdar A, Joshi R, et al. Diagenesis of magnetic minerals in a gas hydrate/cold seep environment off the Krishna–Godavari basin, Bay of Bengal. Marine Geology. 2013;340:57-70.
[355] Tribovillard N, Du Châtelet EA, Gay A, Barbecot F, Sansjofre P, Potdevin J-L. Geochemistry of cold seepage-impacted sediments: Per-ascensum or per-descensum trace metal enrichment? Chemical Geology. 2013;340:1-12.
[356] Drobner E, Huber H, Wächtershäuser G, Rose D, Stetter KO. Pyrite formation linked with hydrogen evolution under anaerobic conditions. Nature. 1990;346:742-4.
[357] Rickard D, Luther GW. Kinetics of pyrite formation by the H 2 S oxidation of iron (II) monosulfide in aqueous solutions between 25 and 125 C: The mechanism. Geochimica et Cosmochimica Acta. 1997;61:135-47.

[358] Conrad R. Contribution of hydrogen to methane production and control of hydrogen concentrations in methanogenic soils and sediments. FEMS Microbiology Ecology. 1999;28:193-202.
[359] Dörr M, Käßbohrer J, Grunert R, Kreisel G, Brand WA, Werner RA, et al. A possible prebiotic formation of ammonia from dinitrogen on iron sulfide surfaces. Angewandte Chemie International Edition. 2003;42:1540-3.
[360] Krause S, Liebetrau V, Gorb S, Sánchez-Román M, McKenzie JA, Treude T. Microbial nucleation of Mg-rich dolomite in exopolymeric substances under anoxic modern seawater salinity: New insight into an old enigma. Geology. 2012;40:587-90.
[361] Raiswell R, Fisher Q. Rates of carbonate cementation associated with sulphate reduction in DSDP/ODP sediments: implications for the formation of concretions. Chemical Geology. 2004;211:71-85.
[362] Luff R, Wallmann K. Fluid flow, methane fluxes, carbonate precipitation and biogeochemical turnover in gas hydrate-bearing sediments at Hydrate Ridge, Cascadia Margin: numerical modeling and mass balances. Geochimica et Cosmochimica Acta. 2003;67:3403-21.
[363] Berner RA, Scott MR, Thomlinson C. Carbonate alkalinity in the pore waters of anoxic sediments. Limnology and Oceanography. 1970;15:544-9.
[364] Maekawa T, Itoh S, Sakata S, Igari S-i, Imai N. Pressure and temperature conditions for methane hydrate dissociation in sodium chloride solutions. Geochemical Journal. 1995;29:325-9.
[365] Neubeck A, Duc NT, Hellevang H, Oze C, Bastviken D, Bacsik Z, et al. Olivine alteration and H 2 production in carbonate-rich, low temperature aqueous environments. Planetary and Space Science. 2014;96:51-61.
[366] Mayhew L, Ellison E, McCollom T, Trainor T, Templeton A. Hydrogen generation from low-temperature water-rock reactions. Nature Geoscience. 2013;6:478-84.
[367] Bayrakci G, Minshull T, Sawyer D, Reston TJ, Klaeschen D, Papenberg C, et al. Fault-controlled hydration of the upper mantle during continental rifting. Nature Geoscience. 2016;9:384-8.
[368] Worman SL, Pratson LF, Karson J, Klein E. Global rate and distribution of H2 gas produced by serpentinization within oceanic lithosphere. Geophysical Research Letters. 2016.
[369] Römer M, Torres M, Kasten S, Kuhn G, Graham AG, Mau S, et al. First evidence of widespread active methane seepage in the Southern Ocean, off the sub-Antarctic island of South Georgia. Earth and Planetary Science Letters. 2014;403:166-77.
[370] Suess E, Torres M, Bohrmann G, Collier R, Greinert J, Linke P, et al. Gas hydrate destabilization: enhanced dewatering, benthic material turnover and large methane plumes at the Cascadia convergent margin. Earth and Planetary Science Letters. 1999;170:1-15.
[371] Krastel S, Bialas J, A V. Im fragilen Gleichgewicht: Deutsch-Neuseeländisches Forscherteam entdeckt bisher unbekanntes Methanvorkommen bei der Untersuchung von instabilen untermeerischen Hängen; . Pressemitteilung 02062014 des GEOMAR Helmholz-Zentrum für Ozeanforschung Kiel und Institut für Geowissenschaften der Christian-Albrechts-Universität zu Kiel vom 12052014. Kiel 2014.
[372] Paull CK, Ussler W, Dallimore SR, Blasco SM, Lorenson TD, Melling H, et al. Origin of pingo-like features on the Beaufort Sea shelf and their possible relationship to decomposing methane gas hydrates. Geophysical Research Letters. 2007;34.
[373] Shakhova N, Semiletov I, Panteleev G. The distribution of methane on the Siberian Arctic shelves: Implications for the marine methane cycle. Geophysical Research Letters. 2005;32.
[374] Serov P, Portnov A, Mienert J, Semenov P, Ilatovskaya P. Methane release from pingo-like features across the South Kara Sea shelf, an area of thawing offshore permafrost. Journal of Geophysical Research: Earth Surface. 2015;120:1515-29.
[375] Berndt C, Feseker T, Treude T, Krastel S, Liebetrau V, Niemann H, et al. Methane hydrates and global warming: Dissolution of hydrates off Svalbard caused by natural processes; . Kiel Pressemitteilung des GEOMAR Helmholz-Zentrum für Ozeanforschung Kiel, Kiel; 2014.
[376] Fischer D, Mogollón JM, Strasser M, Pape T, Bohrmann G, Fekete N, et al. Subduction zone earthquake as potential trigger of submarine hydrocarbon seepage. Nature Geoscience. 2013;6:647-51.
[377] Elvert M, Suess E, Greinert J, Whiticar MJ. Archaea mediating anaerobic methane oxidation in deep-sea sediments at cold seeps of the eastern Aleutian subduction zone. Organic Geochemistry. 2000;31:1175-87.
[378] Shakhova N, Semiletov I, Salyuk A, Kosmach D. Anomalies of methane in the atmosphere over the East Siberian shelf: Is there any sign of methane leakage from shallow shelf hydrates. Geophysical Research Abstracts2008. p. A01526.
[379] Sivan O, Antler G, Turchyn AV, Marlow JJ, Orphan VJ. Iron oxides stimulate sulfate-driven anaerobic methane oxidation in seeps. Proceedings of the National Academy of Sciences. 2014;111:E4139-E47.
[380] Basen M, Krüger M, Milucka J, Kuever J, Kahnt J, Grundmann O, et al. Bacterial enzymes for dissimilatory sulfate reduction in a marine microbial mat (Black Sea) mediating anaerobic oxidation of methane. Environmental microbiology. 2011;13:1370-9.
[381] Sivan O, Adler M, Pearson A, Gelman F, Bar-Or I, John SG, et al. Geochemical evidence for iron-mediated anaerobic oxidation of methane. Limnology and Oceanography. 2011;56:1536-44.
[382] Sivan O, Shusta S, Valentine D. Methanogens rapidly transition from methane production to iron reduction. Geobiology. 2016;14:190-203.
[383] Naqvi S, Bange HW, Farias L, Monteiro P, Scranton M, Zhang J. Marine hypoxia/anoxia as a source of CH4 and N2O. Biogeosciences. 2010;7:2159-90.
[384] Stramma L, Schmidtko S, Levin LA, Johnson GC. Ocean oxygen minima expansions and their biological impacts. Deep Sea Research Part I: Oceanographic Research Papers. 2010;57:587-95.
[385] Duprat LP, Bigg GR, Wilton DJ. Enhanced Southern Ocean marine productivity due to fertilization by giant icebergs. Nature Geoscience. 2016.

[386] Joughin I, Smith BE, Medley B. Marine ice sheet collapse potentially under way for the Thwaites Glacier Basin, West Antarctica. Science. 2014;344:735-8.
[387] Pope F, Braesicke P, Grainger R, Kalberer M, Watson I, Davidson P, et al. Stratospheric aerosol particles and solar-radiation management. Nature Climate Change. 2012;2:713-9.
[388] Pérez-Sanz A, Lucena J. Synthetic iron oxides as sources of Fe in a hydrophonic culture of sunflower. Iron nutrition in soils and plants: Springer; 1995. p. 241-6.
[389] Hochmuth G. ron (Fe) nutrition in Plants; U.S. Department of Agriculture, Extension Service, University of Florida, IFAS Document SL353. Available at http://edis.ifas.ufl.edu/pdffiles/SS/SS55500.pdf 2011.
[390] Morrissey J, Guerinot ML. Iron uptake and transport in plants: the good, the bad, and the ionome. Chemical reviews. 2009;109:4553-67.
[391] Becker M, Asch F. Iron toxicity in rice—conditions and management concepts. Journal of Plant Nutrition and Soil Science. 2005;168:558-73.
[392] Forieri I, Hell R. Micronutrient use efficiency–cell biology of iron and its metabolic interactions in plants. Nutrient use efficiency in plants: Springer; 2014. p. 133-52.
[393] Philpott CC. Iron uptake in fungi: a system for every source. Biochimica et Biophysica Acta (bba)-molecular cell research. 2006;1763:636-45.
[394] Kraemer SM. Iron oxide dissolution and solubility in the presence of siderophores. Aquatic sciences. 2004;66:3-18.
[395] Abadía J, Vázquez S, Rellán-Álvarez R, El-Jendoubi H, Abadía A, Álvarez-Fernández A, et al. Towards a knowledge-based correction of iron chlorosis. Plant Physiology and Biochemistry. 2011;49:471-82.
[396] Basar H, Gürel S, Ataç T, Çelik H. Effect of foliar iron applications on contents of iron forms and mineral composition of sweet cherry (Prunus avium L.). Indo-American Journal of Agriculture and Veterinary Science. 2014;2:1-11.
[397] El-Jendoubi H, Vázquez S, Calatayud Á, Vavpetič P, Vogel-Mikuš K, Pelicon P, et al. The effects of foliar fertilization with iron sulfate in chlorotic leaves are limited to the treated area. A study with peach trees (Prunus persica L. Batsch) grown in the field and sugar beet (Beta vulgaris L.) grown in hydroponics. Frontiers in plant science. 2014;5:2.
[398] Rombolà AD, Tagliavini M. Iron nutrition of fruit tree crops. Iron nutrition in plants and rhizospheric microorganisms: Springer; 2006. p. 61-83.
[399] Fernández V, Sotiropoulos T, Brown PH. Foliar Fertilization: Scientific Principles and Field Pratices: International fertilizer industry association; 2013.
[400] Goos RJ, Johnson BE. A comparison of three methods for reducing iron-deficiency chlorosis in soybean. Agronomy Journal. 2000;92:1135-9.
[401] Yu H, Chin M, Yuan T, Bian H, Remer LA, Prospero JM, et al. The fertilizing role of African dust in the Amazon rainforest: A first multiyear assessment based on data from Cloud-Aerosol Lidar and Infrared Pathfinder Satellite Observations. Geophysical Research Letters. 2015;42:1984-91.
[402] Yu H, Chin M, Bian H, Yuan T, Prospero JM, Omar AH, et al. Quantification of trans-Atlantic dust transport from seven-year (2007–2013) record of CALIPSO lidar measurements. Remote Sensing of Environment. 2015;159:232-49.
[403] Gläser G, Wernli H, Kerkweg A, Teubler F. The transatlantic dust transport from North Africa to the Americas—Its characteristics and source regions. Journal of Geophysical Research: Atmospheres. 2015;120.
[404] Köhler L, Tobón C, Frumau KA, Bruijnzeel LS. Biomass and water storage dynamics of epiphytes in old-growth and secondary montane cloud forest stands in Costa Rica. Plant Ecology. 2007;193:171-84.
[405] Rizzolo JA, Barbosa CGG, Borillo GC, al. e. Mineral nutrients in Saharan dust and their potential impact on Amazonian rainforest ecology. . Atmospheric Chemistry and Physics (under review) DOI: 105194/acp-2016-557. 2016.
[406] Ertel JR, Hedges JI, Devol AH, Richey JE, Ribeiro MdNG. Dissolved humic substances of the Amazon River system. Limnology and Oceanography. 1986;31:739-54.
[407] Abbaspour N, Hurrell R, Kelishadi R. Review on iron and its importance for human health. Journal of Research in Medical Sciences. 2014;19.
[408] WHO. Micronutrient deficiencies: iron deficiency anemia. Geneva: WHO. Available at www.who.int/nutrition/topics/ida/en/. See also www.who.int/nutrition/publications/en/ida_assessment_prevention_control.pdf. 2013.
[409] Avni T, Leibovici L, Gafter-Gvili A. Iron supplementation for the treatment of chronic heart failure and iron deficiency: systematic review and meta-analysis. European journal of heart failure. 2012;14:423-9.
[410] Cohen-Solal A, Leclercq C, Deray G, Lasocki S, Zambrowski J-J, Mebazaa A, et al. Iron deficiency: an emerging therapeutic target in heart failure. Heart. 2014:heartjnl-2014-305669.
[411] Beckett AC, Piazuelo MB, Noto JM, Peek RM, Washington MK, Algood HMS, et al. Dietary composition influences incidence of Helicobacter pylori-induced iron deficiency anemia and gastric ulceration. Infection and Immunity. 2016;84:3338-49.
[412] Medeiros DM. Copper, iron, and selenium dietary deficiencies negatively impact skeletal integrity: A review. Experimental Biology and Medicine. 2016:1535370216648805.
[413] Ünüsan N. The Importance of Iron on Preschool Children and Effect on Cognitive Development. 2013.
[414] Lukowski AF, Koss M, Burden MJ, Jonides J, Nelson CA, Kaciroti N, et al. Iron deficiency in infancy and neurocognitive functioning at 19 years: evidence of long-term deficits in executive function and recognition memory. Nutritional neuroscience. 2013.

[415] Yehuda S, Rabinovitz S, Carasso RL, Mostofsky DI. Long-lasting cognitive, physiological and hematological effects in rehabilitated, early dietary iron-deficiency adult rats, and improvement by treatment with a mixture of essential fatty acids. Nutritional neuroscience. 2013.
[416] Saini RK, Nile SH, Keum Y-S. Food science and technology for management of iron deficiency in humans: A review. Trends in Food Science & Technology. 2016;53:13-22.
[417] Allen LH. Guidelines on food fortification with micronutrients. WHO, FAO. Guidelines on food fortification with micronutrients: World Health Organization. Dept. of Nutrition for Health and Development; 2006.
[418] WHO, FAO, UNICEF. Recommendations on wheat and maize flour fortification meeting report: Interim consensus statement. Interim Consensus Statement. Genova. Available at www.who.int/nutrition/publications/micro-nutrients/wheat_maize_fort.pdf. 2009.
[419] Zuo Y, Zhang F. Soil and crop management strategies to prevent iron deficiency in crops. Plant and Soil. 2011;339:83-95.
[420] Jeong J, Guerinot ML. Biofortified and bioavailable: the gold standard for plant-based diets. Proceedings of the National Academy of Sciences. 2008;105:1777-8.
[421] Zhang Y, Shi R, Rezaul KM, Zhang F, Zou C. Iron and zinc concentrations in grain and flour of winter wheat as affected by foliar application. Journal of agricultural and food chemistry. 2010;58:12268-74.
[422] Wei Y, Shohag M, Yang X, Yibin Z. Effects of foliar iron application on iron concentration in polished rice grain and its bioavailability. Journal of agricultural and food chemistry. 2012;60:11433-9.
[423] Lipson DA, Jha M, Raab TK, Oechel WC. Reduction of iron (III) and humic substances plays a major role in anaerobic respiration in an Arctic peat soil. Journal of Geophysical Research: Biogeosciences. 2010;115.
[424] Miller KE, Lai C-T, Friedman ES, Angenent LT, Lipson DA. Methane suppression by iron and humic acids in soils of the Arctic Coastal Plain. Soil Biology and Biochemistry. 2015;83:176-83.
[425] Lipson D, Miller K, Lai C. Methane Suppression: The Impacts of Fe (III) and Humic Acids on Net Methane Flux from Arctic Tundra Wetlands in Alaska and Finland. AGU Fall Meeting Abstracts2013. p. 02.
[426] Zhang L, Keller J, Yuan Z. Inhibition of sulfate-reducing and methanogenic activities of anaerobic sewer biofilms by ferric iron dosing. Water Research. 2009;43:4123-32.
[427] Zhang L, Derlon N, Keller J, Yuan Z. Dynamic response of sulfate-reducing and methanogenic activities of anaerobic sewer biofilms to ferric dosing. Journal of Environmental Engineering. 2012;138:510-7.
[428] Ali MA, Lee CH, Kim PJ. Effect of silicate fertilizer on reducing methane emission during rice cultivation. Biology and Fertility of Soils. 2008;44:597-604.
[429] Liu S, Zhang L, Liu Q, Zou J. Fe (III) fertilization mitigating net global warming potential and greenhouse gas intensity in paddy rice-wheat rotation systems in China. Environmental pollution. 2012;164:73-80.
[430] Liu D, Dong H, Agrawal A, Singh R, Zhang J, Wang H. Inhibitory effect of clay mineral on methanogenesis by Methanosarcina mazei and Methanothermobacter thermautotrophicus. Applied Clay Science. 2016;126:25-32.
[431] Wang W, Lai DY, Li S, Kim PJ, Zeng C, Li P, et al. Steel slag amendment reduces methane emission and increases rice productivity in subtropical paddy fields in China. Wetlands Ecology and Management. 2014;22:683-91.
[432] Amos R, Bekins B, Cozzarelli I, Voytek M, Kirshtein J, Jones E, et al. Evidence for iron-mediated anaerobic methane oxidation in a crude oil-contaminated aquifer. Geobiology. 2012;10:506-17.
[433] Zhou S, Xu J, Yang G, Zhuang L. Methanogenesis affected by the co-occurrence of iron (III) oxides and humic substances. FEMS microbiology ecology. 2014;88:107-20.
[434] Van Bodegom PM, Scholten JC, Stams AJ. Direct inhibition of methanogenesis by ferric iron. FEMS Microbiology Ecology. 2004;49:261-8.
[435] Teh YA, Dubinsky EA, Silver WL, Carlson CM. Suppression of methanogenesis by dissimilatory Fe (III)-reducing bacteria in tropical rain forest soils: Implications for ecosystem methane flux. Global Change Biology. 2008;14:413-22.
[436] Roden EE, Wetzel RG. Organic carbon oxidation and suppression of methane production by microbial Fe (III) oxide reduction in vegetated and unvegetated freshwater wetland sediments. Limnology and Oceanography. 1996;41:1733-48.
[437] Tagliabue A, Dutkiewicz S. Iron Model Intercomparison Project (FeMIP). Working Group proposal submitted to SCOR April 2016. Available at: http://www.scor-int.org/Annual%20Meetings/2016GM/FeMIP.pdf. . 2016.
[438] Lim M, Chiang K, Amal R. Photochemical synthesis of chlorine gas from iron (III) and chloride solution. Journal of Photochemistry and Photobiology A: Chemistry. 2006;183:126-32.
[439] Meyer-Oeste F-D. Method for Cooling the Troposphere. Int. Patent CA 2748680 A1. (Remark: [Wittmer, 2015] focus only to the side variant of claim 8). 2010.
[440] Platt U, Allan W, Lowe D. Hemispheric average Cl atom concentration from 13 C/12 C ratios in atmospheric methane. Atmospheric Chemistry and Physics. 2004;4:2393-9.
[441] Keene W, Khalil MAK, Erickson D, McCulloch A, Graedel TE, Lobert JM, et al. Composite global emissions of reactive chlorine from anthropogenic and natural sources: Reactive Chlorine Emissions Inventory. Journal of Geophysical Research: Atmospheres. 1999;104:8429-40.
[442] McCulloch A, Aucott ML, Benkovitz CM, Graedel TE, Kleiman G, Midgley PM, et al. Global emissions of hydrogen chloride and chloromethane from coal combustion, incineration and industrial activities: Reactive Chlorine Emissions Inventory. Journal of Geophysical Research: Atmospheres. 1999;104:8391-403.
[443] Sanhueza E. Hydrochloric acid from chlorocarbons: a significant global source of background rain acidity. Tellus B. 2001;53.
[444] Lobert JM, Keene WC, Logan JA, Yevich R. Global chlorine emissions from biomass burning: Reactive chlorine emissions inventory. Journal of Geophysical Research: Atmospheres. 1999;104:8373-89.
[445] Jaenicke R. Atmospheric aerosols and global climate. Journal of Aerosol science. 1980;11:577-88.

[446] Penner JE, Andreae M, Annegarn H, Barrie L, Feichter J, Hegg D, et al. Aerosols, their direct and indirect effects. Climate Change 2001: The Scientific Basis Contribution of Working Group I to the Third Assessment Report of the Intergovernmental Panel on Climate Change: Cambridge University Press; 2001. p. 289-348.
[447] Kumar P, Robins A, Vardoulakis S, Britter R. A review of the characteristics of nanoparticles in the urban atmosphere and the prospects for developing regulatory controls. Atmospheric Environment. 2010;44:5035-52.
[448] Gupta D, Kim H, Park G, Li X, Eom H-J, Ro C-U. Hygroscopic properties of NaCl and NaNO3 mixture particles as reacted inorganic sea-salt aerosol surrogates. Atmospheric Chemistry and Physics. 2015;15:3379-93.
[449] Biskos G, Malinowski A, Russell L, Buseck P, Martin S. Nanosize effect on the deliquescence and the efflorescence of sodium chloride particles. Aerosol Science and Technology. 2006;40:97-106.
[450] Oeste FD. Controlling concentration of active materials necessary for life; air pollution control. US Patents 08/534535; 2009.
[451] Ito T, Nenes A, Johnson M, Meskhidze N, Deutsch C. Acceleration of oxygen decline in the tropical Pacific over the past decades by aerosol pollutants. Nature Geoscience. 2016.
[452] Sullivan RC, Guazzotti SA, Sodeman DA, Tang Y, Carmichael GR, Prather KA. Mineral dust is a sink for chlorine in the marine boundary layer. Atmospheric Environment. 2007;41:7166-79.
[453] Hoshyaripour G, Hort M, Langmann B. Ash iron mobilization through physicochemical processing in volcanic eruption plumes: a numerical modeling approach. Atmospheric Chemistry and Physics. 2015;15:9361-79.
[454] Martin R, Wheeler J, Ilyinskaya E, Braban C, Oppenheimer C. The uptake of halogen (HF, HCl, HBr and HI) and nitric (HNO 3) acids into acidic sulphate particles in quiescent volcanic plumes. Chemical Geology. 2012;296:19-25.
[455] Ayris PM, Delmelle P, Cimarelli C, Maters EC, Suzuki YJ, Dingwell DB. HCl uptake by volcanic ash in the high temperature eruption plume: Mechanistic insights. Geochimica et Cosmochimica Acta. 2014;144:188-201.
[456] Myriokefalitakis S, Mihalopoulos N, Baker A, Kanakidou M. The anthropogenic influence on Iron deposition over the oceans: a 3-D global modeling. EGU General Assembly Conference Abstracts2014. p. 8310.
[457] Keeling RF, Shertz SR. Seasonal and interannual variations in atmospheric oxygen and implications for the global carbon cycle. Nature. 1992;358:723-7.
[458] Manning AC, Keeling RF. Global oceanic and land biotic carbon sinks from the Scripps atmospheric oxygen flask sampling network. Tellus B. 2006;58:95-116.
[459] Oeste FD. The ISA method (IM). Climate Engineering Research Symposium 2015, Current State and Future Perspectives. Berlin2015.
[460] Oeste FD, Ries E. IOA, the CO2- and methane-carbon capturing process: Effective and secure carbon sequestration from troposphere into ocean sediment by flue gas conditioning of coal power plants. . 2nd ICEPE 2011 International Conference on Energy Process Engineering, Frankfurt am Main, Book of Extended Abstracts: Efficient carbon capture for coal power plants Frankfurt DECHEMA Gesellschaft für Chemische Technik & Biotechnologie e.V., Frankfurt am Main; 2011. p. 207-9.
[461] Kammler HK, Mädler L, Pratsinis SE. Flame synthesis of nanoparticles. Chemical engineering & technology. 2001;24:583-96.
[462] Buyukhatipoglu K, Clyne AM. Controlled flame synthesis of αFe2O3 and Fe3O4 nanoparticles: effect of flame configuration, flame temperature, and additive loading. Journal of Nanoparticle Research. 2010;12:1495-508.
[463] Kim D, Song K, Kaushik R. Fuel Additives for Particulate Matter/Dust Reduction. Asian Journal of Chemistry. 2008;20:5797.
[464] Madhu S, Nagaraju J, Sridhar P. Evaluation of four stroke diesel engine performance with ferrocene as fuel additive. International Journal & Magazine of Engineering, Technology, Management and Research. 2015;2:2199-204.
[465] Rubasinghege G, Lentz RW, Scherer MM, Grassian VH. Simulated atmospheric processing of iron oxyhydroxide minerals at low pH: roles of particle size and acid anion in iron dissolution. Proceedings of the National Academy of Sciences. 2010;107:6628-33.
[466] Rustad D, Gregory N. Photoreduction of gaseous iron (III) chloride with sunlight and other light sources. Inorganic and Nuclear Chemistry Letters. 1980;16:521-4.
[467] Ming T. Solar Chimney Power Plant Generating Technology: Academic Press, 246p. ISBN: 978-0-12-805370-6. ; 2016.
[468] Michaud L, Renno N. the sky's the limit. Mechanical Engineering. 2011;133:42.
[469] Davidson P, Burgoyne C, Hunt H, Causier M. Lifting options for stratospheric aerosol geoengineering: advantages of tethered balloon systems. Philosophical Transactions of the Royal Society of London A: Mathematical, Physical and Engineering Sciences. 2012;370:4263-300.
[470] Kuo KA, Watson I, Hunt HE. The SPICE project: an example of geoengineering research. Water and Climate: Policy Implementation Challenges; Proceedings of the 2nd Practical Responses to Climate Change Conference: Engineers Australia; 2012. p. 479.
[471] Anderson K. Duality in climate science. Nature Geoscience. 2016;8:898-900.
[472] Jones A, Haywood J, Jones A. Climatic impacts of stratospheric geoengineering with sulfate, black carbon and titania injection. Atmospheric Chemistry & Physics Discussions. 2015;15.
[473] Herzog HJ. Scaling up carbon dioxide capture and storage: From megatons to gigatons. Energy Economics. 2011;33:597-604.
[474] Betz G, Brachatzeck N, Cacean S, Güssow K, Heintzenberg J, Hiller S, et al. Gezielte Eingriffe in das Klima? Eine Bestandsaufnahme der Debatte zu Climate Engineering. ISBN: 3-89456-324-9, Kiel Earth Institute. 2011.

[475] Myriokefalitakis S, Daskalakis N, Mihalopoulos N, Baker A, Nenes A, Kanakidou M. Changes in dissolved iron deposition to the oceans driven by human activity: a 3-D global modelling study. Biogeosciences. 2015;12:3973-92.
[476] Annett AL, Skiba M, Henley SF, Venables HJ, Meredith MP, Statham PJ, et al. Comparative roles of upwelling and glacial iron sources in Ryder Bay, coastal western Antarctic Peninsula. Marine Chemistry. 2015;176:21-33.
[477] Bhatia MP, Kujawinski EB, Das SB, Breier CF, Henderson PB, Charette MA. Greenland meltwater as a significant and potentially bioavailable source of iron to the ocean. Nature Geoscience. 2013;6:274-8.
[478] Raiswell R, Benning LG, Tranter M, Tulaczyk S. Bioavailable iron in the Southern Ocean: the significance of the iceberg conveyor belt. Geochem Trans. 2008;9:9.
[479] Boyd PW. Development of geopolitically-relevant ranking criteria for geoengineering methods. DOI: 10.1002/2016EF000447. Earth's Future. 2017.
[480] Wang B, O'Brien RE, Kelly ST, Shilling JE, Moffet RC, Gilles MK, et al. Reactivity of liquid and semisolid secondary organic carbon with chloride and nitrate in atmospheric aerosols. The Journal of Physical Chemistry A. 2014;119:4498-508.
[481] Laskin A, Moffet RC, Gilles MK, Fast JD, Zaveri RA, Wang B, et al. Tropospheric chemistry of internally mixed sea salt and organic particles: Surprising reactivity of NaCl with weak organic acids. Journal of Geophysical Research: Atmospheres. 2012;117.
[482] Okin GS, Baker AR, Tegen I, Mahowald NM, Dentener FJ, Duce RA, et al. Impacts of atmospheric nutrient deposition on marine productivity: Roles of nitrogen, phosphorus, and iron. Global Biogeochemical Cycles. 2011;25.
[483] Zhang Z, Moore JC, Huisingh D, Zhao Y. Review of geoengineering approaches to mitigating climate change. Journal of Cleaner Production. 2014.
[484] Lackner M. Geoengineering for Climate Stabilization. New York: Springer; 2015.
[485] Williams J, Reus Md, Krejci R, Fischer H, Ström J. Application of the variability-size relationship to atmospheric aerosol studies: estimating aerosol lifetimes and ages. Atmospheric Chemistry and Physics. 2002;2:133-45.
[486] Davidson P. Up and away! : TCE www.tcetoday.com; 2012. p. 28-32.
[487] Boyd PW, Jickells T, Law C, Blain S, Boyle E, Buesseler K, et al. Mesoscale iron enrichment experiments 1993-2005: Synthesis and future directions. science. 2007;315:612-7.
[488] Harrison DP. A method for estimating the cost to sequester carbon dioxide by delivering iron to the ocean. International Journal of Global Warming. 2013;5:231-54.
[489] Aumont O, Bopp L. Globalizing results from ocean in situ iron fertilization studies. Global Biogeochemical Cycles. 2006;20.
[490] Nedwell DB, Watson A. CH 4 production, oxidation and emission in a UK ombrotrophic peat bog: influence of SO 4 2− from acid rain. Soil Biology and Biochemistry. 1995;27:893-903.
[491] Watson A, Nedwell DB. Methane production and emission from peat: the influence of anions (sulphate, nitrate) from acid rain. Atmospheric Environment. 1998;32:3239-45.
[492] Gauci V, Matthews E, Dise N, Walter B, Koch D, Granberg G, et al. Sulfur pollution suppression of the wetland methane source in the 20th and 21st centuries. Proceedings of the National Academy of Sciences of the United States of America. 2004;101:12583-7.
[493] Gauci V, Dise N, Fowler D. Controls on suppression of methane flux from a peat bog subjected to simulated acid rain sulfate deposition. Global Biogeochemical Cycles. 2002;16.
[494] Gauci V, Dise N, Blake S. Long-term suppression of wetland methane flux following a pulse of simulated acid rain. Geophysical research letters. 2005;32.
[495] Krishnamurthy A, Moore JK, Mahowald N, Luo C, Doney SC, Lindsay K, et al. Impacts of increasing anthropogenic soluble iron and nitrogen deposition on ocean biogeochemistry. Global Biogeochemical Cycles. 2009;23.
[496] Moore JK, Doney SC, Lindsay K. Upper ocean ecosystem dynamics and iron cycling in a global three-dimensional model. Global Biogeochemical Cycles. 2004;18.
[497] Martin JH, Coale KH, Johnson KS, Fitzwater SE, Gordon RM, Tanner SJ, et al. Testing the iron hypothesis in ecosystems of the equatorial Pacific Ocean. Nature. 1994;371:123-9.
[498] Wang R, Balkanski Y, Bopp L, Aumont O, Boucher O, Ciais P, et al. Influence of anthropogenic aerosol deposition on the relationship between oceanic productivity and warming. Geophysical Research Letters. 2015;42.